THE PRE-EVENT STIMULUS ENSEMBLE

an analysis of the stimulus-response relation for complex stimuli applied to auditory neurons

jan l. groshuis

THE PRE-EVENT STIMULUS ENSEMBLE

an analysis of the stimulus-response relation

for complex stimuli

applied to auditory neurons

THE PRE-EVENT STIMULUS ENSEMBLE

an analysis of the stimulus-response relation

for complex stimuli

applied to auditory neurons

proefschrift

ter verkrijging van de graad van
doctor in de wiskunde en natuurwetenschappen
aan de Katholieke Universiteit te Nijmegen
op gezag van de rector-magnificus
prof.mr. F.J.F.M. Duynstee
volgens besluit van het college van decanen
in het openbaar te verdedigen
op vrijdag 18 januari 1974
des middags te 14.00 uur precies

door

Jan Lammert Grashuis
geboren te Delft

pour tous

TABLE OF CONTENTS

MOTIVATION AND BACKGROUND

Signal processing in the central nervous system is very complex.
Signals of continuous nature arrive from the outer world at the various
kinds of sensors and are converted, via a number of stages, different
for the various sensory organs, into neural events (actionpotentials or
spikes) which are transmitted further into the central nervous system.
Many nerve endings converge on one neuron and one neuron influences
many other neurons. These neural connections are very specific, but
also very complex.
Actionpotentials arriving at a synaps are causing post-synaptic potentials
at the post synaptic membrane. Those post-synaptic potentials have a
continuous nature and can undergo decremental conduction in the dendrites.
The outgoing signals have in most cases an all or none pulse type
character (actionpotentials), while their generation is often influenced
by stochastic components. The picture for one neuron thus is : many
input channels, continuous signals as well as pulse type signals,
stochastic influences, and one, diverging output channel.

The complexity is a great barrier for theoretical descriptions of
neural information processing.
The fact, however, that every neuron has only one output channal enables
the observation of the responses of aneuron by means of (extra cellular)
recordings of the actionpotential. And through the variation of
stimuli presented (to e.g. the auditory system of the cat) one could
try to obtain information about the functional and/or structural properties
of the neuron.
Therefore, neurophysiology concerns about finding the stimuli which
alters the response of neurons in such a way that information is
obtained about the properties of the neurons. This approach is
characterized by applying a group of simple stimuli and studying the
responses of the neurons and trying to extract from these stimulus-
response relations general transfer properties of the neurons.

In 1968,however, de Boer et al introduced their important theory and
results of the reverse correlation (de Boer,Kuyper,de Jongh, 1968
to 1974) in which they used noise as a stimulus.
As for linear systems the crosscorrelation between (noise) input
and output results in the impulse response of the system, the cross-
correlation between the (noise) stimulus and the recorded action-
potentials results in a non-zero function representing in some way the
linear aspects of the peripheral auditory system. De Boer et al thus
proved that also with non-structured stimuli information could be
obtained about the nervous system.
At about that time Johannesma worked in our laboratory on theoretical
stochastic descriptions of neural activity, resulting in his thesis
(Johannesma 1968,1969) describing neural activity in terms of diffusion
equations and introducing a stochastic transfer matrix.
In 1969 the need was felt to combine his theoretical work with electro-
physiological experiments and a group was formed (Johannesma,van
Gisbergen, Grashuis, Krijt, Braks) to investigate theoretical and
experimental aspects of the nervous system
The aim was to study stimulus-response relations for single neurons
by extra-cellular recordings of the actionpotentials. Using both,
the more conventional approach of applying well-defined stimuli and
studying the response properties, and the approach initiated by de
Boer, using stochastic, complex stimuli and studying the stimulus
properties which gave rise to the generation of the actionpotentials.
however, because of the non-linearities in the system, different
methods may lead to different results and the bringing together of these
different results is an important part of the research

The first method we used is the presentation of a simple repetitive
stimulus of which the average response is determined, the well-known
post-stimulus time histogram,(PSTH). The averaging is necessary
because of the statistical fluctuations in the elicited spikes
causing the individual responses to be irreproducible. The PSTH in
general is reproducible. This method was extended with sets of
stimuli in which the frequency and/or intensity are changing

10

stochastic transfer function.

As research objest the auditory system of the cat was chosen, because
of the possibilities in generation, processing and registration of
auditory stimuli. In the auditory system the cochlear nuclei were chosen
as they are a rather low but not the lowest level in the auditory
system. Here it is possible to compare the results of the various
analyses for rather simple neurons. Also an impression as to whether
or not the same analysis could be applied to neurons at higher levels
in the auditory system can be obtained from the more complex neurons

Within this frame work, many activities were undertaken in the past four
years.
The experimental equipment has been build up to a rather sophisticated
degree and was interfaced to the laboratory computer and software for
on-line experiments and off-line computations were developed
(here we must mention the contributions and supports of the computer
group and the electronics department of our laboratory)
The existing auditory electrophysiological techniques were adopted and
evaluated and new methods and techniques were added (complex stimuli,
amplitude and frequency modulation of tones and noise, scans)   Results
have been or will be published (van Gisbergen 1971,1974, Johannesma 1971a).
Research was done on the condition of the animal and on influences of
anaesthesia on the neural responses. Recordingsites were histologically
traced (van Gisbergen 1974, Kevenzel 1974).
The crosscorrelation method (reverse coorelation) was adopted and extended
to the analysis of the pre-event stimulus ensemble (Johannesma 1971,
this thesis, chapter III). An attempt was made to characterize and
parametrize the reverse correlation functions (Olde Heuvelt 1971,   ◢
this thesis, chapter IV)
Investigations concerning the complex energy density of the pre-event
stimulus ensemble were started (van Bloemendaal).
A model of a first-order auditory neuron (Johannesma 1969) was extended
and analysed, to support the neurophysiological experiment (methodological
aspects) as well as to facilitate thoughts and discussions (Johannesma

1971, Koldewijn 1973). Furthermore thought was given to the invariance
property introduced by Siebert (1965) and Gestri and Petracchi (1970)
stating that possibly the expectation density of events elicited by
different stimuli is invariant after an appropriate time transformation
for each stimulus (Joosten).
Very recently also attempts were made to use the same kind of analysis
for the visual system (lateral geniculate body) which give promissing
results (Sak, Boezeman).

I.2   THIS THESIS

This thesis presents the part of the investigations concerning the Pre-
Event Stimulus Ensemble, resulting in a functional description of
responses to complex stationary stimuli. It should, therefore, be
emphasised that this thesis is closely connected to the thesis presented
by van Gisbergen : Characterization of responses to tone and noise
stimuli of neurons in the cat's cochlear nuclei (van Gisbergen, 1974).

As a necessary introduction, Chapter II is a complete reproduction of the
paper presented by Johannesma at the Symposium on Hearing Theory in
Eindhoven (1972). In this paper the following are introduced and
properly defined : the Pre-Event stimulus Ensemble, the Post-Stimulus
Response Ensemble and the connections of both via the Bayes relation.
Moreover this paper gives a wider scope to the presented material.

Chapter III gives a detailed description of the analyses carried out of
the Pre-Event Stimulus Ensemble, resulting in prediction algorithms for
stationary complex stimuli. It also gives the results of the analyses
for several neurons, together with a number of results from other kinds
of experiments. The rather ad hoc presentation as given in chapter III-3
was necessary as at present a more integrated treatment was not possible.

Chapter IV is an attempt to characterize and parametrize the cross-
correlation functions (the average pre-event stimulus).
This chapter is written as and intended to be an article to be published.

This chapter, which is an introduction to Chapters III and IV is a
paper presented by Johannesma on the IPO-symposium on Hearing Theory
in Eindhoven (1972).
It is a complete reproduction except for some errata and a renumbering
of the equations, to render it more suitable for this thesis. The
notes at the bottom of the pages are from the author of this thesis.
Since the appearance of this paper, the terminology has changed with
regard to 'response', which in the following is called 'event', e.g.
the Pre-Response Stimulus Ensemble is identical to the Pre-Event
stimulus Ensemble etc.

14

II   THE PRE-RESPONSE STIMULUS ENSEMBLE OF NEURONS IN THE COCHLEAR NUCLEUS

Peter I M. Johannesma

Lab. of Biophysics and Medical Physics, Univ. Nijmegen, Nijmegen,
The Netherlands.

II.1   INTRODUCTION

Presentation of an auditory stimulus
$$x(t) , 0 \leq t \leq t_0$$
may elicit a sequence of action potentials
$$z(t) = \sum_n \delta(t-t_n) , n = 1,N \qquad (II-1)$$
from a neuron in the auditory system.

Periodically repeated presentation of the stimulus
$$x(t) : x(t+kt_0) = x(t) , k = 1,K \qquad (II-2)$$
allows the formation of the ensemble of elicited responses.

Definition : The Post Stimulus Response Ensemble (PSRE) of stimulus
$x(t) , 0 \leq t < t_0$, is the ensemble of responses induced
by the repetitive presentation of stimulus $x(t)$:
$$z(t+kt_0) . 0 \leq t < t_0 , k = 1,K \qquad (II-3)$$
If no systematic changes dependent on k are visible in this ensemble,
e.g. no habituation, then the PSRE is homogeneous. In this case the
average value of the PSRE, i.e. the Post Stimulus Time Histogram
(PSTH) or event-density $n(t)$

$$n(t) = \frac{1}{K} \sum_{k=1}^{K} z(t+kt_0) , 0 \leq t < t_0 \qquad (II-4)$$

is the function normally used for the representation of the dynamic

aspects of the single cell response.

The relation between stimulus $x(t)$ and pulse sequence $z(t)$ is always essentially nonlinear; the relation between stimulus $x(t)$ and event-density $n(t)$ may be nonlinear, but is usually not essentially nonlinear. For the study of the stochastic dynamics, i.e. the dynamic relation between stimulus $x(t)$ and averaged or expected response $n(t)$, the computation of the crosscorrelations forms a general and useful approach (Wiener, 1958).
The first-order crosscorrelation

$$R(\tau) = \frac{1}{t_0} \int_0^{t_0} dt \; x(t-\tau) \; n(t) \qquad\qquad (II-5)$$

represents the linear relation between $x(t)$ and $n(t)$: the harmonic part of the (average) response.
The second-order crosscorrelation

$$R(\sigma,\tau) = \frac{1}{t_0} \int_0^{t_0} dt \; x(t-\sigma) \; x(t-\tau) \; n(t) \qquad\qquad (II-6)$$

represents the dependence of the average response $n(t)$ on the quadratic properties of the stimulus $x(t)$; e.g. on the second harmonic for a sinusoidal stimulus.
Higher-order crosscorrelations represent more complex and usually less important aspects of the stimulus-response relations.

This approach to the analysis of single-cell responses on repetitive stimuli, will be generalised in this paper for non-repetitive stimuli where no PSTH can be constructed and the event-density $n(t)$ cannot be measured. The exploitation of the fact that the response is a pulse sequence allows a more general analysis including a relation with the concepts and methods used in pattern recognition.

The correlation of stimulus $x(t)$ and PSTH $n(t)$

$$R(\tau) = \frac{1}{t_0} \int_0^{t_0} dt \; x(t-\tau) \; n(t)$$

$$= \frac{1}{t_0} \int_0^{t_0} dt \; x(t-\tau) \; \frac{1}{K} \sum_{k=1}^{K} z(t+kt_0), \quad \text{because of Eq. (II-4)}$$

$$R(\tau) = \frac{1}{K} \sum_{k=1}^{K} \frac{1}{t_0} \int_0^{t_0} dt \; x(t-\tau) \; z(t+kt_0)$$

$$= \frac{1}{K} \sum_{k=1}^{K} \frac{1}{t_0} \int_0^{t_0} dt \; x(t+kt_0-\tau) \; z(t+kt_0), \quad \text{because of Eq. (II-2)}$$

$$= \frac{1}{T_0} \int_0^{T_0} dt \; x(t-\tau) \; z(t) \; , \qquad T_0 = K \, t_0 \qquad \text{(II-7)}$$

This equation states that the crosscorrelation between stimulus $x(t)$
and PSTH or event-density $n(t)$ is, always and exactly, equal to the
crosscorrelation between stimulus $x(t)$ and pulse sequence $z(t)$. The
same can easily be derived for the second-order crosscorrelation

$$R(\sigma,\tau) = \frac{1}{t_0} \int_0^{t_0} dt \; x(t-\sigma) \; x(t-\tau) \; n(t)$$

$$= \frac{1}{T_0} \int_0^{T_0} dt \; x(t-\sigma) \; x(t-\tau) \; z(t) \qquad \text{(II-8)}$$

and for the crosscorrelation of arbitrary order.

These mathematical results imply that the information with respect to
the response of a cell on the repetitive stimulus $x(t)$ contained in
the PSTH $n(t)$ is also present in the crosscorrelations between
stimulus $x(t)$ and pulse-sequence $z(t)$.
Eq. (II-7) and Eq. (II-8) will from here on form the basic definitions
of $R(\tau)$ and $R(\sigma,\tau)$ which apply both for repetitive and non-repetitive

stimuli. The fact that the response $z(t)$ is a pulse-sequence, leads to the following equations

$$R(\tau) = \frac{1}{T_0} \int_0^{T_0} dt\ x(t-\tau)\ z(t)$$

$$= \frac{1}{T_0} \int_0^{T_0} dt\ x(t-\tau) \sum_{n=1}^{N} \delta(t-t_n), \text{ because of Eq. (II-1)}$$

$$= \frac{1}{T_0} \sum_{n=1}^{N} \int_0^{T_0} dt\ x(t-\tau)\ \delta(t-t_n)$$

$$R(\tau) = \frac{1}{T_0} \sum_{n=1}^{N} x(t_n-\tau) \tag{II-9}$$

Eq. (II-9) states that the crosscorrelation of stimulus $x(t)$ and pulse-sequence $z(t)$ equals the average value of the stimulus preceding an action potential (de Boer and Kuyper, 1968). *)

In the same way, it can be shown that

$$R(\sigma,\tau) = \frac{1}{T_0} \int_0^{T_0} dt\ x(t-\sigma)\ x(t-\tau)\ z(t)$$

$$= \frac{1}{T_0} \sum_{n=1}^{N} x(t_n-\sigma)\ x(t_n-\tau) \tag{II-10}$$

Analogous results again follow for the higher-order crosscorrelations. The meaning of these equations can be made more clear by definition of the pre-response stimulus ensemble.

---

*) A better definition of the average value of the stimulus preceding an action potential is

$$\frac{1}{N} \sum_{n=1}^{N} x(t_n-\tau) = \frac{T_0}{N} R(\tau)$$

(cf. Eq. (III-1) and Eq. (IV-4)).

<u>Definition</u> : The Pre-Response Stimulus Ensemble (PRSE) is the ensemble
of stimuli preceding an action potential

$$x_n(\tau) = x(t_n-\tau) \ , \quad n = 1,N \qquad\qquad (II-11)$$

The next step is to recognise the fact that the mth-order cross-
correlation functions of stimulus $x(t)$ and pulse-sequence $z(t)$
defined as

$$R_m = R(\tau_1, \tau_2, \ . \ , \tau_m) = \int dt \ x(t-\tau_1) \cdot x(t-\tau_2) \cdot .. \cdot x(t-\tau_m) \ z(t) \quad (II-12)$$

is identical with the mth-order moment-function of the PRSE, defined as
(Stratonovich, 1963)

$$R_m = R(\tau_1, \tau_2, \ . \ , \tau_m) = \sum_{n=1}^{N} x_n(\tau_1) \cdot x_n(\tau_2) \cdot .. \cdot x_n(\tau_m) \quad (II-13)$$

Several important conclusions may now be drawn.

<u>Conclusion 1</u> :

The information on stimulus-response relations contained in the PSTH
$n(t)$ is also present in the crosscorrelation-functions of stimulus $x(t)$
and pulse sequence $z(t)$ and in the moment-functions of the Pre-Response
Stimulus Ensemble.

<u>Conclusion 2</u> :

For the definition of the Pre-Response Stimulus Ensemble and
computation of the moment-functions R_m there is no need for the
stimulus $x(t)$ to be repetitive and/or simple   In fact complex,
non-repetitive stimuli may be more adequate in this approach because
of the potential richness of PRSE (e.q. Gaussian white noise, Poisson-
distributed clicks, randomly in amplitude and frequency-modulated
tones).

<u>Conclusion 3</u> .

Since the stimulus does not have to be repetitive the correlation
method does not need controllability of the stimulus; observability
may be sufficient. If the stimulus is not controllable formation and
analysis of the PRSE seems the most adequate approach.

19

Conclusion 4 :

The characteristics of the PRSE may be investigated and represented through the moment-functions R_m, by means of other characteristics or directly through the probability density distribution

In order to be able to extract quantative information from the PRSE and to establish the relation with pattern recognition we introduce a geometrical representation of the Pre-Response Stimulus Ensemble. Given a complex, repetitive or not, stimulus $x(t)$ with highest-frequency components $\leq W$, the assumption is made that apriori physiological knowledge implies that the response $z(t)$ does not depend on the part of the stimulus $x(s)$ with $s < t-T$. (For the Cochlear Nucleus T might be ~20 msec.) As a consequence each element of the PRSE

$$x_n(\tau) = x(t_n-\tau) \; ; \; n = 1,N \; ; \; 0 \leq \tau \leq T$$

can be represented by 2WT sample-values at

$$0 \leq \tau = \frac{m}{2W} \leq T \; , \; m = 1,M \; , \; M = 2WT$$

This implies that the function $x_n(\tau)$ may be replaced by the 2WT-dimensional vector $\vec{x}_n$. Defining now a 2WT-dimensional signal space, then each 2WT-dimensional signal vector defines a point in this space and the PRSE forms a cloud, possibly even a cluster, in this space. The characteristics of this cloud (e.g. location, size, form) will now become the point of interest. However, these characteristics can only be evaluated through a comparison with some standard form.

Definition · The (original or complete) Stimulus Ensemble (SE) is the ensemble of stimuli contained in the complete stimulus of bandwidth W and duration T_0

$$\vec{x}_p = x(t_p-\tau)$$

where

$$0 \leq t_p = \frac{p}{2W} \leq T_0 \; ; \; p = 1,P \; , \; P = 2WT$$

$$0 \leq \tau = \frac{m}{2W} \leq T \; , \; m = 1,M \; , \; M = 2WT \qquad , \; T_0 \gg T$$

This implies that stimuli are taken from the signal $x(t)$ at distances $\frac{1}{2W}$ over the total duration T_0 and each again sampled at $\frac{1}{2W}$ over a time T. The relation between stimulus $x(t)$ and response $z(t)$ can now be represented in five Probability Density Functions (PDF).

1. $f(\vec{x})$ is the P.D.F. of the stimulus ensemble; this function describes the probability density of occurrence of stimulus $\vec{x}$ and may or may not be under experimental control.

2. $f(z)$ represents the probability of occurrence of an action potential per unit of time $(1/2W)$ and equals the average frequency (N/T_0) for the given stimulus ensemble.

3. $f(\vec{x},z)$ is the combined PDF of stimulus and response ensemble; this function represents the probability density of occurrence of a stimulus $\vec{x}$ and an action potential at the end of $\vec{x}$.

4. $f(\vec{x}|z)$ is the conditional PDF of stimulus with respect to response; this function gives the probability density of occurrence of stimulus $\vec{x}$ when an action potential is known to occur.

5. $f(z|\vec{x})$ is the conditional PDF of response with respect to stimulus; this function gives the probability of occurrence of an action potential directly following the presentation of stimulus $\vec{x}$, is identical with the event-density $n(t)$ and follows directly from the PSTH.

These five probability density functions are, however, not independent. The Bayes'relation implies

$$f(\vec{x}) \cdot f(z|\vec{x}) = f(\vec{x},z) = f(z) \, f(\vec{x}|z) \qquad (II\text{-}14)$$

Since stimulus $x(t)$ and response $z(t)$ are observable, the PDF of the stimulus ensemble $f(\vec{x})$ and of the response ensemble $f(z)$ can be measured. This implies that, because of Eq. (II-14) the following two approaches yield the same information.

Forward approach

Determination of $f(z|\vec{x})$ from the average value of the Post-Stimulus Response Ensemble (PSTH). This approach fits well into the framework of system theory. It represents response prediction from the experimenters point of view.

Backward approach

Determination of $f(\vec{x}|z)$ from the distribution of the Pre-Response Stimulus Ensemble. This type of approach, which is strongly related to the theory of pattern recognition is focused upon stimulus estimation from the animal's point of view.

With the simple relation between these two approaches ·

$$\frac{f(z|\vec{x})}{f(z)} = \frac{f(\vec{x},z)}{f(\vec{x}) \cdot f(z)} = \frac{f(\vec{x}|z)}{f(\vec{x})} \qquad (II-15)$$

In words : the normalised response density is equal to the quotient of   of aposteriori and apriori stimulus density.

The forward approach directly studies $f(z|\vec{x})$, i.e. the PSTH for a limited set of stimuli $\vec{x}$ These stimuli are presented repetitively, as a consequence full stimulus control is needed.

The backward approach evaluates $f(\vec{x}|z)$ or $f(\vec{x},z)$, usually but not necessarily for comples stimuli, and compares these with $f(\vec{x})$.

The determination of the functions $R_m = R(\tau_1, \tau_2, \ldots, \tau_m)$ can be formulated both in the forward approach as the crosscorrelations between stimulus $x(t)$ and PSTH $n(t)$ (Eq. (II-5) and Eq. (II-6)) and in the backward approach as the crosscorrelations between pulse-sequence $z(t)$ and stimulus $x(t)$ (Eq. (II-7) and Eq. (II-8)) as well as the moments of the Pre-Response Stimulus Ensemble (Eq. (II-9) and Eq. (II-10)).

Since the Pre-Response Stimulus Ensemble is a selection out of the original Stimulus Ensemble it is possible to define the complement of the PRSE with respect to the SE. The collection of stimuli contained in the SE but not in the PRSE forms the Complementary PRSE. A comparative evaluation of PRSE and CPRSE is a well-known problem in the realm of pattern recognition.

22

II.3   EXPERIMENTAL APPLICATION ON EXTRACELLULAR SINGLE CELL RECORDINGS IN
        THE COCHLEAR NUCLEUS OF THE ANAESTHETISED CAT.

II.3.1   First-order analysis

Gaussian white noise (random or pseudorandom) with a frequency content
W large with respect to the characteristic frequency of the cell was
used as auditory stimulus.
Computation of first-order crosscorrelation

$$R(\tau) = \int dt\; x(t-\tau)\; z(t) = \sum_n x(t_n-\tau) = \sum_n x_n(\tau)$$

gave three types of results.
a. $R(\tau)$ equals zero. This is the case for cells with a CF $\geq$ 3kC, but,
   differing from results for primary auditory fibers, this may also
   occur for cells with a much lower CF.
b. Complex $R(\tau)$. either consisting of two well discernible types of
   oscillations or with a complex envelope in time and frequency.
c. Simple $R(\cdot)$: describable as an amplitude modulation of a sine wave
   of approximately the CF of the cell.
Five parameters were extracted from $R(\tau)$
    average time μ_τ time duration σ_τ phase ϕ
    average frequency ω_0, spectral width σ_ω,
The uncertainty product of time duration and spectral width was for
the simple $R(\tau)$ only slightly above the theoretical limit of 0 5 *)

$$0\;5 < \sigma_\tau \cdot \sigma_\omega < 0.7 \tag{II-16}$$

This implies that the average pre-spike stimulus is (nearly) as narrow
in the frequency-domain as is compatible with its duration in the time-
domain.
The waveform could be well approximated through

$$R(\tau) \propto c \left(\frac{\tau-\alpha}{\beta}\right)^{\gamma-1} e^{-\frac{\tau-\alpha}{\beta}} \sin(\omega_0\tau+\phi) \tag{II-17}$$

---

*) The upper limit of 0.7 appeared to be too low when more units were
investigated (cf. chapter IV).

23

where the parameters α, β and γ follow from τ_0, σ_τ and σ_ω.
The form of $R(\tau)$ is not in an obvious way related with the type of
neuron characterised by the PSTH on CF tone-bursts (Pfeiffer, 1966).
The quality of $R(\tau)$ seems clearly related with the amount of phase-
lock in tone-burst response and with cell-type (compare Lavine, 1971).
$R(\tau)$ forms the average value of the PRSE. If $R(\tau)$ differs
significantly from zero, then the following analysis of the dispersion
of this ensemble appears attractive. For each stimulus $\vec{x}_n$ the energy
and similarity with the average pre-response stimulus $R(\tau)$ is computed:

$$\text{Energy .} \quad e_n = \int_0^T d\tau \ \{x_n(\tau)\}^2 = \vec{x}_n \cdot \vec{x}_n \qquad (II-18)$$

$$\text{Similarity:} \quad \rho_n = \frac{\int_0^T d\tau \ x_n(\tau) \ R(\tau)}{\left[\int_0^T d\tau \ \{x_n(\tau)\}^2 \cdot \int_0^T d\tau \ \{R(\tau)^2\}\right]^{\frac{1}{2}}} = \frac{\vec{x}_n \cdot \vec{R}}{|\vec{x}_n| \cdot |\vec{R}|} \qquad (II-19)$$

The square root of the energy $\sqrt{e_n} = |\vec{x}_n|$ represents the length of $\vec{x}_n$,
while ρ_n equals the cosine of the angle between arbitrary pre-response
stimulus $\vec{x}_n$ and average pre-response stimulus $\vec{R}$.
Distribution of similarity ρ and energy e for the Stimulus Ensemble

$$f(\rho,e)$$

and for the Pre-Response Stimulus Ensemble

$$f(\rho,e,z)$$

result in the probability density function of spike generation as
function of similarity and energy of a signal $x(t)$

$$f(z|\rho,e) = \frac{f(\rho,e,z)}{f(\rho,e)} \qquad (II-20)$$

This function supplies information concerning selectivity and
threshold of the neuron.

Second-order analysis

For this analysis, which can be applied both on low- and on high-
frequency cells, the stimuli were Gaussian white noise and/or randomly
in amplitude and frequency modulated tones. Subject of investigation

is the second-order crosscorrelation of stimulus $x(t)$ and pulse
sequence $z(t)$

$$R(\sigma,\tau) = \int dt\ x(t-\sigma)\ x(t-\cdot)\ z(t) = \sum_n x_n(\sigma)\ x_n(\tau) = \sum_n r_n(\sigma,\tau)$$

which equals the ensemble-averaged second moment or the autocorrelation
of the PRSE. In an analogous way as the first-order moment $R(\tau)$ may
be represented as a 2WT-dimensional vector $\vec{R}$, the second-order moment
$R(\sigma,\tau)$ can be regarded as a 2WT x 2WT-dimensional matrix R. The
eigen-vectors of this matrix form an orthogonal set spanning the
signal-space; the eigen-vectors with the largest eigen-values form
the main axes for the representation of the PRSE. Though this
approach does well fit in with the theory of pattern recognition
(Karhunen - Loève expansion) it does not appear well matched to the
general characteristics of auditory signal transformation. A better
suited description may be found by considering the signal both as
function of time and as function of frequency.

Definition : The complex energy density of the signal
$x_n(\tau)$, $0 \le \tau \le T$, is given through the expression
(Rihaczek, 1968)

$$\varepsilon_n(\omega,\tau) = x(\tau)\ e^{-i\omega\tau}\ \tilde{x}_n^*(\omega) \tag{II-21}$$

where
$$\tilde{x}_n^*(\omega) = \int_0^T d\sigma\ e^{i\omega\sigma}\ x_n(\sigma)$$

Some symbol manipulations leads to

$$\varepsilon_n(\omega,\tau) = \int d\sigma\ e^{-i\omega\sigma}\ r_n(\tau,\tau-\sigma) \tag{II-22}$$

$$E(\omega,\tau) = \sum_n \varepsilon_n(\omega,\tau) = \sum_n \int d\sigma\ e^{-i\omega\sigma}\ r_n(\tau,\tau-\sigma) =$$

$$= \int d\sigma\ e^{-i\omega\sigma}\ R(\tau,\tau-\sigma) \tag{II-23}$$

This implies that the (average) complex energy density is the Fourier-
transform of the (average) autocorrelation.

The complex energy density has some interesting and relevant properties
for auditory signal processing. The integral over all frequencies
gives the energy density as function of time

$$\int_{-W}^{W} d\omega \; \varepsilon_n(\omega,\tau) = e_n(\tau) \quad , \quad \int_{-W}^{W} d\omega \; E(\omega,\tau) = E(\tau) \quad (II-24)$$

integration over time gives energy density as function of frequency

$$\int_0^T d\tau \; \varepsilon_n(\omega,\tau) = e_n(\omega) \quad , \quad \int_0^T d\tau \; E(\omega,\tau) = E(\omega) \quad (II-25)$$

and integration over both frequency and time gives the total energy of the signal

$$\int_{-W}^{W} d\omega \int_0^T d\tau \; \varepsilon_n(\omega,\tau) = e_n \quad , \quad \int_{-W}^{W} d\omega \int_0^T d\tau \; E(\omega,\tau) = E \quad (II-26)$$

The complex energy density $\varepsilon_n(\omega,\tau)$ may be considered as the complex energy of $x_n(\tau)$ as function of both frequency and time, $E(\omega,\tau)$ is the average energy differentiated with respect to frequency and time of the PRSE. The deviations of the complex energy densities of the individual pre-response stimuli $\varepsilon_n(\omega,\tau)$ from the average complex energy density of the PRSE $E(\omega,\tau)$ can be evaluated in an analogous way as the deviations of the pre-response stimuli from the average pre-response stimulus

The (average) uncertainty product $\sigma_\omega \cdot \sigma_\tau$, i e the combined frequency-time resolution of this cell for complex stimuli can be computed from the (average) complex energy density

There does not necessarily exist a general apriori relation between the spectral density of the first-order crosscorrelation

$$I(\omega) = |\bar{R}(\omega)|^2 = |\int d\tau \; e^{-i\omega\tau} R(\tau)|^2 \quad (II-27)$$

and the spectral density derived from the complex energy density of the PRSE

$$E(\omega) = \int d\tau \; E(\omega,\tau) \quad (II-25)$$

The proportion of these two densities

$$0 \le C(\omega) = \frac{I(\omega)}{E(\omega)} \le 1 \quad (II-28)$$

appears to be the obvious definition of a synchronisation-coefficient, at least for complex stimuli.

A related approach realisable with analog equipment in real time and
resulting in the real energy as function of frequency and time can be
implemented with a set of band-pass filters and quadratic rectifiers

If $h_k(\tau)$ is the impulse response of the band-pass filter with center
frequency at $\omega = \omega_k$ then the filtered signal is

$$x_k(t) = \int d\tau \; h_k(\tau) \; x(t-\tau) \qquad (II-29)$$

and the energy density of frequency components around $\omega = \omega_k$ at time t
is $\quad e(\omega_k,t) = \{x_k(t)\}^2 \qquad (II-30)$

The crosscorrelation of the energy density and the sequence of action
potentials

$$E(\omega_k,\tau) = \int dt \; e(\omega_k,t-\tau) \; z(t)$$

$$= \sum_n e(\omega_k,t_n-\tau) = \sum_n e_n(\omega_k,\tau) \qquad (II-31)$$

equals the sum of the pre-spike energy densities.
The relation with the second-order crosscorrelation or the average
auto-correlation of the PRSE is

$$E(\omega_k,\tau) = \int d\lambda \; h_k(\lambda) \int d\mu \; h_k(\mu) \; R(\tau+\lambda,\tau+\mu) \qquad (II-32)$$

and with the average complex energy density of the PRSE

$$E(\omega_k,\tau) = \int d\omega \int d\sigma \; H_k^*(\omega,\sigma) \; E(\omega,\tau+\sigma) \qquad (II-33)$$

where $\quad H_k(\omega,\sigma) = h_k(\sigma) \; e^{-i\omega\sigma} \; h_k^*(\omega) \qquad (II-34)$

is the complex energy density of the filter impulse response.
The real, time and frequency dependent, energy density $E(\omega_k,\tau)$ is an
integration over frequency and time with a weighting function determined
by the characteristics of the band-pass filter. This function may be
considered as the sonogram of this neuron averaged over the PRSE.

An inherent problem with this hardware analysis is that frequency and
time resolution of the sonogram depend on the characteristics of the
filters.

Knowledge of the probability density function of the energy $e(\omega,\tau)$
for the original Stimulus Ensemble

$$f(e(\omega,\tau)) = f(e(\omega))$$

and for the Pre-Response Stimulus Ensemble

$$f(e(\omega,\tau),z)$$

allows the computation of the related forward distributions.

<u>Dynamic Response Area</u> (DRA) defined as the probability density of occurrence of an action potential a time τ after presentation of a signal with energy e at frequency ω :

$$f(z|e(\omega,\tau)) = \frac{f(e(\omega,\tau),z)}{f(e(\omega,\tau))} \tag{II-35}$$

<u>Response Area</u> (RA) defined as the probability density of occurrence of an action potential induced by the presentation of a signal with energy e at frequency ω

$$f(z|e(\omega)) = \frac{f(e(\omega),z)}{f(e(\omega))} = \frac{\int_0^T d\tau\ f(e(\omega,\tau),z)}{\int_0^T d\tau\ f(e(\omega,\tau))} \tag{II-36}$$

<u>Dynamic Response</u> (DR) defined as the probability density of occurrence of an action potential a time τ after the presentation of a signal with energy e

$$f(z|e(\tau)) = \frac{f(e(\tau),z)}{f(e(\tau))} = \frac{\int_{-W}^{W} d\omega\ f(e(\omega,\tau),z)}{\int_{-W}^{W} d\omega\ f(e(\omega,\tau))} \tag{II-37}$$

For the original Stimulus Ensemble any wide-band stimulus may, in principle, be choosen. The central question, which can only be answered experimentally, is to what extent the normalised distributions $f(z|x)$, $f(z|\rho,e)$ and $f(z|\varepsilon(\omega,\tau))$ which characterise the cell, are independent of the stimulus ensemble. For a model study see Johannesma, 1971.

In the backward approach random and pseudo-random Gaussian white noise and randomly or pseudo-randomly in amplitude and/or frequency modulated tones are used for determination of DRA $f(z|e(\omega,\tau))$, RA $f(z|e(\omega))$ and DR $f(z|e(\tau))$ (compare Van Gisbergen e.a., 1971).

In the forward approach tone-bursts are used for determination of the frequency dependent dynamic characteristics (DRA), tones of gradually increasing intensity for the response area (RA) and amplitude modulated noise for investigation of wide-band dynamic response (DR).

Preliminary experimental data and computational results will be presented to illustrate applicability and effectiveness of this approach.

Boer, E. de and Kuyper, P. (1968): Triggered correlation,
    IEEE Tr. on Bio-Med. Eng. BME 15-3, 169-179.
Gisbergen, J.A.M. van, Grashuis, J.L., Johannesma, P.I.M., and
Vendrik, A.J.H. (1971): Single cells in the auditory system investigated
with stochastic stimuli,
    Proc. XXV Intern. Congress of Physiol. Sciences, Munich, 1971.
Johannesma, P.I.M. (1971): Dynamical aspects of the transmission of
stochastic neural signals,
    Proc. first European Biophysics Congress, Wiener Med. Akademie,
    V, 329-333.
Lavine, R.A. (1971): Phase-locking in response of single neurons in
cochlear nuclear complex of the cat to low-frequency tonal stimuli,
    J. Neurophysiol. 34, 467-483.
Pfeiffer, R.R. (1966): Classification of response patterns of spike
discharges for units in the cochlear nucleus: tone burst stimulation,
    Exp. Brain Res. 1, 220-235.
Rihaczek, A.W. (1968): Signal energy distribution in time and frequency,
    IEEE Tr. on Information Theory, IT 14-3, 360-374.
Stratonovich, R.L.: Topics in the theory of random noise;
    Gordon and Breach (1963).
Wiener, N.: Nonlinear problems in random theory;
    MIT-press (1958).

III   THE PRE-EVENT STIMULUS ENSEMBLE
        DESCRIPTION AND APPLICATIONS

Table of contents

The previous chapter introduced the concept of the pre-event stimulus ensemble (PESE) and the use of the Bayes relation in this context

As stated in Chapter II 1 the relation between a stimulus $x(t)$ and the elicited event sequence $z(t)$ is essentially non-linear and has a stochastic nature

In the forward approach the essential non-linearity can be eliminated by the linearising operation of ensemble averaging over the post-stimulus event ensemble (PSEE), yielding the event density or PSTH $n(t)$. Therefore linear approximations can be made for the relations between stimulus $x(t)$ and event density $n(t)$, and concepts as stochastic linearity and stochastic tranfer functions can be introduced (Johannesma, 1971, 1971a) While however, $x(t)$ can be positive and negative as well and $n(t)$ can only be positive, it is useful to separate $n(t)$ in an even part $n_e(t)$ and an odd part $n_o(t)$.

If $\quad n_+(t) = n(t,\{x\})$

is the event density or PSTH for the stimulus $x(t)$ and

$$n_-(t) = n(t,\{-x\})$$

is the event density for the same, but sign-inverted, stimulus $-x(t)$

then $\quad n_o(t) = \tfrac{1}{2}\{n_+(t) - n_-(t)\}$

is the odd part of the event density or compound PSTH (cf. Goblick and Pfeiffer, 1969 and Johannesma, 1971a) and

$$n_e(t) = \tfrac{1}{2}\{n_+(t) + n_-(t)\}$$

is the even part of the event density or summated PSTH. It will be clear that a linear relation can only exist between $x(t)$ and $n_o(t)$. On the other hand quadratic properties of $x(t)$, like the intensity, being even functions of $x(t)$ only can be linearly related to $n_e(t)$.

In the backward approach the essential non-linearity between $x(t)$ and $z(t)$ is eliminated through the linearising effects of the time

averaging in the correlation procedures for complex stimuli (cf. equation (II-5) and equation (II-6)).
This implies that equation (II-9) :

$$R(\tau) = \frac{1}{T_0} \sum_{n=1}^{N} x_n(t-\tau) \qquad (II-9)$$

is the linear approximation to the impulse response of the system (cf. Chapter IV.1) and as such can be compared to the compound PSTH for clicks (cf. Johannesma, 1971, also cf. Møller, 1969).

In Chapter III.2 analyses of the PESE are described in an attempt to extract from the PESE information about the functional properties of the neurons, using the first order analysis only, resulting in prediction algorithms consisting of a linear part followed by an algebraic non-linearity.

The stimulus given to the cat is Gaussian white noise, so a stationary complex stimulus. This implies that non-stationary relations between stimulus and response (all kinds of amplitude modulations) are not studied, and a time-invariant preparation is also assumed.
The power of the stimulus used, is, in the analysis, always assumed to be unity (unless stated otherwise).

Chapter III.3 shows some results from the analyses for several neurons in the cochlear nuclei of the cat and compares the predictions with experimentally recorded PSTH's. Furthermore some comparisons will be made with other kinds of (forward) experiments for the same neurons (see also van Gisbergen, 1974).

III.2.1   The center of mass

When the signal space concept is used for the PESE, every stimulus preceding a spike $x_n(\tau)$, is a point in the 2WT dimensional space. The most important point in this signal space apart from the origin is the center of mass of the PESE.
The (complete or original) stimulus ensemble SE, when a Gaussian white noise stimulus is used, has a multidimensional normal distribution so the center of mass of the SE coincides with the origin.
The center of mass of the PESE is

$$\vec{R} = \frac{1}{N} \sum_{n=1}^{N} \vec{x}_n \tag{III-1}$$

where $\vec{x}_n$ is the 2WT dimensional vector representing the pre-event stimulus $x(t_n-\tau)$.
Comparing equation (III-1) with the crosscorrelation function defined in equation (II-9)

$$R(\tau) = \frac{1}{T_0} \sum_{n=1}^{N} x(t_n-\tau) \tag{II-9}$$

the difference is the factor $\frac{N}{T_0}$, being the average firing rate of the neuron.
When we ignore this factor as being some scaling factor, it becomes apparent that the center of mass of the PESE being identical to the average pre-event stimulus, is equal to the crosscorrelation of stimulus and pulse sequence.
The analysis of $R(\tau)$ is carried out in Chapter IV and deals with wave-shape, spectrum and delay times and will be accompanied by the introduction of a mathematical function representing $R(\tau)$.
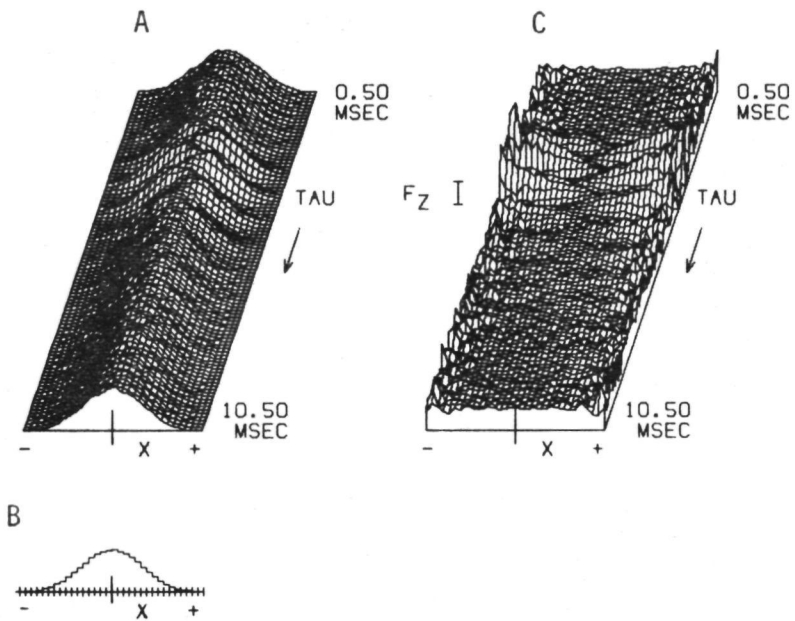
Fig. III-1 A Signal value distributions of the stimulus at different
moments τ_i before the action potential $f(x_i|z)$

B Signal value distribution of the stimulus $f(x)$

C Normalized signal value distributions

$$f(z|x_i) = \frac{f(x_i|z)}{f(x)}\ f(z)$$

The coordinates R_i, $i = 1, 2WT$, of the center of mass $\hat{R}$ are the mean values of the distributions along the 2WT axes, or in other words the distributions of signal values at the various times before the spike. The attention will now be given to those distributions.

For axis i, representing the time $\tau_i = \frac{i}{2W}$ before the event the distribution is given for the PESE by

$$f(x(t-\tau_i)|z(t)) \equiv f(x_i|z) \qquad (III-2)$$

Because the stimulus is Gaussian white noise, the distributions of the SE are independent of τ_i, so for all τ_i the same normal distribution is obtained.

$$f(x(t-\tau_i)) = f(x(t)) = f(x) \qquad (III-3)$$

Figure III-1 shows the set of distributions for unit 59-5 for $50 < \tau < 10.50$ msec or $5 < i < 105$ of the PESE and the SE distribution. According to the Bayes relation (II-14)

$$f(x_i,z) = f(x_i|z)\, f(z)$$
$$= f(z|x_i)\, f(x_i) = f(z|x_i)\, f(x) \qquad (III-4)$$

Rearranging :

$$\frac{f(z|x_i)}{f(z)} = \frac{f(x_i|z)}{f(x)} \qquad (III-5)$$

$$f(z|x_i) = \frac{f(x_i|z)}{f(x)}\, f(z)$$

Equation III-5 states that the probability of the occurrence of an event a time τ_i after a stimulus value x is present, is proportional to the quotient of the PESE probability of the value x at the ith axis and the SE probability of x.
So $f(z|x_i)$ predicts the occurrence of a spike a time τ_i after a stimulus value x is present.

The entire set $f(z|x_i)$ for all i is a predictor set for the occurrence of spikes at times τ_i (0 < i < 2WT) after a stimulus value x. This set (figure III-1) can be considered as the stochastic impulse response, to be understood as the response (i.e. the probability density function of the action potentials or event density) to a small stimulus pulse, buried in noise (cf. stochastic linearisation procedure, Johannesma, 1971, 1971a). As can be seen in figure III-1 this stochastic impulse response is non-linear with respect to the amplitude of the stimulus pulse. Mind that this impulse response should be strictly interpreted as the response to an impulse and that no inferences are made so far about the response to combinations of impulses.

When, however, a continuous stimulus is presented to the cat, of which we like to predict the response, we must make an assumption about the temporal relations or interactions between the individual $f(z|x_i)$. In a first order approximation we then assume the individual $f(z|x_i)$ to be independent. For this assumption two necessary conditions are met, viz. the stimulus is stationary and the x_i are independent (sampled at 2WT moments). In a second-order approximation the $f(z|x_i)$ will not be independent because the $f(x_i|z)$ will have some relation through the occurrence of the spike.

The temporal relation thus becomes the superposition of independent probabilities, i.e. the product of the probabilities (note that for linear systems the superposition of independent contributions is a summation, viz. the convolution integral). So the relative probability of a spike to occur at a time $t = t_n$ when a continuous stimulus is presented is approximated through

$$\frac{f(z(t_n)|x(t_n-\tau),\ 0<\tau<T)}{f(z)} = \prod_{i=1}^{2WT} \frac{f(z|x_i)}{f(z)}$$

or

$$f(z|\vec{x}_n) = \prod_{i=1}^{2WT} \frac{f(z|x_i)}{f(z)} \quad f(z) \qquad (III-6)$$

38

PREDICTED PSTH

EXPERIMENTAL PSTH

10 MSEC
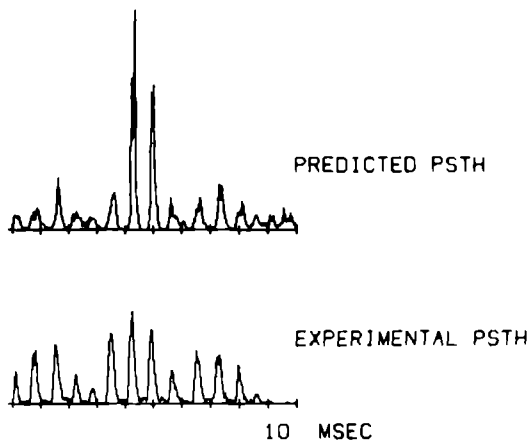
Fig. III-2 Predicted and experimentally recorded PSTH's for a pseudo-
            noise stimulus for unit 59-5. Predictor: $f(z|\vec{x}) = \pi\ f(z|x_i)$.

This means that we have derived a predictor to predict the expected value
of the response to a stimulus $x(t)$ or in other words, we can predict the
event density or PSTH. Figure III-2 shows a PSTH predicted in this way
for a short pseudonoise stimulus, and the PSTH for the same stimulus
recorded from the animal. The similarity of both supports the assumption
about the temporal interaction, made above. For an evaluation
we refer to Chapter III 2.4.

For a fruitful application of the predictor derived it is necessary that
the $f(z|x_1)$ do have some structure. When all the $f(x_1|z)$ of the PESE are
normal distributions the $f(z|x_1)$ are all identical to $f(z)$. In general
this will be the case when the uncertainty in the time relation between
the relevant stimulus and the elicited neural event is of the order of
one half to one period of the characteristic frequency of the neuron, i.e.
the time lock between stimulus and response deteriorated too much. In
that case also no non-zero $R(\tau)$ will be obtained. This implicates that
the analysis only can be made successfully for low frequency neurons
(up till 1 to 3 kHz, depending on the location). See also Chapter IV.

39

M,cosφ-analysis

In the previous paragraph we merely observed the distributions along the axes and treated them as being independent of each other. In this paragraph we will analyse the locations of the individual points of the PESE in the signal space i.e. the structure of the PESE.

Let us first look to the density of points in the signal space. Assume that we recorded 10,000 spikes (a reasonable number) so we have 10^4 pre event stimuli or points in the signal space. When we now assume a very bad resolution along the axis, e.g. 5 positive and 5 negative values, a stimulus with frequencies up till 5 kHz and taking the relevant stimulus duration as 10 msec (so 2WT = 100) the number of space cells is 10^{100}.

Therefore the density in the space is $10^4/10^{100} = 10^{-96}$ which is extremely low. We thus have to reduce the number of dimensions considerably. We ,therefore, suggest to look at the energy contained in each stimulus $x_n(t)$ and the similarity with $R(\tau)$. However, $\vec{R} = R(\tau)$ is contaminated by the residual noise, and before any computation is done with $R(\tau)$ we will remove this residual noise. This is done by some weighting procedure in both time and frequency domain, as described in more detail in Chapter IV.4.1.

In the remainder of this chapter we will consider $R(\tau)$ to be the weighted version, unless stated otherwise.

As defined in equations II-18 and II-19, the energy and similarity are respectively

$$e_n = \int_0^T \{x_n(\tau)\}^2 \, d\tau = \vec{x}_n \cdot \vec{x}_n \qquad \text{(III-7)}$$

$$\rho_n = \frac{\vec{x}_n \cdot \vec{R}}{|\vec{x}_n| \cdot |\vec{R}|} \qquad \text{(III-8)}$$

In the signal space concept it may be more suitable to use, instead of the energy, the square root of the energy, which represents the length of the vector $\vec{x}_n$ or the modulus

$$M_n = \sqrt{E_n} = (\vec{x}_n \cdot \vec{x}_n)^{\frac{1}{2}} = |\vec{x}_n| \qquad \qquad (III-9)$$

(here and in the following e_n is replaced by E_n, so $E_n \equiv e_n$)

and the similarity can be interpreted as the cosine of the angle between $\vec{x}_n$ and $\vec{R}$

$$\cos \phi_n = \rho_n \qquad \qquad (III-10)$$

Furthermore the projection of $\vec{x}_n$ on the $\vec{R}$ can be defined, or the scalar product of $\vec{x}_n$ and the normalised $\vec{R}$, being

$$P_n = \frac{\vec{x}_n \cdot \vec{R}}{|\vec{R}|}$$

$$= M_n \cos \phi_n \qquad \qquad (III-11)$$

Figures III-3, 4A show the distributions $f(M|z)$ of the modulus, $f(\cos \phi|z)$ for $\cos \phi$ and $f(P|z)$ for the scalar product of the PESE, and figures III-3, 4B the distributions $f(M)$, $f(\cos \phi)$ and $f(P)$ of the SE for two different units.

According to the Bayes relation we arrive at the predictors :

$$f(z|M) = \frac{f(M|z)}{f(M)} f(z) \qquad \qquad (III-12)$$

$$f(z|\cos \phi) = \frac{f(\cos \phi|z)}{f(\cos \phi)} f(z)$$

$$f(z|P) = \frac{f(P|z)}{f(P)} f(z)$$

These are shown in figures III-3, 4C. About these distributions a general remark must be made. As can be seen in figures III-3, 4B the SE distributions are Gaussian or approximately Gaussian. Although this theoretically means that all values for $\cos \phi$, M and P should occur, in a finite time duration there will be values that in practice do not occur in the stimulus and thus also cannot be present in the PESE. Therefore the sudden breakdown at the edges is due to lack of data. Furthermore it will be clear from figures III-3, 4A and B that the
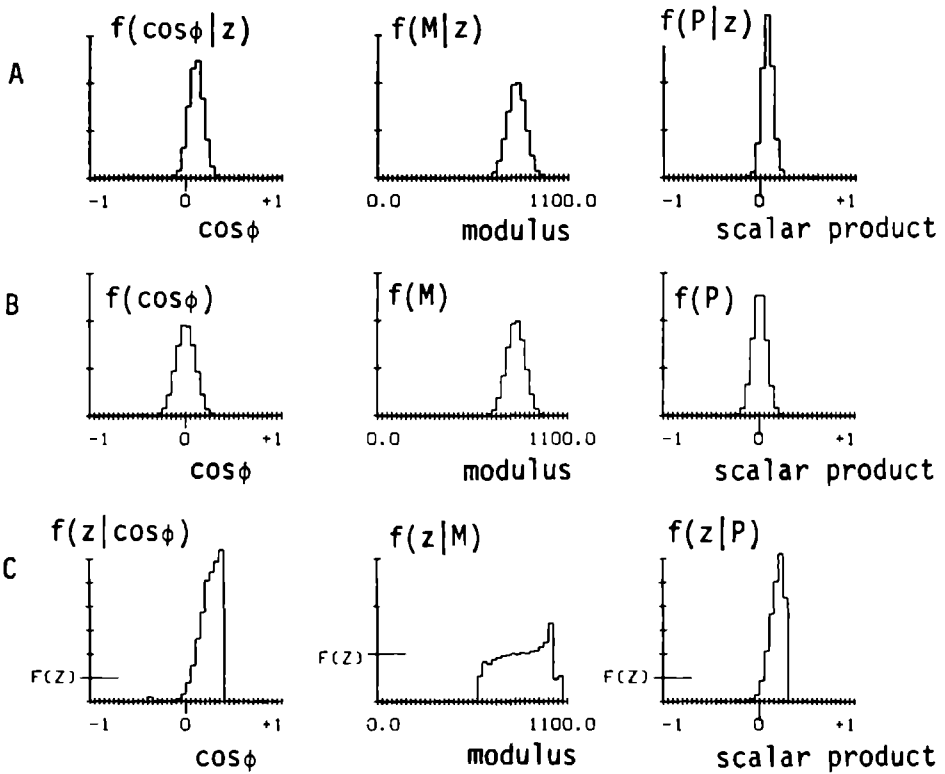
Fig. III-3 M-, cosφ- and scalar product distributions for unit 45-3.

      A PESE distributions

         $f(\cos\phi|z)$, $f(M|z)$, $f(P|z)$

      B SE distributions

         $f(\cos\phi)$, $f(M)$, $f(P)$

      C Normalized distributions or predictors

         $f(z|\cos\phi)$, $f(z|M)$, $f(z|P)$

         The mark $F(Z)$ indicates $f(z)$

      (figures along the modulus axis are arbitrary,

      +1 along the P-axis represents $(\cos\phi = 1)$ · (max. modulus))
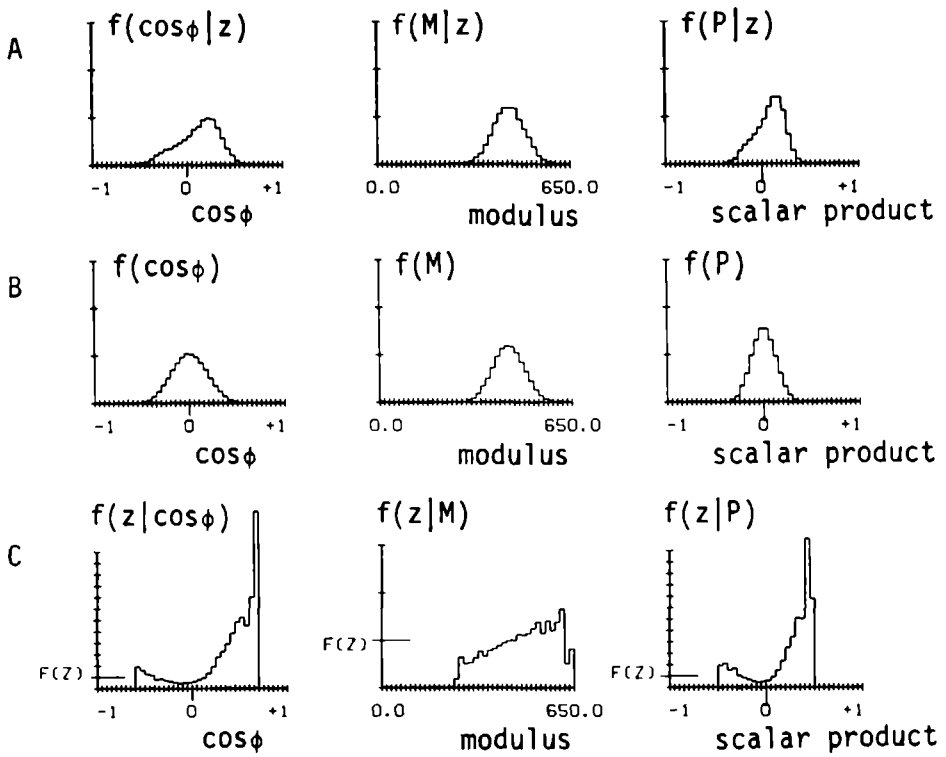
Fig. III-4   M-, cosφ- and scalar product distributions for unit 44-9
(see legend figure III-3)
The width of the figures of figure III-4 and figure III-3
differ because of a different dimensionality was used for
both units (N = 2WT, W = 5 kHz for both units   T = 100 msec.
for unit 45-3 and T = 30 msec. for unit 44-9).
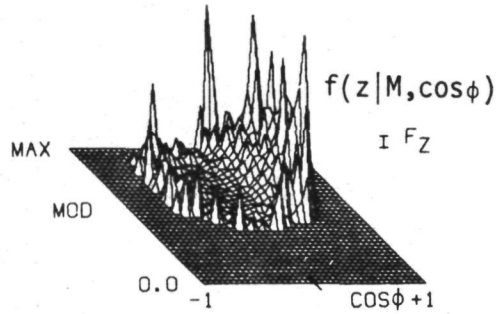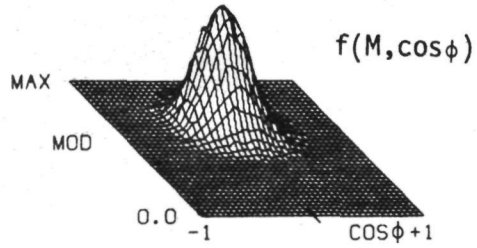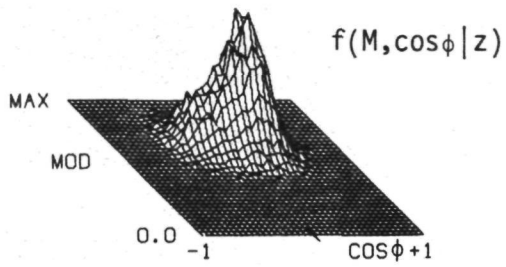
Fig. III-5   Combined M,cosφ-distributions for unit 44-9

    A   PESE distribution
    B   SE distribution
    C   normalized distribution or predictor

significance of figures III-3, 4C is decreasing toward the edges.

From figures III-3, 4C the following conclusions can be drawn.

1. The modulus M, so the energy E of the stimulus only slightly affects the probability of the generation of a spike, at least under this kind of stimulation (stationary noise), and in the observed modulus-range.

2. The similarity (cos ϕ) and the scalar product P = M cos ϕ are strongly affecting the probability of the occurrence of a spike.

At this point it may be worthwile to look in more detail into the interpretation of M, cos ϕ and P in terms of time signals.
The energy $E_n = M_n^2$ is merely the energy of the stimulus as it is presented to the ear, so an input property   The similarity $\rho_n = \cos \phi_n$ can also be interpreted as the correlation coefficient between $x_n(\tau)$ and $R(\tau)$ which is in fact a quantity indicating the similarity of two signals. When $\rho = 1$ the $x_n(\tau)$ and $R(\tau)$ have exactly the same form i.e. are identical apart from a multiplicative constant, whereas when $\rho = -1$ they are equal but opposite in sign. The multiplicative constant, as can be seen in equation (III-11), is the modulus M, so $P_n = M_n \cos \phi_n$ can be interpreted as the amount of $R(\tau)$ present in $x_n(\tau)$

For linear systems P_n would be the output at time t = t_n if the system has an impulse response R(τ), and an input signal x(t) is applied. The reason for this is that the output of a linear system can be found from the convolution of the input signal and the impulse response h(τ) as

$$y(t) = \int_0^T h(\tau) \, x(t-\tau) \, d\tau \qquad\qquad (III-13)$$

Now substituting $h(\tau) = \dfrac{R(\tau)}{|\vec{R}|}$ and t = t_n :

$$y(t_n) = P_n \qquad\qquad (III-14)$$

So in linear system theory P would be the important variable and not

45

the individual M and cos ϕ.

To see whether for our results, this also will be the case we will have to compare the P distributions with the simultaneous M,cos ϕ distributions (figure III-5). These are f(M,cosϕ|z) and f(M,cosϕ) resulting in

$$f(z|M,\cos\phi) = \frac{f(M,\cos\phi|z)}{f(M,\cos\phi)} \; f(z) \qquad\qquad (III-15)$$

Now we have to verify if

$$f(z|M,\cos\phi) = f(z|M\cdot\cos\phi) = f(z|P) \qquad\qquad (III-16)$$

No significant deviations from equation (III-16) were indeed observed in the obtained results, so we can focus on f(z|P) and leave the M,cosϕ-analysis.

It should be noted, however, that in the non-stationary situation the above result may not be achieved.

When we now turn our attention to the f(z|P) in figures III-3, 4C we observe that for unit 45-3 the probability of a spike increases for increasing positive P only (as far as we obtained P-values in the analysis), whereas for unit 44-9 the probability increases for increasing both positive and negative P. This will be explained in the following.

P-values that are equally large, but opposite in sign will be obtained for equal, but opposite x(τ), so when $x_1(\tau)$ = -$x_2(\tau)$ then P_1 = -P_2. We can think of $x_1(\tau)$ and $x_2(\tau)$ as identical waveforms, of which one is shifted in phase 180° with respect to the other over the whole frequency range.

While R(τ) indicates a narrow bandpass filter (cf. Chapter IV), we may think of the output of this filter as the relevant part of x(τ), being an oscillation of approximately one frequency (the characteristic frequency, CF). This means that 180° phaseshift has practically the same effect as a timeshift of one half of the period of the CF. It is well known that there is an uncertainty in the moment of the

occurrence of a spike, and this uncertainty can be explained in terms
of timejitter (loss of time lock) as well as in terms of phasejitter
(loss of phase lock). Both kinds of jitter, can be translated into
each other easily, and while the source of the jitter is not known we
will speak of phase-jitter $\Delta\psi$ in the following. It must be stated,
however, that all the effects that we will explain by some kind of
jitter, can equally well be explained by low-pass filter effects
(cf. the model of Johannesma, 1971). We now assume that the increase
of $f(z|P)$ for negative P is due to relevant, but jittered stimuli.
While, however, the jitter may be assumed to have a monomodal distribut-
ion around $\Delta\psi = 0^0$ ($\Delta\psi$ is defined with respect to the direction of $\vec{R}$),
there appears to be a discrepancy, in so far as the effects are only
(at least strongest) observed at $\Delta\psi = 180^0$ (note that $\llcorner\psi = 180^0$ for
an arbitrary but relevant stimulus gives rise to a P < 0 but not
necessary P = -1) and not at $\Delta\psi = 90^0$ which yields P = 0. We will
solve this discrepancy with an example. Assume that the stimulus x(t)
elicited 10100 spikes of which 100 $x_n(\tau)$ yielded a P = 0.5 when no jitter
was present. Now we assume a discrete jitter, so that 50 $x_n(\tau)$ have
a $\psi = 0^0$, 40 have a $\Delta\psi = \pm 90^0$ and 10 have a $\Lambda\psi = 180^0$ The remaining
x_n will be assumed to have the same P-distribution as the SE.
Now when P = 0.5 for $\Delta\psi = 0^0$, then P = -0.5 for $\Delta\psi = 180^0$, but for
$\Delta\psi = \pm 90^0$ P will be zero, because 90^0 phaseshift causes an orthogonal
vector which implicates a scalar product being zero (compare sine and
cosine, which are orthogonal). The P-distribution of the SE is
Gaussian with the mean at P = 0, and here P = 0 indicated that the
stimuli are uncorrelated with $R(\tau)$. Assume this SE-distribution to
have the following values :

$$f(P) = 0.005 \text{ for } P = \;\; 0.5$$
$$= 0.1 \quad \text{for } P = \;\; 0 \qquad\qquad\qquad (III-17)$$
$$= 0.005 \text{ for } P = -0.5$$

With the above assumptions this will result in a distribution of the
PESE as

$$f(P|z) = 0.005 \cdot 10^4 + 50 = \;\; 100 \quad \text{for } P = \;\; 0.5$$
$$= 0.1 \quad \cdot 10^4 + 40 = 1040 \quad \text{for } P = \;\; 0 \qquad (III-18)$$
$$= 0.005 \cdot 10^4 + 10 = \;\; 60 \quad \text{for } P = -0.5$$

So we get

$$\frac{f(z|P)}{f(z)} = \frac{f(P|z)}{f(P)}$$

$$= \frac{100}{0.005} = 2 \quad \cdot 10^4 \qquad \text{for } P = 0.5$$

$$= \frac{1040}{0.1} = 1.04 \cdot 10^4 \qquad \text{for } P = 0 \qquad (III-19)$$

$$= \frac{60}{0.005} = 1.2 \cdot 10^4 \qquad \text{for } P = -0.5$$

This result is roughly comparable with the result in figure III-4C.
It is clear now that the apparent discrepancy is caused by the fact
that the P = 0 values originating from a $\Delta\psi = \pm 90^o$ are drowned in the
P = 0 values originating from uncorrelated stimuli.
The contaminating effect caused by these uncorrelated stimuli does of
course not only affect the P = 0 results, but also the other ones, so
the f(z|P) picture is a disturbed one. To bring these disturbances into
account, we shall have to extend the analysis.

III.2.3.2 P,Q-analysis

To solve the problems that arose in the previous paragraph we need to
have a possibility to discriminate between the correlation and the
phaseshifting contributions to the specific P-values. When we again
focus on P = 0, we observe that the problem in fact was the large amount
of uncorrelated stimuli yielding P = 0. This amount is so large
because of the many orthogonal $x_n(\tau)$ which in turn is due to the high
dimensionality of the signal space. In a 2WT dimensional space there
are 2WT-1 orthogonal directions with respect to $\vec{R}$ and the case for
which $\Delta\psi = 90^o$, is only one direction out of the 2WT-1.
From the above considerations it is clear that we must give more
attention to the special direction for which $\Delta\psi = 90^o$ than to the
other 2WT-2 directions.
Therefore we now introduce the second, special direction, orthogonal
to R(τ) and being the 90° phaseshift of R(τ), denoted as $\tilde{R}(\tau)$ and then

48

attention will be given to the two-dimensional plane spanned by $\vec{R}$ and $\tilde{R}$, because a phaseshift of $\Delta\psi^{0}$ in the relevant part $y(t)$ of the stimulus $x(t)$, is equivalent to a rotation over $\Delta\psi^{0}$ in the $(\vec{R},\tilde{R})$ plane. The equivalence of a $\Delta\psi$ phaseshift in the time signal and a $\Delta\psi$ rotation in the $(\vec{R},\tilde{R})$ plane can be illustrated with the following example. When $\vec{R} = A(t) \sin \omega t$ and $\tilde{R} = A(t) \cos \omega t$, then

$$A(t) \sin (\omega t + \Delta\psi) = A(t) \{\sin \omega t \cos \Delta\psi + \cos \omega t \sin \Delta\psi\}$$

$$= \vec{R} \cos \Delta\psi + \tilde{R} \sin \Delta\psi \qquad \text{(III-20)}$$

Indeed equation (III-20) is a rotation of $\Delta\psi$ in the $(\overset{\circ}{R},\tilde{R})$ plane.

So now the relevant part of the stimulus $x(t)$ is supposed to be represented by the projection on the $(\vec{R},\tilde{R})$ plane.
The $\tilde{R}$ that we seek, must meet the following conditions

1. $\vec{R}$ and $\tilde{R}$ must be orthogonal

$$\vec{R} \cdot \tilde{R} = 0 \qquad \text{(III-21)}$$

   or

$$\int_{0}^{T} R(\tau) \, \tilde{R}(\tau) \, d\tau = 0$$

2. $\tilde{R}(\tau)$ must be the same as $R(\tau)$ apart from a phaseshift of 90^{0}.

These conditions are met by the Hilberttransform of $R(\tau)$ defined as (Deutsch, 1969)

$$\tilde{R}(\tau') = \frac{1}{\pi} \fint_{-\infty}^{\infty} \frac{R(\tau)}{\tau'-\tau} \, d\tau \qquad \text{(III-22)}$$

where the symbol $\fint$ stands for the Cauchy principle value.

Now $\tilde{R}(\tau)$ has the same time envelope as $R(\tau)$, and the same amplitude spectrum, but their phase spectra differ 90^{0} over the whole frequency range. $\tilde{R}(\tau)$ is often referred to as the quadrature signal of $R(\tau)$. $\tilde{R}(\tau)$ can be computed easily according to the following flow scheme (see also Chapter IV)

$$R(\tau) \xrightarrow{\quad F \quad} \hat{R}(\omega) \xrightarrow{\quad \epsilon \quad} \hat{\rho}(\omega) \xrightarrow{\quad F^{-1} \quad} \rho(\tau)$$
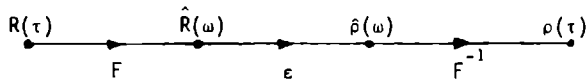
where F = fast fourier transform

$\hat{R}(\omega)$ = complex spectrum of $R(\tau)$

ϵ denotes $\epsilon(y) = 2y \quad y > 0$

$\qquad\qquad \epsilon(y) = y \quad y = 0$

$\qquad\qquad \epsilon(y) = 0 \quad y < 0$

$\hat{\rho}(\omega)$ = complex spectrum of $\rho(\tau)$

$\rho(\tau) = R(\tau) + i \, \tilde{R}(\tau)$

$\rho(\tau)$ is called the pre-envelope of $R(\tau)$ and is an analytic signal of which the imaginary part is the quadrature signal of the real part.

Now we have defined a two dimensional plane, and the analysis will be extended to the relation of $\vec{x}_n$ to this plane. Therefore we define the projection of $\vec{x}_n$ on $\vec{R}$ as before (equation (III-11))

$$P_n = \frac{\vec{x}_n \cdot \vec{R}}{|\vec{R}|} \tag{III-11}$$

but also the projection of $\vec{x}_n$ on $\overset{\rightthreetimes}{R}$

$$Q_n = \frac{\vec{x}_n \cdot \overset{\rightthreetimes}{R}}{|\overset{\rightthreetimes}{R}|} \tag{III-23}$$

and while

$$|\vec{R}| = |\overset{\rightthreetimes}{R}|$$

$$Q_n = \frac{\vec{x}_n \cdot \overset{\rightthreetimes}{R}}{|\vec{R}|} \tag{III-24}$$

$$= \frac{1}{|\vec{R}|} \int_0^T x_n(\tau) \, \tilde{R}(\tau) \, d\tau$$

The projection of the modulus on the $(\vec{R}, \overset{\rightthreetimes}{R})$plane then is

$$M_{PQ,n} = (P_n^2 + Q_n^2)^{\frac{1}{2}} \tag{III-25}$$

50

In the system theoretical point of view $E_{PQ,n} = M^2_{PQ,n}$ is the intensity of the output at $t = t_n$ of a linear filter with impulse response $R(\tau)$ when a stimulus $x(t)$ is applied (cf. Deutsch, 1969), so it can be interpreted as that part of the energy that is passed through the filter.

The total energy of the stimulus $x_n(\tau)$ is equal to

$$E_{T,n} = M^2_n$$ (equation (III-9)), so the energy that did not pass

the filter E_R (the remaining part of the energy) is

$$E_{R,n} = E_{T,n} - E_{PQ,n} \tag{III-26}$$

In terms of the signal space, the modulus of the remaining vector $(\dot{x}_n - $ (projection of $\vec{x}_n$ on the $(\vec{R}, \overset{\tau}{R})$ plane)) is

$$M_{R,n} = (M^2_n - M^2_{PQ,n})^{\frac{1}{2}} \tag{III-27}$$

For every pre-event stimulus $x_n(\tau)$ we thus compute P, Q, E_{PQ}, E_T and E_R according to the following scheme
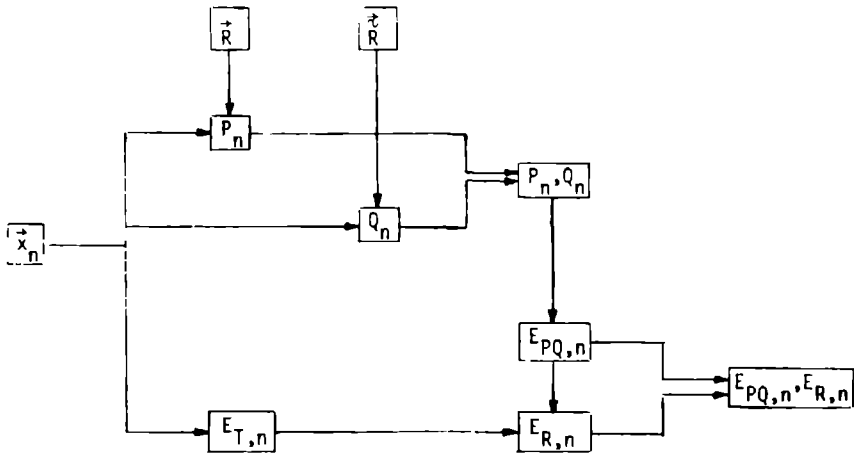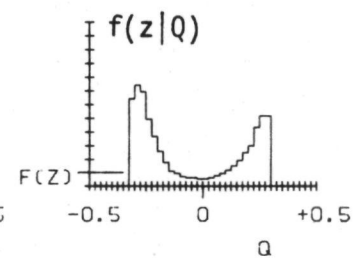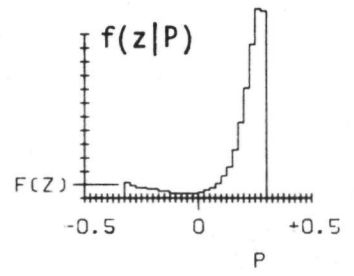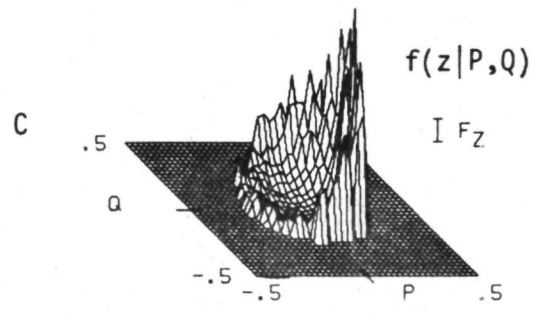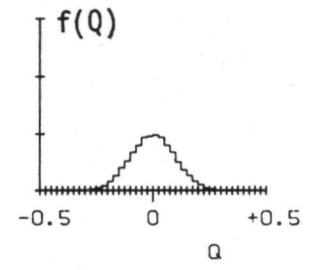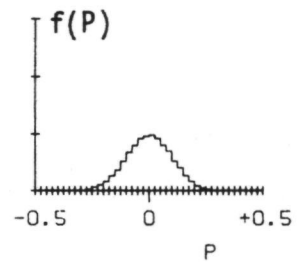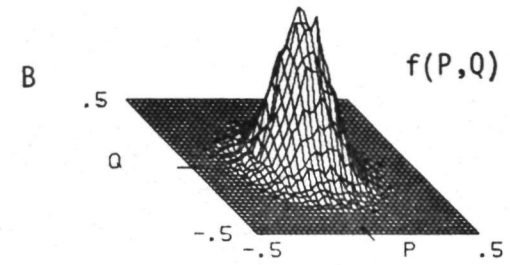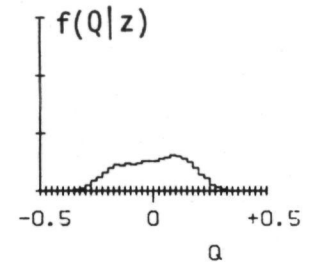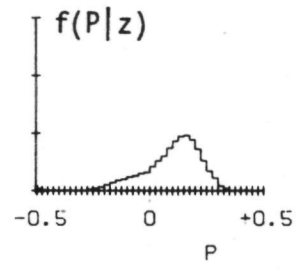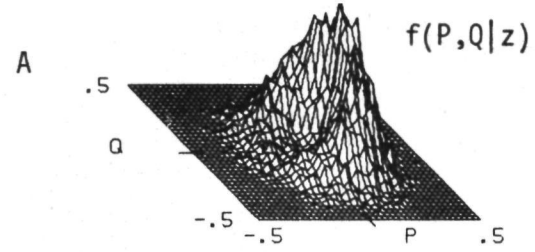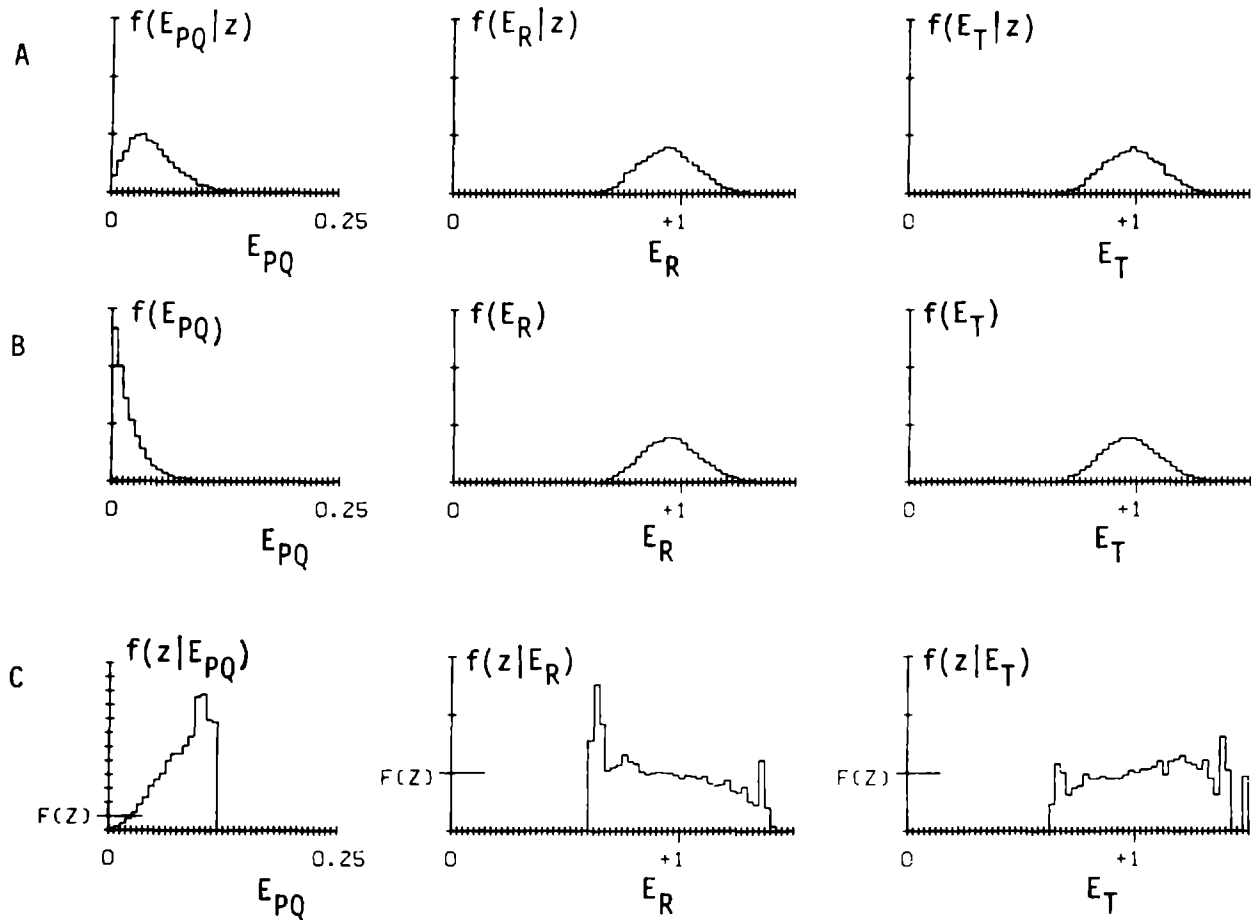
Fig. III-6 Distributions for unit 52-7

A PESE distributions
B SE distributions
C normalized distributions or predictors (F(Z) = f(z))
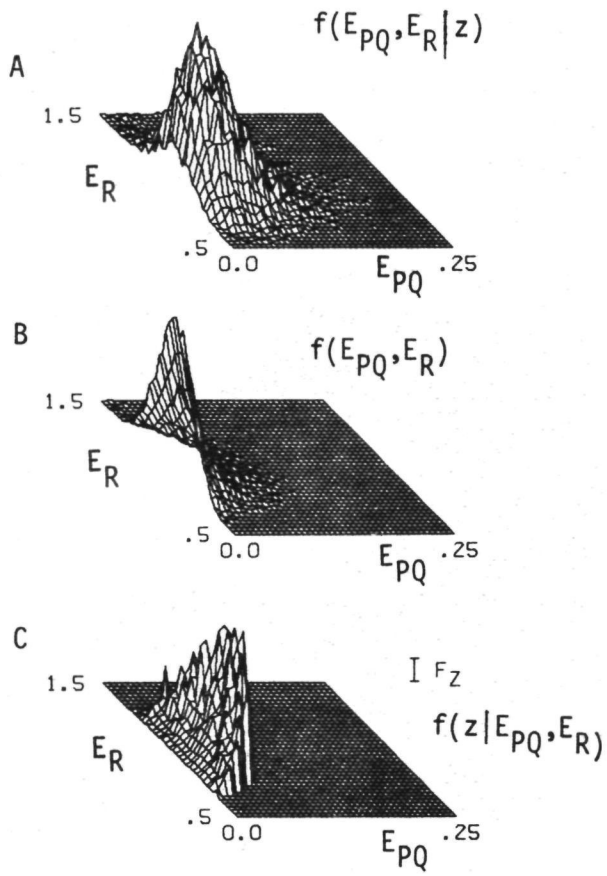
Fig. III-7 E_{PQ} - E_R distributions for unit 52-7

    A PESE distribution
    B SE distribution
    C normalized distribution ($F_Z = f(z)$)

54

In this way the PESE-distributions

$$f(P|z), \quad f(Q|z), \quad f(E_{PQ}|z), \quad f(E_R|z) \quad \text{and} \quad f(E_T|z)$$

are obtained and the combined distributions

$$f(P,Q|z) \quad \text{and} \quad f(E_{PQ},E_R|z)$$

(Note that $f(P|z)$ and $f(Q|z)$ are the marginal distributions of $f(P,Q|z)$ and $f(E_{PQ}|z)$ and $f(E_R|z)$ are the marginal distributions of $f(E_{PQ},E_R|z)$).

For the SE analogously the distributions are made up for $f(P)$, $f(Q)$, $f(P,Q)$, $f(E_{PQ})$, $f(E_R)$, $f(E_T)$ and $f(E_{PQ},E_R)$.

Applying the Bayes relation to each corresponding pair we arrive at

$$f(z|P,Q) \quad = \quad \frac{f(P,Q|z)}{f(P,Q)} \quad f(z)$$

$$f(z|P) \quad = \quad \frac{f(P|z)}{f(P)} \quad f(z)$$

$$f(z|Q) \quad = \quad \frac{f(Q|z)}{f(Q)} \quad f(z) \qquad\qquad \text{(III-28)}$$

$$f(z|E_{PQ}) \quad = \quad \frac{f(E_{PQ}|z)}{f(E_{PQ})} \quad f(z)$$

$$f(z|E_R) \quad = \quad \frac{f(E_R|z)}{f(E_R)} \quad f(z)$$

$$f(z|E_T) \quad = \quad \frac{f(E_T|z)}{f(E_T)} \quad f(z)$$

and

$$f(z|E_{PQ},E_R) = \frac{f(E_{PQ},E_R|z)}{f(E_{PQ},E_R)} \quad f(z) \qquad\qquad \text{(III-29)}$$

Note that now $f(z|P)$ and $f(z|Q)$ are no longer the marginal distributions of $f(z|P,Q)$ and $f(z|E_{PQ})$ and $f(z|E_R)$ are no longer the marginal

distributions of $f(z|E_{PQ},E_R)$.
In figure III-6 and figure III-7 all the distributions mentioned above
are shown for unit 52-7.

From figure III-6 it is clear that the problem we had in III.2.3.1 for
$f(z|P)$ around $P = 0$ is also present in $f(z|Q)$ for $Q = 0$, as could be
expected. In the twodimensional $f(z|P,Q)$, however, a clear distinction
can be made between uncorrelated stimuli ($P = 0$ and $Q = 0$) and relevant
but shifted stimuli (e.g. $P = 0$ and $Q \neq 0$). The symmetrical shape of
$f(z|Q)$ indicates that the distribution of deviations from $P = 0$
(distribution of $\Delta\psi$) is a regular symmetric one.
$f(z|E_{PQ})$ predicts the response of the neuron to the intensity of the
relevant stimulus. It can be interpreted as a local dynamic response
(local because the stimulus itself is stationary, and therefore the E_{PQ}
range is limited) $f(z|E_{PQ})$ is dependent on the stimulus intensity, cf.
figure III-17 and figure III-19.

$f(z|E_T)$ gives the response to the total stimulus intensity and is much
less salient than $f(z|E_{PQ})$, because in E_T also the non-relevant part of
the stimulus is present.

$f(z|E_R)$ predicts the response to the non-relevant part of the stimulus
and thus should be independent of E_R. So possibly there is an
indication to what extend the P,Q-analysis is a complete functional
description in the course of $f(z|E_R)$. E.g. an increasing $f(z|E_R)$ for
increasing E_R indicates that E_R positively influences the probability
for the occurrence of a spike signifying that there are relevant
stimuli not represented by $R(\tau)$. On the other hand, a decreasing $f(z|E_R)$
might indicate that stimuli not represented by $R(\tau)$ are inhibiting the
spike probability.
However, a decreasing $f(z|E_R)$ might also be found when E_R and E_{PQ} are
not independent (and in fact E_R and E_{PQ} are dependent through
$E_{PQ} + E_R = E_T$). So the interpretation of a decreasing $f(z|E_R)$ is not
unique.

In the combined $f(z|E_{PQ},E_R)$ distribution the dependence of E_{PQ} and E_R
is not a problem while for every E_{PQ} the course of $f(z|E_R)$ can be
observed (figure III-7). While, however, the most significant part of
the $f(z|E_{PQ},E_R)$ distribution lies in the range where $f(z|E_{PQ},E_R)$ is very
small no definite conclusions can be drawn so far. Possibly a more
detailed study may yield clearer results.

$f(z|P,Q)$ is the most important predictor we arrived at. It predicts in
detail the responses for stationary complex stimuli and possibly also
for other stimuli. It should also be noted that the distributions for
P, Q and E_{PQ} can be derived from the P,Q distributions. That the
P,Q-analysis describes reasonably well the functional properties of a
lot of neurons is affirmed by comparing the prediction results and the
responses recorded from the animal (cf. Chapters III.2.4 and III.3.2
where these comparisons are made).

III.2.4   Prediction algorithms and functional description

In the previous paragraphs we arrived at three different predictors

1. $\prod_1 f(z|x_1)$ (III-6)

2. $f(z|P)$ (III-12)
3. $f(z|P,Q)$ (III-28)

In this paragraph we will compare these predictions and the underlying
functional descriptions.

When we first turn our attention to linear system theory, it is well
known that when the impulse response of a linear system is known, the
output of the filter can be found by the convolution of the input signal
and the impulse response. When we assume $R(\tau)$ to be the impulse response
of the peripheral auditory system, the output of the system, applying
a stimulus $x(t)$ would be

$$y(t) = \frac{1}{|\vec{R}|} \int_0^\infty R(\tau)\ x(t-\tau)\ d\tau = P(t)$$ (III-30)
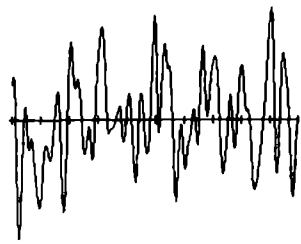
A stimulus
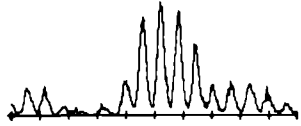
B experimental PSTH
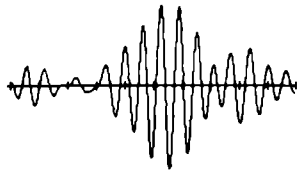
C convolution
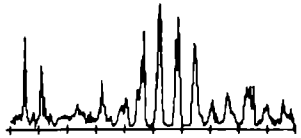
D prediction $\prod f(z|x_i)$
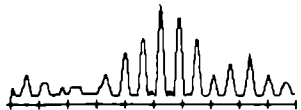
E prediction $f(z|P)$
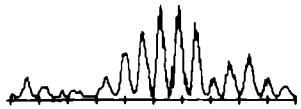
F prediction $f(z|P,Q)$

0   5   MSEC

Fig. III-8   Stimulus, recorded PSTH and several predictions for
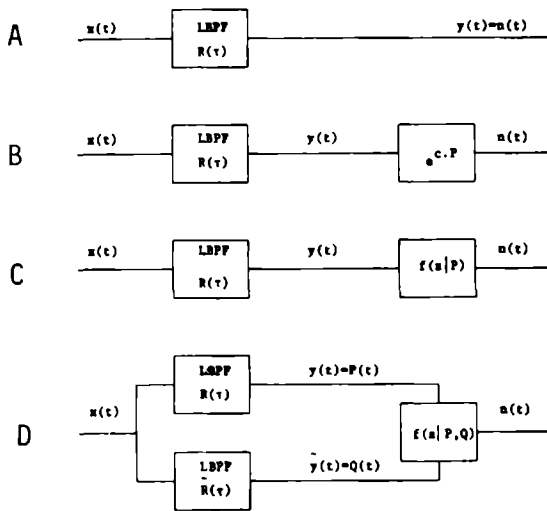   unit 65-2.

Fig. III-9 Functional models representing the prediction algorithms.
The input to each model is the stimulus $x(t)$, the output
the event density or PSTH $n(t)$.

A   a linear bandpass filter (LBPF) with impulse response $R(\tau)$,
$n(t) = y(t)$ is the convolution of $x(t)$ and $R(\tau)$

B   a linear bandpass filter ($y(t) = P(t)$) followed by an
exponentiator representing the $\prod_i f(z|x_i)$ predictor

C   a linear bandpass filter ($y(t) = P(t)$) followed by the
nonlinearity $f(z|P)$

D   two parallel bandpass filters with impulse responses
$R(\tau)$ and $\tilde{R}(\tau)$ followed by the nonlinearity $f(z|P,Q)$

This in fact is also a predictor for the response of a neuron (see also
de Jongh, 1972).

Figure III-8A shows the input $x(t)$, a short pseudonoise of 5.11 msec
duration, and figure III-8C the $y(t)$, computed according to equation
(III-30). Figure III-8B is the PSTH recorded from the cat (unit 65-2)
for the same stimulus repeated continuously. The predictor III-30 can
be replaced by the model in figure III-9A.

The predictor we arrived at in Chapter III.2.2 was

$$\prod_{i} \frac{f(z|x_i)}{f(z)} \tag{III-6}$$

The product was a consequence of the superposition of independent
probabilities. As already mentioned in Chapter III.2 for linear systems
the superposition of independent contributions is a summation or
integration.

Furthermore the courses of the individual $\dfrac{f(z|x_i)}{f(z)}$ seem to be
exponential.

We thus try

$$\frac{f(z|x_i)}{f(z)} = \exp \{g_i(x)\} \tag{III-31}$$

where $g_i(x)$ is an arbitrary function of x_i.

Then

$$g_i(x) = \ln \frac{f(z|x_i)}{f(z)} \tag{III-32}$$

and

$$\prod_{i} \frac{f(z|x_i)}{f(z)} = \exp \{\sum_{i} g_i(x)\} \tag{III-33}$$

Experimentally it appears that the $g_i(x)$ are all approximately linear
functions of x, with a proportionality factor varying with i

$$g_i(x) = c_i x_i \tag{III-34}$$

and it appears futhermore that for different i c_i is proportional to $R(\tau_i)$

$$c_i = c' \, R(\tau_i) \qquad\qquad\qquad\qquad \text{(III-35)}$$

so

$$g_i(x) = c' \, x_i R(\tau_i) \qquad\qquad\qquad\qquad \text{(III-36)}$$

Substituting into equation (III-33) we arrive at

$$\prod_i \frac{f(z|x_i)}{f(z)} \;=\; \exp\{\textstyle\sum_i c' \, x_i R(\tau_i)\}$$

$$= \exp c' \, \vec{x}\cdot\vec{R}$$

and with

$$P = \frac{\vec{x}\cdot\vec{R}}{|\vec{R}|} \qquad\qquad\qquad\qquad \text{(III-11)}$$

$$\prod_i \frac{f(z|x_i)}{f(z)} \;=\; \exp c' \, P|\vec{R}| \qquad\qquad \text{(III-37)}$$

$$= \exp cP$$

The experimental evidence for the derivation above is illustrated in figure III-10 where for several i are shown

$$f(z|x_i) \quad \text{and} \quad \frac{\ln \dfrac{f(z|x_i)}{f(z)}}{R(\tau_i)} \quad \text{and the average over } i \text{ of the last one.}$$

We thus arrived at the conclusion that because of the experimental evidence the predictor (III-6) may be functionally separated into a linear part (linear bandpass filter) with impulse response $R(\tau)$ and an algebraic non-linearity e^{cP} as shown in figure III-9B.

Figure III-8D shows the result of the predictor with equation (III-6) for the short pseudonoise of figure III-8A.

The predictor arrived at in Chapter III.2.3.1 was

$$f(z|P) \qquad\qquad\qquad\qquad \text{(III-12)}$$
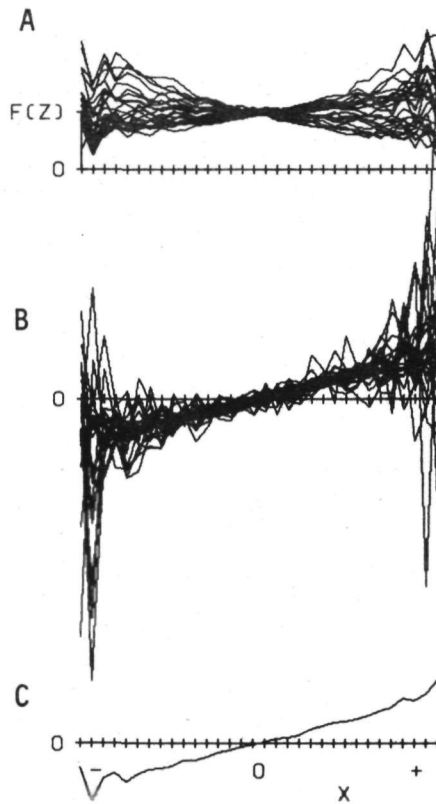
Fig. III-10 A $f(z|x_i)$ for several τ_i

$$ B \quad \frac{\ln \dfrac{f(z|x_i)}{f(x)}}{R(\tau_i)} $$

C   average over i of figure B

Fig. C approximates a straight line indicating that

$$ \prod_i \frac{f(z|x_i)}{f(z)} = \exp\{cP\} $$

The result of this predictor is shown in figure III-8E and equation (III-12) can be represented by figure III-9C.

The last predictor we found was

$$f(z|P,Q) \tag{III-28}$$

which resulted in the predicted PSTH of figure III-8F and is represented in figure III-9D.

Comparing the four predictions the following remarks can be made.
The first prediction, the convolution, does not reckon with any non-linearity, so that even negative values occur, which is certainly wrong.
The second prediction is an extension of the first one, through the addition of an exponentiator. This is an improved predictor, but it has the disadvantage that the form of the non-linearity is a fixed one (exponential) resulting in the average firing rate $f(z)$ for $P = 0$, i.e. a lot of spikes for possibly non-relevant stimuli.
The third prediction, having an experimentally determined non-linearity, sometimes shows proper predictions, namely when there is a perfect time lock between relevant stimulus and elicited event. However, parts of the predictions deteriorate when the time lock becomes worse, (around $P = 0$ no longer distinction can be made between relevant and non-relevant stimuli).
The fourth predictor $f(z|P,Q)$ is, as can be seen in figure III-8F, by far the best one, as it resembles the experimentally recorded PSTH (figure III-8B) in detail. This indicates that over the entire P,Q range the prediction is correct and no systematic deviations are found. Therefore it can be stated that (apart from higher order effects as adaptation and refractoriness) the P,Q-analysis gives a proper functional description of the spike generation of (at least a number of) neurons.

So far, we assumed the crosscorrelation procedure to result in a
non-zero $R(\tau)$, with which our structure analysis could be started.
When, however, the center of mass of the PESE coincides with the origin,
the analysis cannot be started. But we now know that for the P,Q-
analysis, we only require some point of the $(\vec{R},\vec{R})$ plane, apart from the
origin, because when one point is defined, a second can be found through
the Hilberttransformation, and the whole plane is determinded.
Therefore, when $R(\tau)$ is identical zero, the problem is to find one point
of the $(\vec{R},\vec{R})$ plane. From the results obtained with the P,Q-analysis
for low frequency units it can be assumed that the disappearance of
$R(\tau)$ can be due to jitter or low-pass filter effects (cf. Chapter
III.2.3.1).
Therefore, we developed a procedure (see appendix I) in which we tried
to neutralize these effects and to shift the spikes to the moments at
which a non-zero crosscorrelation function can be obtained (the
shifting procedure).
With the shifted spikes a function $R_1(\tau)$ was obtained of which we
assumed that it indeed represented some point in the $(\vec{R},\vec{R})$ plane, and
from which we could start the P,Q-analysis.
The correctness of the assumptions underlying the shifting procedure
and the relevance of $R_1(\tau)$ will be proven by the results of the P,Q-
analysis and the comparison of predicted and recorded PSTH's.
Figures III-24, 25 and 26 show the $R(\tau)$, the $R_1(\tau)$, $f(z|P,Q)$, $f(z|E_{PQ})$
and a predicted and recorded PSTH for 3 units.
From these results we conclude that :

1. The shifting procedure can be used and yields the proper result, at
   least for a number of neurons.
2. The P,Q-analysis also holds true for high frequency units, having an
   $R(\tau) \equiv 0$.

Refering to figures III-24, 25 and 26 two remarks must be made.

1. Because the center of mass coincides with the origin $(R(\tau) \_ 0)$, a

point-symmetrical shape of $f(z|P,Q)$ with respect to the origin must be expected. The rotation-symmetrical shape indicates that indeed jitter- or lowpass filter effects may cause the deterioration and disappearance of $R(\tau)$.

2. The rotation symmetrical shape implicates that $f(z|P,Q)$ contains the same information as $f(z|E_{PQ})$ so the probability for the generation of spikes only depends on the energy of the stimulus in the relevant frequency region. Therefore, the analysis concerning the complex energy density, introduced in Chapter II, is a rational extension of the P,Q-analysis.

III 3   APPLICATIONS

III.3.1   Experimental methods

About the experimental methods only a few remarks will be made. For a complete description we refer to van Gisbergen (1974). We also refer to Chapter IV 2 where a brief description is given.

The stimulus given to the cat was a pseudonoise with an upper frequency of 5 kHz or 15 kHz, depending on the frequency of the unit. The intensity of the stimulus was in general chosen 20 dB above the intensity at which a response could be heard.
The intensities that are mentioned in the following pages are in dB with reference to the maximum sound pressure that could be reached in our acoustic system, i.e. about 80 dB SPL (see van Gisbergen, 1974). The predictions were verified for stimuli which were short pseudonoise sequences (cf. figure III-8) Sometimes a small timeshift can be observed between the predicted and the experimental PSTH. In general this shift does not exceed 0.1 msec, and timeshifts of this order can be attributed to differences in the level setting of the level discriminator in which the spikes are converted to unit pulses.
On average the positive slope of the spike has a duration of 0.3 to 0.4 msec, so a different setting of the level in different experiments

for the same unit can cause a systematic timeshift of the order of 0.1 msec.

Results and comparisons

Because of the diverging results obtained for e.g. $f(z|P,Q)$ and $f(z|E_{PQ})$ it is not possible at this moment to present an integral view on the results obtained in the cochlear nuclei of the cat.

Therefore, the results of several neurons are given individually and briefly commented on and only sometimes comparisons are made with other kinds of experiments (cf. van Gisbergen, 1974).
The PESE analysis was performed for 25 neurons, of which one was stimulated at three different intensities and one at four different intensities.
8 units were possibly auditory nerve fibers (but fibers anyhow) of which 3 are given on the following pages. 11 units were ventral cochlear nucleus units of which 7 gave a non-zero $R(\tau)$. The other 4 were successfully treated with the shifting procedure. Of these 7 resp. 4, the results for 4 resp. 3 units are given. 6 units were dorsal cochlear nucleus units, of which 2 gave a non-zero $R(\tau)$. For the remaining 4 the shifting procedure was successful for 2 units. Of these units the results of one are given.

Concerning the predictions some general remarks must be made.
The predictions are predictions of the probability of the occurrence of an action potential, so the result always is and only can be the expected value of the number of spikes, i e. the event density or PSTH.

The predictors (and $R(\tau)$) are derived from complex stimuli (Gaussian white noise). This implies that the prediction is in general the best one for any arbitrary stimulus, but that no specific details will be predicted for some specific stimulus.

66

This means that for every specific stimulus (like the short pseudonoise used) a better, more specific predictor can be derived, but this will be a worse one for any other stimulus.

Also special effects like adaptation and refractoriness will not appear in the predictions.

The results presented in the following pages are organised in the same way for all neurons. When no result was obtained (e.g. no PSTH to compare with the prediction) or the result was irrelevant (signal distribution when $R(\tau)$ was identical zero) its place is left blank.

The picture representing the results are to be read as indicated on the next pages. The column on the right pages gives some data for the unit.

Because the pictures on the left pages are computer drawings, only capital letters could be used. Therefore, e.g. F_Z should be read as $f(z)$.

R(τ), crosscorrelation function
magnified to equal amplitude
(except when R(τ) $\sim$ 0)

$\hat{R}$(f), spectral envelope of
R(τ)

weighted R(τ)
or function used for P,Q-analysis

weighted $\hat{R}$(f)
spectrum of weighted R(τ)

predictor set
$f(z|x_1)$
cf. equation (III-5)
bar indicates $F_z \equiv f(z)$
= mean firing rate
X-axis ranging from -3σ to $+3\sigma$

predictor
$f(z|P,Q)$
cf. equation (III-28)
bar indicates $F_z \equiv f(z)$
= mean firing rate
values along the axes are
normalised to stimulus
intensity unity $(\sigma^2 = 1)$

$f(z|E_{PQ})$ $f(z|E_R)$ $f(z|E_T)$
cf. equations (III-28)
vertical axis in multiples of $f(z)$ = mean firing rate
horizontal axis normalised to stimulus intensity unity $(\sigma^2 = 1)$

experimental PSTH   experimental PSTH   predicted PSTH
                           and predicted PSTH
              normalised to equal number of spikes

explanation of following pages

		this column can be folded out on page 103	figures of unit 54-4
		unit number	54-4
AN(?) possibly auditory nerve fiber VCN ventral cochlear nucleus DCN dorsal cochlear nucleus		location	AN(?)
spontaneous activity in spikes/sec		spont act sp/sec	65
lowest threshold at CF in dB determined from IFS		CF threshold dB	-48
Bandwidth noise stimulus 0-5000 or 0-15000 Hz		upper limit noise	5000
intensity of noise stimulus in dB		intens. noise dB	-10
number of spikes recorded during stimulus		number of spikes	14708
mean firing rate during stimulus spikes/sec		$F_z = f(z)$ sp/sec	78
modulus of $R(\tau) \equiv \|\vec{R}\|$ (equal to $\sqrt{E}$ of chapter IV)		$\|\vec{R}\| = \sqrt{E}$	0.120
cf. Chapter IV	mean of spectral envelope	μ_f kHz	1.51
	standard deviation of spectral envelope	σ_f kHz	0.10
	mean of time envelope	μ_τ msec	5.71
	standard deviation of time envelope	σ_τ msec	1.65
	$\sigma_\omega \sigma_\tau = 2\pi \sigma_f \sigma_\tau$	$\Delta = \sigma_\omega \sigma_\tau$	1.08
quotient of mean values of $E_{PQ}\|z$ and E_{PQ}		$\overline{E_{PQ}\|z}/\overline{E_{PQ}}$	1.515
$E_R\|z$ and E_R		$\overline{E_R\|z}/\overline{E_R}$	0.996
$E_T\|z$ and E_T		$\overline{E_T\|z}/\overline{E_T}$	1.006
number of spikes predicted in PSTH per stimulus		N spikes pred.	0.39
" " " of experimental PSTH per "		N spikes rec.	0.38
quotient of the quantities above		$\dfrac{\text{N pred.}}{\text{N rec.}}$	1.03
time shift of pred. PSTH $\leftrightarrow$ exper. PSTH in msec		time shift pred.	0.08

explanation of following pages

20.00
MSEC

0

6250
HERZ

← TAU

20.00
MSEC

0

6250
HERZ

2.50
MSEC

UNIT 54- 4

F_Z I

TAU

+0.5

I F_Z

Q

−0.5

12.50
MSEC

−0.5

P

+0.5

−   X   +

F_Z

0   E_{PQ} .25

F_Z

0   E_R 1.0

F_Z

0   E_T 1.0

0   EXP   5   0   EXP AND PRED   5   0   PRED   5
MSEC
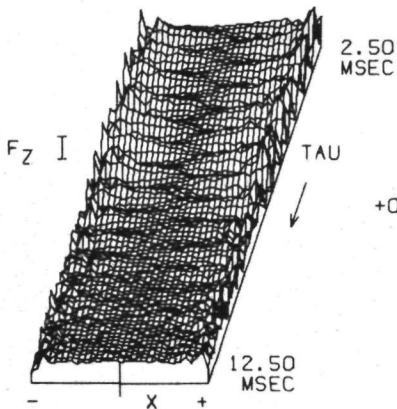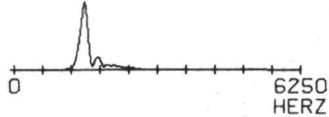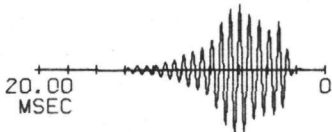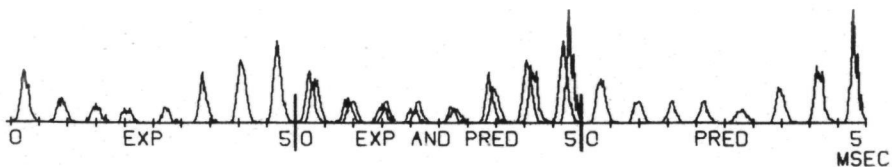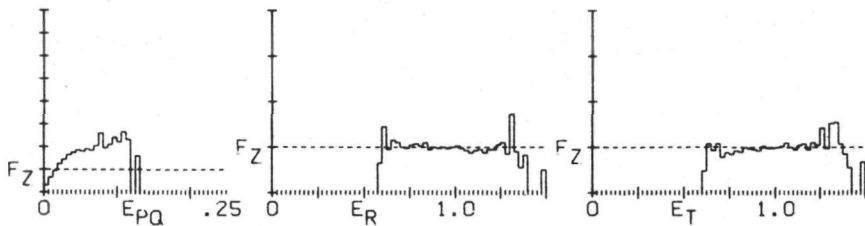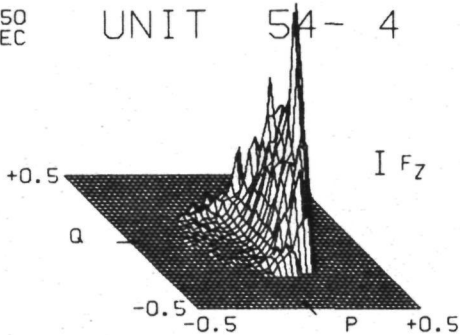
The PSTH's shown on the right
side of this page are those
for positive clicks and negative
clicks, and the compound PSTH
(cf. III-1). The resemblence
with $R(\tau)$ is striking,
confirming the functional
models of figure III-9.
The interrupted line in the
compound PSTH is the envelope
of $R(\tau)$.
The average firing rate during
click stimulation was about
two spikes per stimulus.
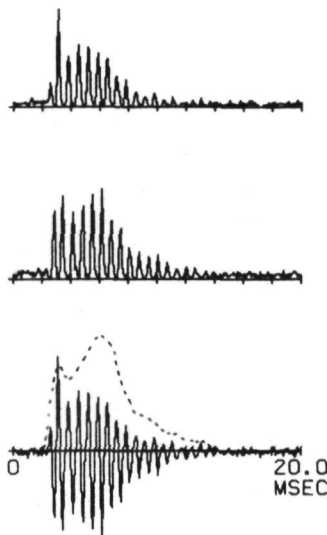
54-4

AN(?)

65

-48

5000

-10

14708

78

0.120

1.51

0.10

5.71

Comparing the figures for $f(z|P,Q)$ and $f(z|E_{PQ})$, one could say
that for this neuron (AN(?)) the most important response to a
stimulus is not an increase in the firing rate but a time
locking to the relevant stimulus (synchronisation).

1.65

1.08

The timeshift of the predicted PSTH with respect to the
experimental PSTH is so small that it can be ignored (cf.
Chapter III.2.1).

1.515

0.996

1.006

0.39

0.38

1.03

0.08
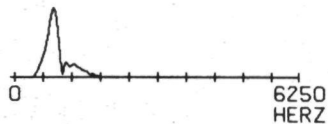
Fig. III-11   for explanation of figures see pages 68 and 69

71

Although R(τ) of this neuron (fiber) is very different from
that of unit 54-4 (previous figure) the several predictors
look very much alike.

Note the weak dependence of $f(z|E_{PQ})$, $f(z|E_R)$ and $f(z|E_T)$
on their arguments and the independence of $f(z|P,Q)$ on Q.

The mentioned weak dependences seem to be a property for most
auditory nerve fibers.

59-5

AN(?)

55

-80

5000

-40

12126

105

0.117

1.38

0.17

3.73

0.74

0.79

1.425

0.992

1.001

1.03

1.03

1.00

0.08

Fig. III-12   for explanation of figures see pages 68 and 69

20.00 MSEC

0

6250 HERZ

← TAU

20.00 MSEC

0

6250 HERZ

0.50 MSEC

UNIT   59- 5

F_Z I

TAU

I F_Z

+0.5

Q

-0.5
-0.5

P

+0.5

10.50 MSEC

−   X   +

Z

0   E_{PQ} .25

F_Z

0   E_R 1.0

F_Z

0   E_T 1.0

0   EXP   10 0   EXP AND PRED   10 0   PRED   10 MSEC
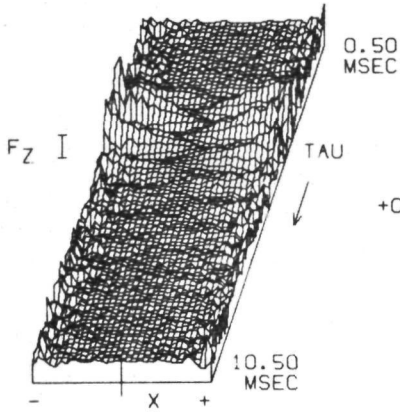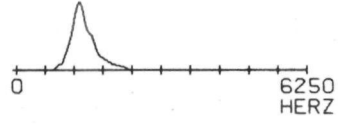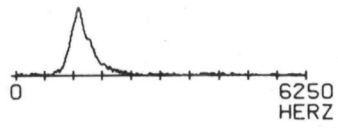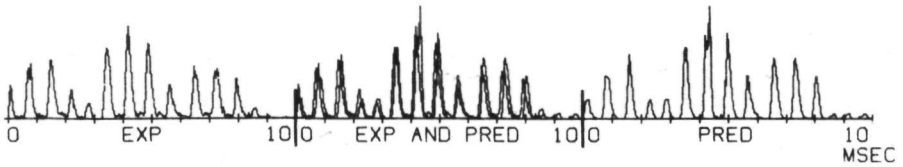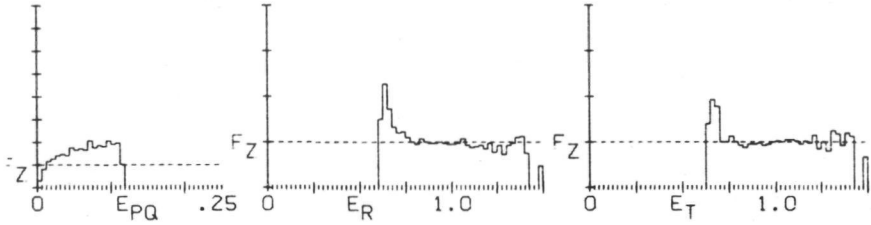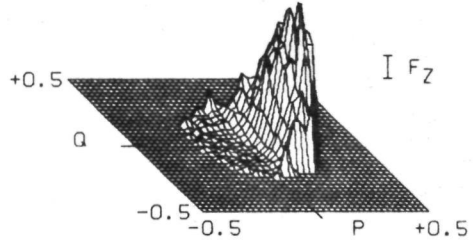
This unit differs from the previous and other AN(?) units in
that respect that it has no spontaneous activity.

60-8

The several predictors are much more salient than the previous   AN(?)
ones (note that the F_Z bars are smaller than in the other
figures).   0

-40

Although, of course, predictions are possible, none is given   5000
because no experimental PSTH could be obtained (unit was lost),
so no comparison can be made.   -20

∠169

10.9

0.214

0.84

0.14

5.27

1.20

1.08

3.081

0.979

1.022

-

-

-

-

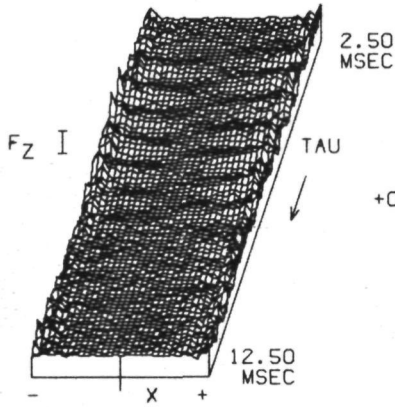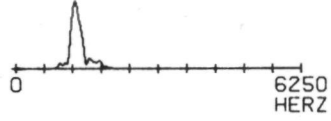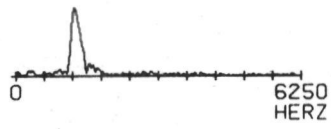Fig. III-13   for explanation of figures see pages 68 and 69

20.00
MSEC

← TAU

0

0

6250
HERZ

20.00
MSEC

0

0

6250
HERZ

F_Z I

1.50
MSEC

TAU

11.50
MSEC

−   X   +

UNIT   60− 8

+0.5

Q

−0.5
−0.5

ɪ F_Z

P   +0.5

F_Z

0   E_{PQ} .25

F_Z

0   E_R 1.0

F_Z

0   E_T 1.0
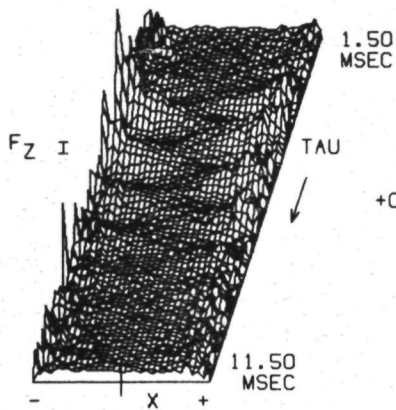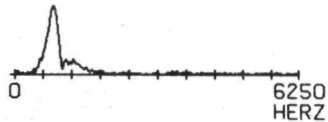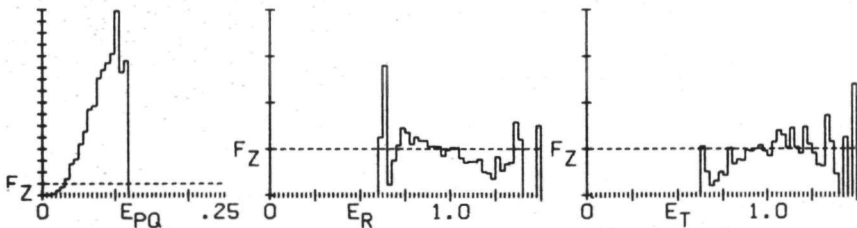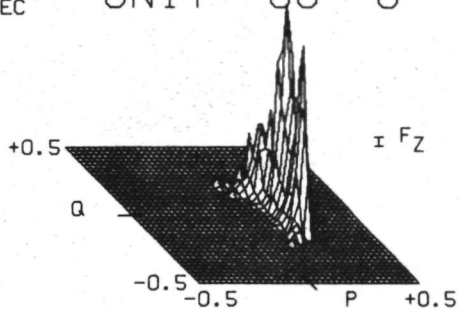
For this unit it is clear that the P,Q-analysis is superior
to the P-analysis alone.

In the comparison of experimental and predicted PSTH it is striking
that the peaks are coinciding perfectly but their heights differ.
This may be due to adaptation or refractoriness effects, which
are not present in the predicted PSTH (the analysis can only
predict responses for stationary stimuli).

That this unit has a strong adaptation can be seen below, where
a PSTH on tone bursts of the characteristic frequency is given.
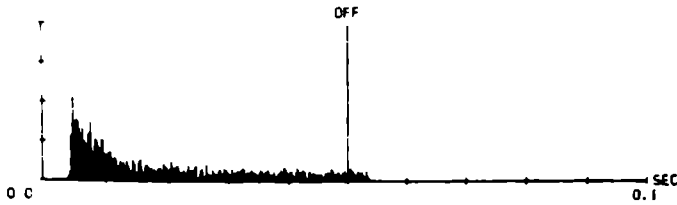
OFF

0 c   SEC
                                                            0.1

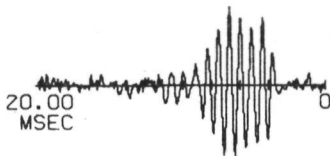F . III-14   for explanation of figures see pages 68 and 69

UNIT 52- 7
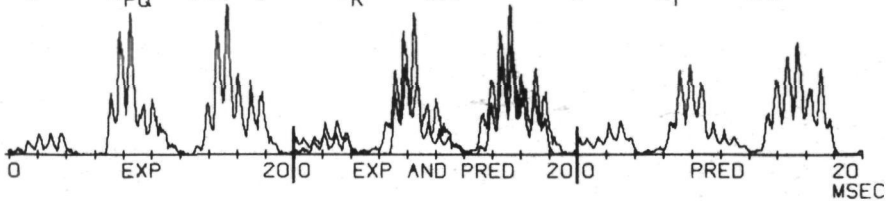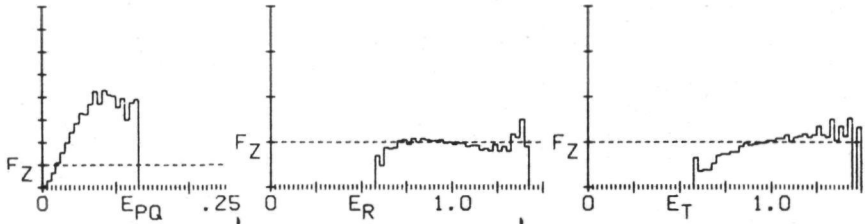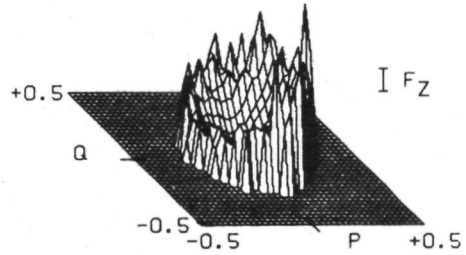
20.00
MSEC

← TAU

0   6250
           HERZ

20.00
MSEC

0   6250
           HERZ

2.50
MSEC

F_Z I

TAU

UNIT 54- 3

I F_Z

+0.5

Q

-0.5
  -0.5   P   +0.5

12.50
MSEC

−   X   +

F_Z F_Z F_Z

0   E_{PQ} .25   0 E_R 1.0   0 E_T 1.0

0   EXP   20 0   EXP AND PRED   20 0   PRED   20
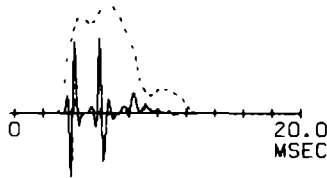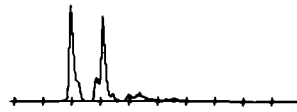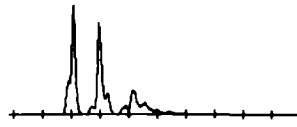   MSEC
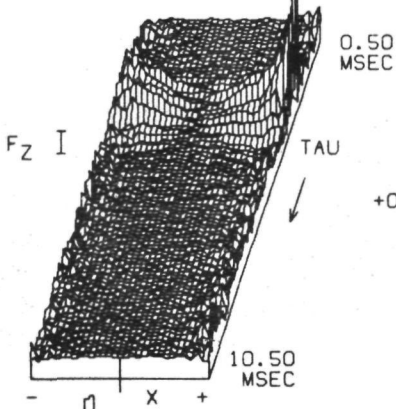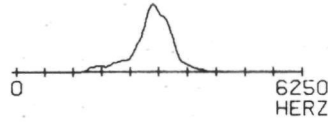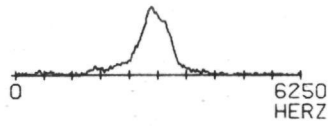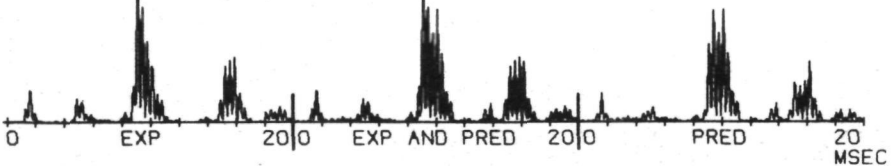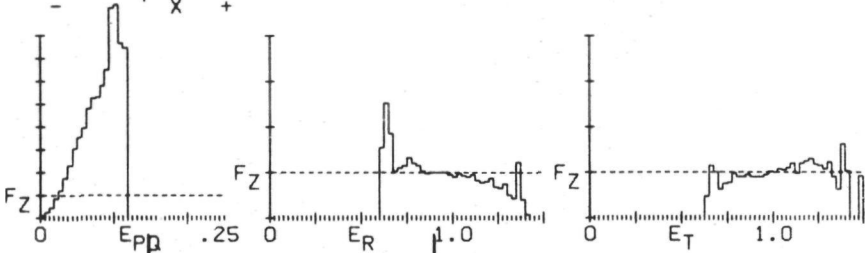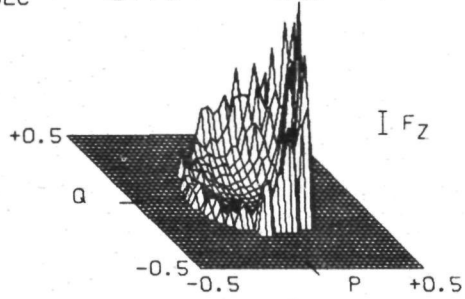
This neuron we have stimulated at three different intensities (figures III-15, 16, 17).

Clicks were also used as stimuli and the PSTH's are shown on the right (position click, negative click, compound PSTH). The resemblence of the compound PSTH with R(τ) (interrupted line is envelope of R(τ)) is much less than for unit 54-4 (figure III-11).
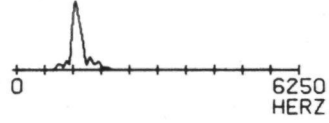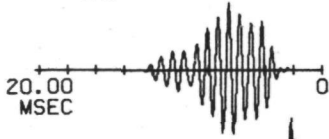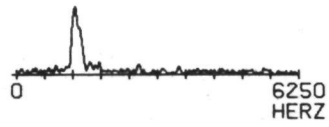
The spikes elicited by the click (2 à 3 spikes per stimulus) arrive at very regular moments after the click (contrary to the click PSTH's for unit 54-4). This could be attributed to refractoriness but it is more likely that it is due to temporal integration mechanisms (cf. van Gisbergen, 1974, Chapter III). This mechanism does not come forward in R(τ), but in the interval histogram of the spike train elicited by the noise stimulus also a dominant interval is present.

VCN
20
-39

5000
0
32881
93

0.042
1.30
0.095
6.17
1.47
0.83

2.028
0.995
1.016

1.92
2.41
0.60
0.1

20.0
MSEC

0

Fig. III-15   for explanation of figures see pages 68 and 69

UNIT 54- 3

20.00
MSEC

TAU

20.00
MSEC

0

6250
HERZ

0

6250
HERZ

2.50
MSEC

F_Z I

TAU

I F_Z

+0.5

Q

-0.5
-0.5

P

+0.5

12.50
MSEC

−   X   +

F_Z 0 E_{PQ} .25

F_Z 0 E_R 1.0

F_Z 0 E_T 1.0

0   EXP   20 0   EXP AND PRED   20 0   PRED   20
MSEC
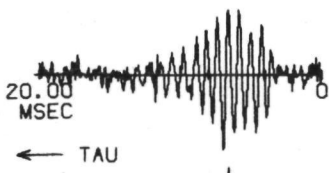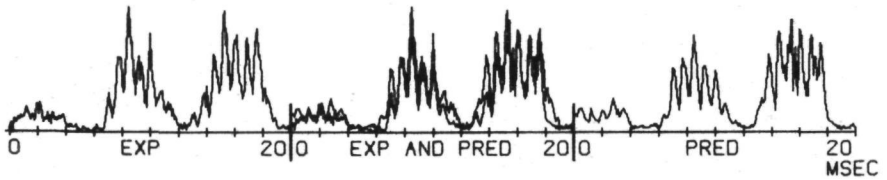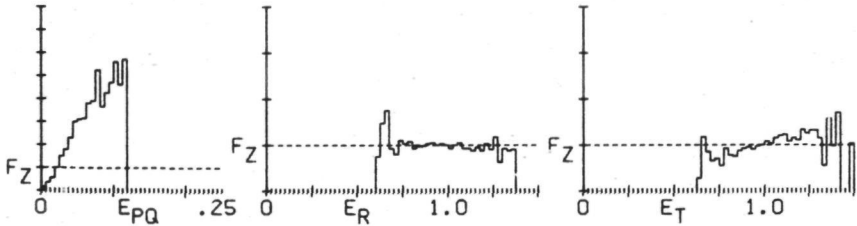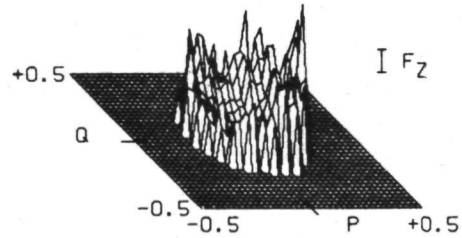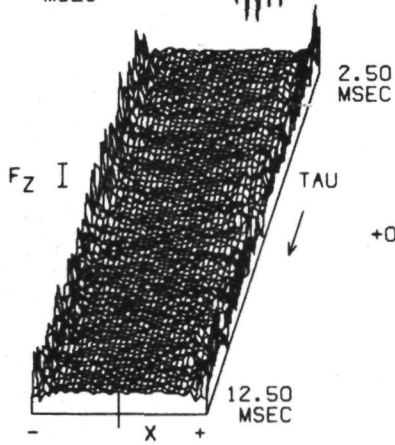
Comparing this figure with the previous one, very few differences
can be observed, although the stimulus intensity is 10 dB lower
here (so the scaling along the axes that are related to the
intensity differ 10 dB).

Below, a comparison is made between the two spectra of
figure III-15 and figure III-16 and the intensity frequency
scan measured with pure tones (cf. Chapter IV and van Gisbergen,
1974).
That these rather complex spectra match so precisely is striking.

54-3-2

VCN

20

-39

5000

-10

8064

63

0.039

1.30

0.094

6.42

1.62

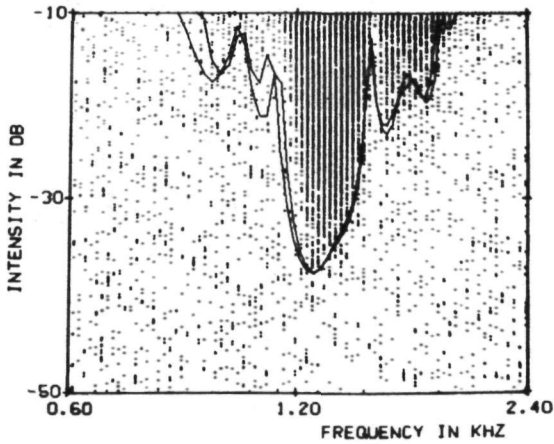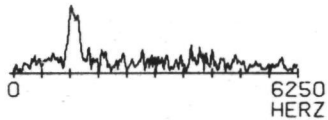0.96

2.050

0.997

1.018

1:69

1.68

1.01

0

Fig. III-16   for explanation of figures see pages 68 and 69
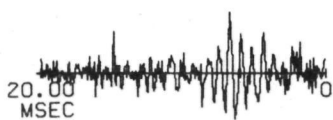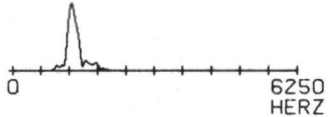
UNIT 54- 3
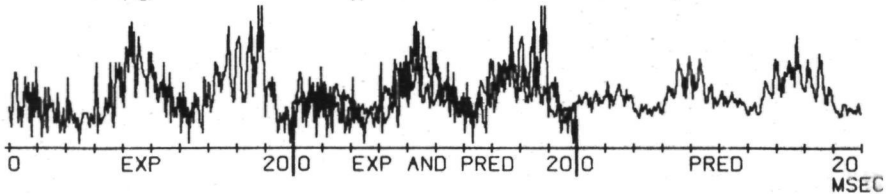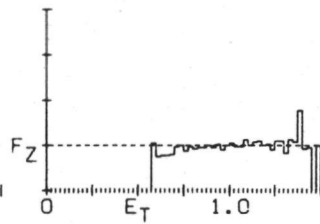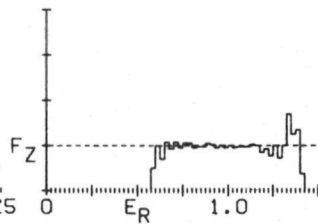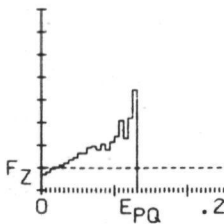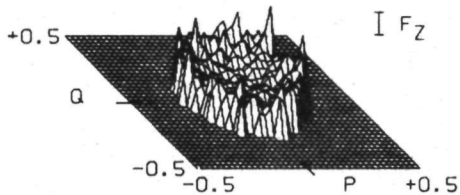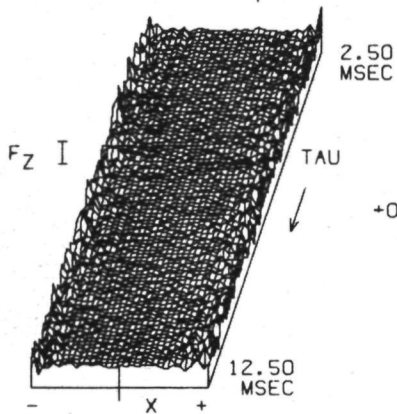
The intensity in this figure is again 10 dB lower than in the
previous one (same unit), and now the results differ substantially.

The effects of stimulation at the different intensities are
illustrated in the figure below in which the $f(z|E_{PQ})$ are given
for the different intensities   The arrow indicates the
spontaneous activity and the interrupted lines indicate the
individual $f(z)$.
The curves have a similar course, indicating that at the several
intensity levels approximately the same relative sensitivity is
obtained. (cf. the situation of light flashes with different
background illumination in the visual system, Werblin, 1973).

Unfortunately we did not stimulate at higher intensities, so
we cannot give a complete picture.
Connecting the interrupted lines one should obtain the well-known
S-shaped overall rate intensity curve (Ruggero, 1973).

54-3-3

VCN

20

-39

5000

-20

14435

63

0.012

1.31

0.114

6.45

1.63

1.16
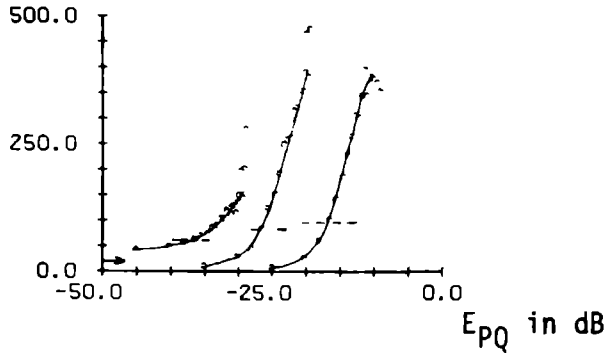
1.338

0.998

1.005

1 30

0 64

2.02

0.15

Fig. III-17   for explanation of figures see pages 68 and 69

20.00 MSEC   0   0   6250 HERZ

← TAU

20.00 MSEC   0   0   6250 HERZ

F_Z I

0.50 MSEC

UNIT 65-2

TAU

10.50 MSEC

$-$ X $+$

+0.5

Q

-0.5

-0.5 P $+0.5$

I F_Z

F_Z 0 E_{PQ} .25

F_Z 0 E_R 1.0

F_Z 0 E_T 1.0

0   EXP   5 0   EXP AND PRED   5 0   PRED   5 MSEC
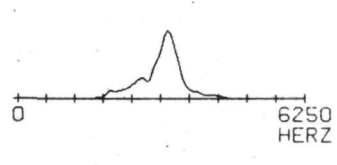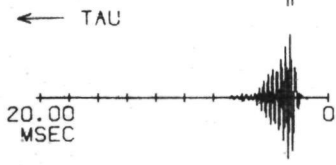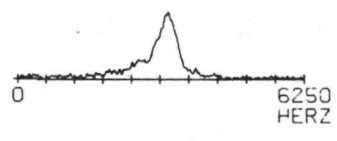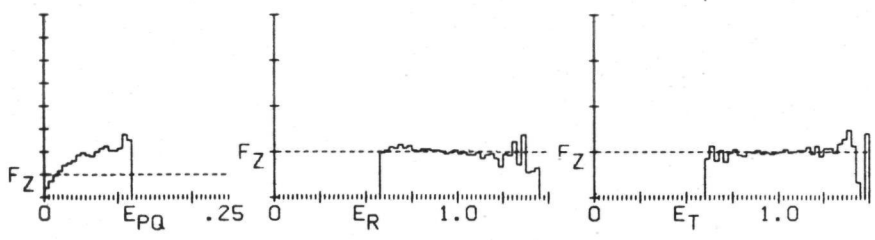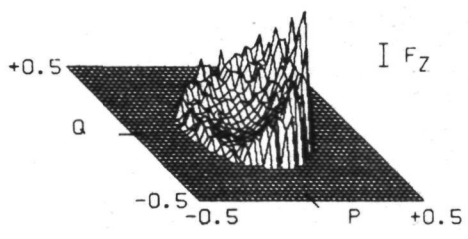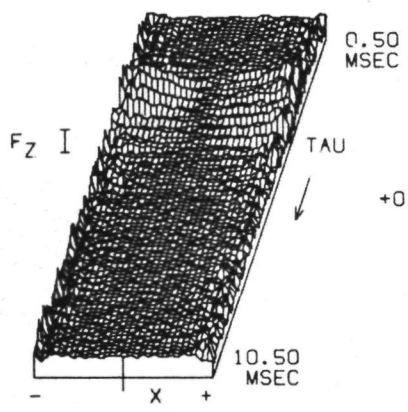
These and the following figures are also obtained from stimulating
the same neuron with different intensities.

For these records all the P,Q-analyses have been made with the
same R(ι), namely the one in this figure (III-18), because no
systematic differences can be observed in the different R(ι)
and this seems to be the best one.

5000

-40

17427

139

0.069

3.14

0.27

3.08

0.62

1.06

1 474

0.993

1.003

0.61

0.56

1.08

0.02

Fig. III-18   for explanation of figures see pages 68 and 69

20.00
MSEC

← TAU

20.00
MSEC

0   6250
         HERZ

0   6250
         HERZ

0.50
MSEC

UNIT   65- 2

F$_Z$ I

TAU

←0.5

Q

I F$_Z$

-0.5
-0.5   P   +0.5

10.50
MSEC

−   X   +

F$_Z$

0   E$_{PQ}$ .25

F$_Z$

0   E$_R$ 1.0

F$_Z$

0   E$_T$ 1.0

0   EXP   5 0   EXP AND PRED   5 0   PRED   5
                                                                MSEC
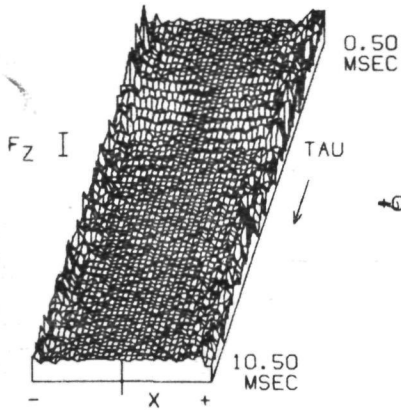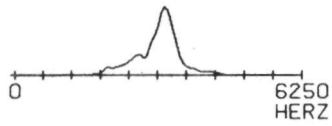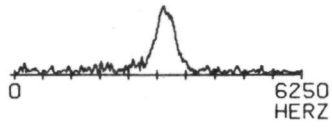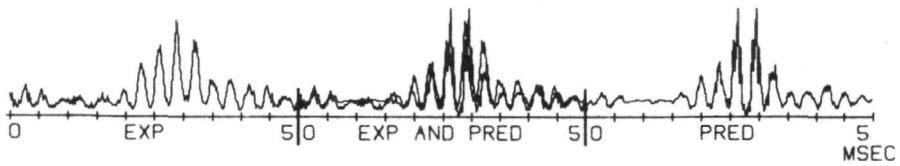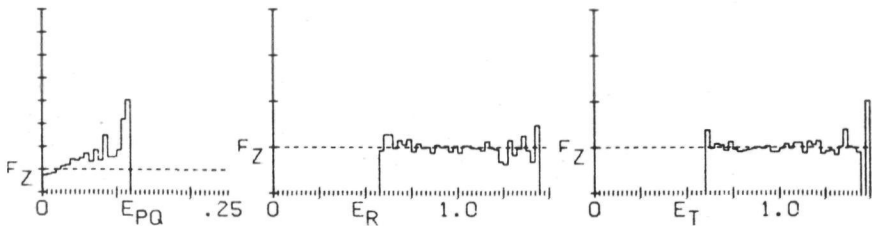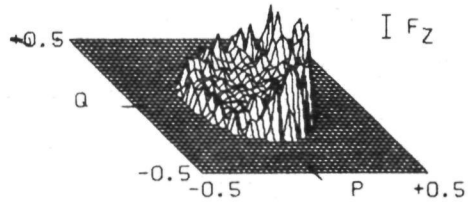
The stimulus intensity is 20 dB lower than for figure III-18.

The figure below, as in figure III-17, shows the $f(z|E_{PQ})$ for different intensities for this unit.
The arrow indicates the spontaneous activity and the interrupted lines the individual $f(z)$.
As can be seen, the relative sensitivity is decreasing for the lower intensity levels but the highest two intensities again show about equal relative sensitivity. Here too, no higher intensities were used.

$f(z|E_{PQ})$
spikes/sec
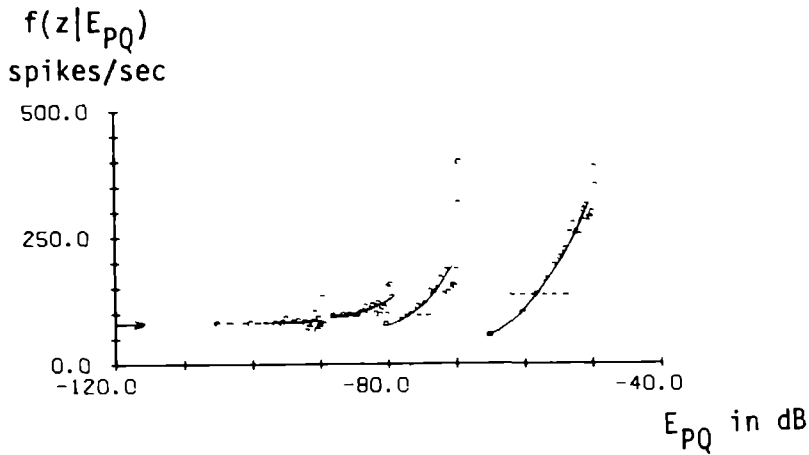
Fig. III-19   for explanation of figures see pages 68 and 69
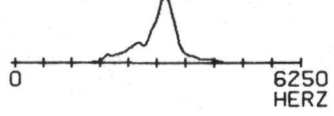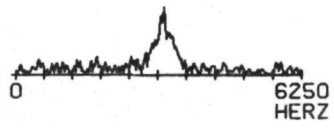
UNIT 65- 2
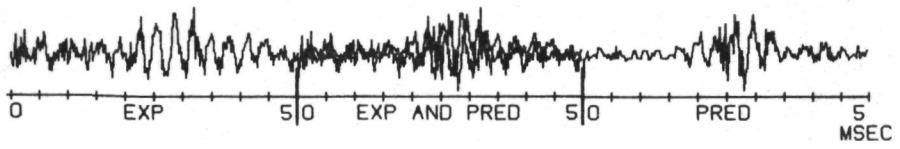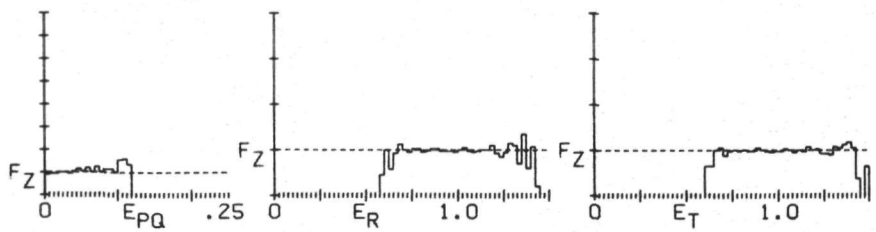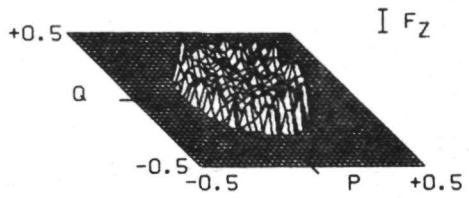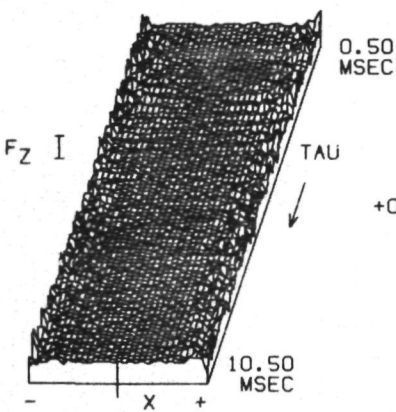
Stimulus intensity 10 dB lower than figure III-19 so 30 dB
lower than figure III-18.

Below, the comparison of IFS and the weighted spectrum is given.

65-2-3

VCN

80

-78

5000

-70

18681

97

0.014

3.19

0.17

3.22

0.65

0.69

1.059

0.999

1.001

0.48

0.40

1.21

0.08
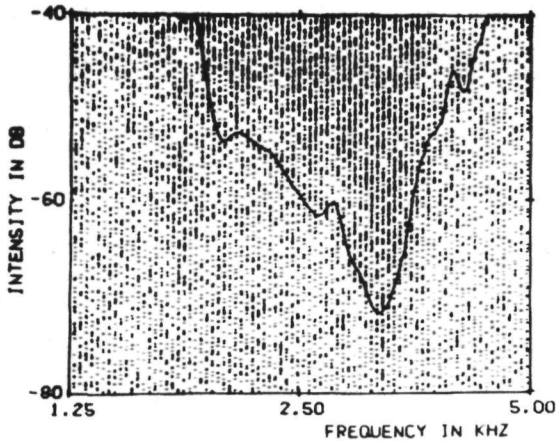
Fig. III-20   for explanation of figures see pages 68 and 69

20.00
MSEC

← TAU

0

6250
HERZ

20.00
MSEC

0

6250
HERZ

0.50
MSEC

UNIT   65- 2

F_Z I

TAU

I F_Z

+0.5

Q

−0.5
−0.5

P   +0.5

10.50
MSEC

−   X   +

F_Z

0   E_{PQ} .25

F_Z

0   E_R 1.0

F_Z

0   E_T 1.0

0   EXP   5|0   EXP AND PRED   5|0   PRED   5
MSEC

Stimulus intensity again 10 dB lower so 40 dB lower than
figure III-18.

65-2-4

VCN

80

-78

5000

-80

21500

82

0.005

3.21

0.12

3.52

0.96

0.71

1.008

0.997

0.997

0.40

0.41

1.04

-

Fig. III-21   for explanation of figures see pages 68 and 69

20.00 MSEC   0

← TAU

0   6250 HERZ

20.00 MSEC   0

0   6250 HERZ

2.50 MSEC

UNIT 42- 3
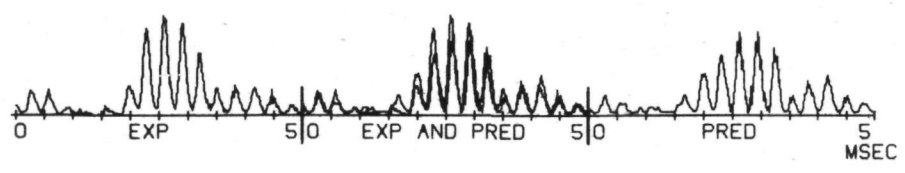
F_Z I

TAU

+0.5

Q

I F_Z

12.50 MSEC

−0.5
−0.5   P   +0.5

− X +

F_Z

0   E_{PQ} .25

F_Z

0   E_R 1.0

F_Z

0   E_T 1.0
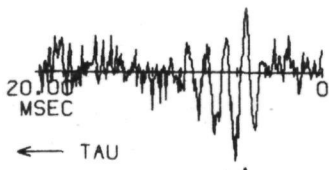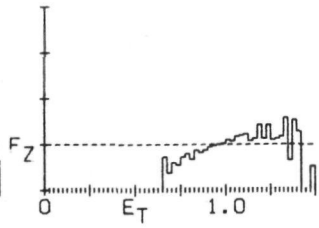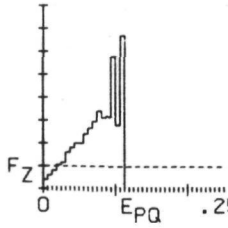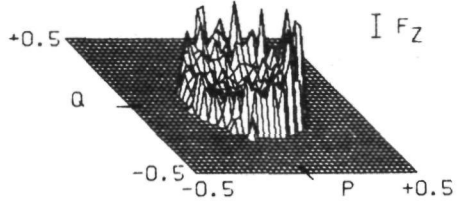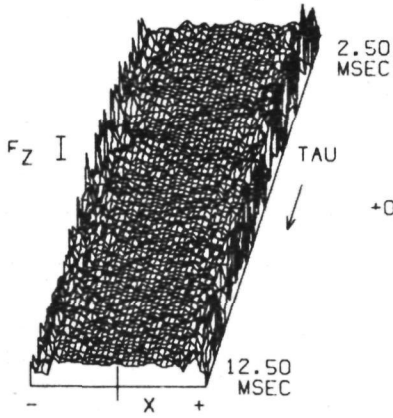
In the previous results the P,Q-analysis gave a rather complete
description of the functional properties of the neurons. This
unit, however, gives rise to some problems.

The low frequency waveform, lying over $R(\tau)$ is, however,
artificial and so is the low frequency peak in the spectrum.
These are due to the use of a noise stimulus that was not
Gaussian white noise (cf. Chapter IV.2).
These effects are therefore eliminated through the weighting-
procedure.

The increasing $f(z|E_R)$ for increasing E_R indicates that E_R still
contains some part relevant for the neuron. So for this unit
the P,Q-analysis is not a complete description.
This can also be observed in the comparison of the spectrum with
the intensity frequency scan (IFS). The IFS shows a very complex
I-F dependence in which non-monotonic and suppression-effects
are visible. These aspects are not present in the correlation
function $R(\tau)$.

(continued)

42-3

DCN

17

-73

5000

-50

4482

20.4

0.030

0.73

0.076

6.39

1.31

0.63

1.673

1.006

1.019

-

-

-

-
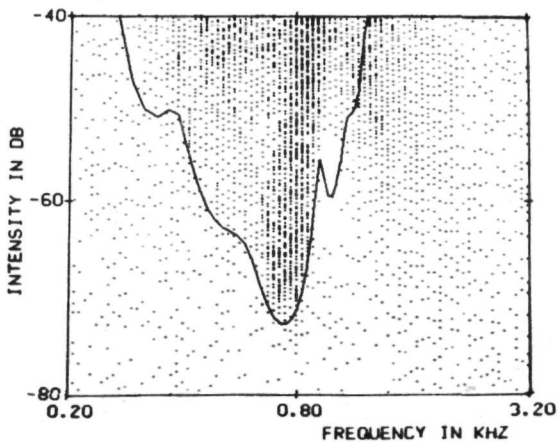
Fig. III-22   for explanation of figures see pages 68 and 69

6.67
MSEC

← TAU

6.67
MSEC

0   18740
                     HERZ

0   18740
                     HERZ

0.83
MSEC

UNIT   64 - 1

F$_Z$ I

TAU

I F$_Z$

+0.5

Q

-0.5
-0.5   P   +0.5

F$_Z$

0   E$_{PQ}$ 25

F$_Z$

0   E$_R$ 1.0

F$_Z$

0   E$_T$ 1.0

0   EXP   80 0   EXP AND PRED   80 0   PRED   80
                                                              MSEC
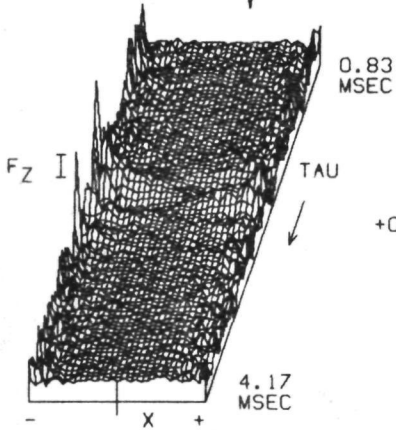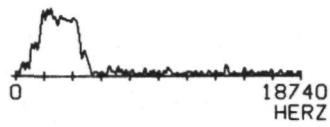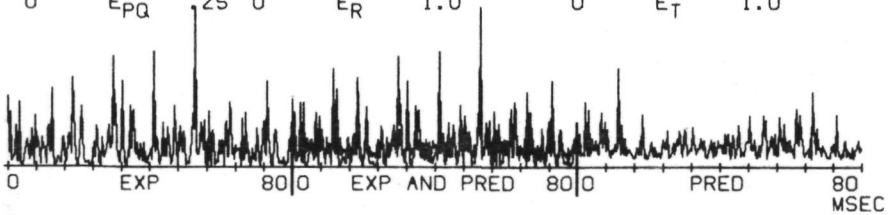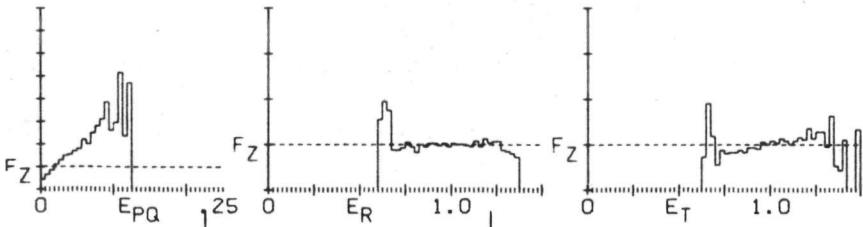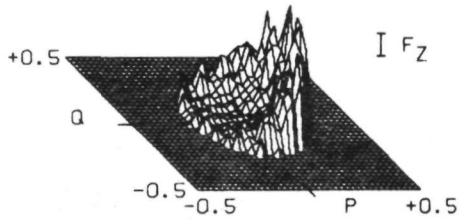
This figure gives another example of an incomplete description by the P,Q-analysis.

In the comparison of predicted and experimental PSTH only a partial resemblence is observed and the predicted PSTH has much less structure than the experimental PSTH.
The $f(z|E_R)$ is not decreasing and the $f(z|E_{PQ})$ for $E_{PQ} = 0$ is higher than that for other comparable neurons. All these arguments point towards an $R(\tau)$ that is incomplete.
This also can be seen in the comparison of spectrum and IFS (below). It seems to be that $R(\tau)$ is only representing the low frequency part of the response area. (cf. the low-pass filter in the model of Johannesma, 1971).
The shifting procedure did not yield an improvement for $R(\tau)$.

64-1

VCN

5

-50

15000

0

7842

28

0.072

2.73

0.83

2.35

0.16

0.82

1.577

1.001

1.012

2.22

2.24

0.99

0
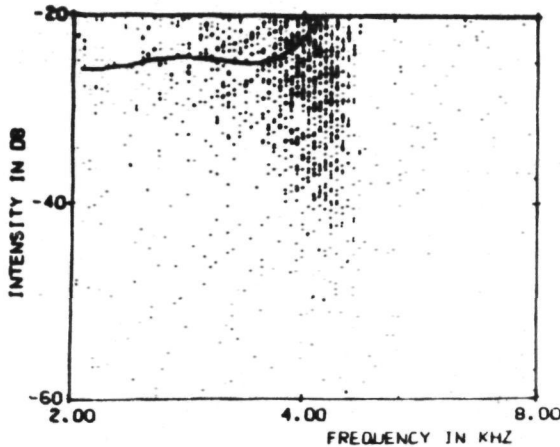
Fig. III-23   for explanation of figures see pages 68 and 69

20.00
MSEC

0

0

6250
HERZ

← TAU

20.00
MSEC

0

0

6250
HERZ

UNIT   56- 7

+0.5

I F_Z

Q

-0.5
-0.5

P   +0.5

F_Z

0   E_{PQ} .25

F_Z

0   E_R 1.0

F_Z

0   E_T 1.0

0   EXP   S│0   EXP AND PRED   S│0   PRED   5
MSEC
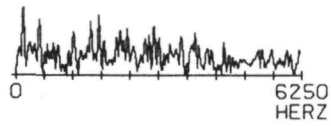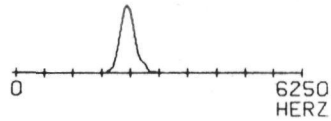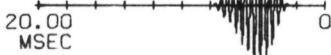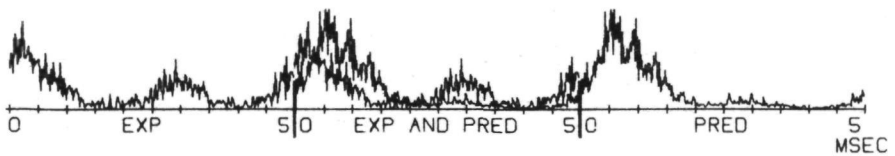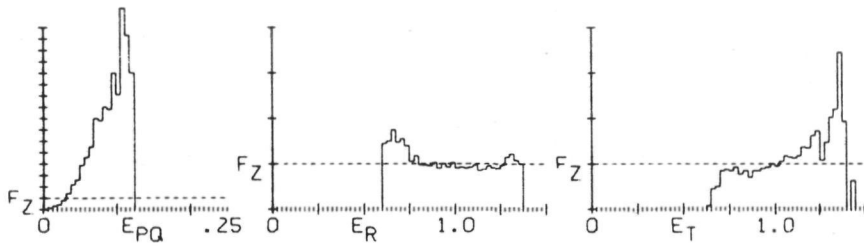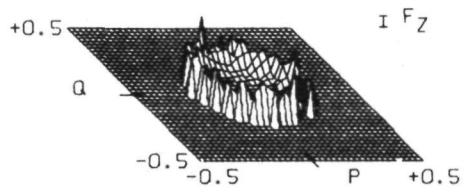
This unit is one of those who gave an R(ι) not discernable
from zero. This, however, was remedied with the help of the
shifting procedure.

The rotation symmetrical shape of f(z|P,Q) indicates that no
preference for phase exists, but the steep slope indicates that
the extracted $R_1(\tau)$ is not far from the truth

VCN

0

-ɔ0

Because of this rotation symmetry $f(z|E_{PQ})$ is giving the same
information as f(z|P,Q) apart from this symmetry.
The prediction is not very good, but we are unable to say why.

ɔ000

-10

63∠1

At the right the click PSTH's
(positive and negative clicks
and compound PSTH) are given.
Every click elicited one spike,
at a fixed click - spike
interval, and no relation with
the frequency of $R_1(\tau)$ is
observed.

1ɔ

0 000

∠ 39

0 11

4 7ɔ

0.80

0 ɔ5

∠ 767

0 989

1 0∠6

0 20.0
MSEC

0.05

0.06

0 80
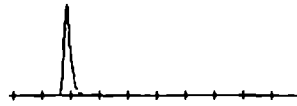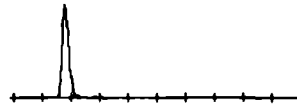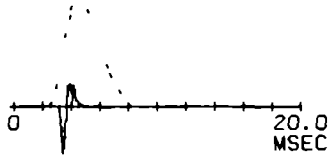
0 ∠6

Fig. III-24   for explanation of figures see pages 68 and 69

6.67
MSEC
0

0
18740
HERZ

← TAU

6.67
MSEC
0

0
18740
HERZ

UNIT   64- 5

+0.5

Q

-0.5
-0.5

I F_Z

P   +0.5

F_Z

0   E_{PQ} .25

F_Z

0   E_R 1.0

F_Z

0   E_T 1.0

0   EXP   80|0   EXP AND PRED   80|0   PRED   80
MSEC
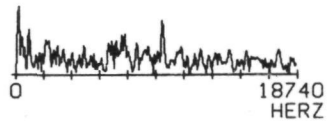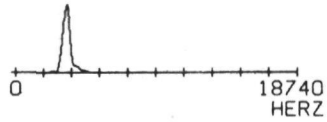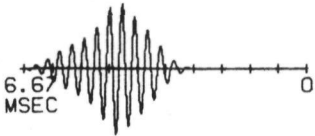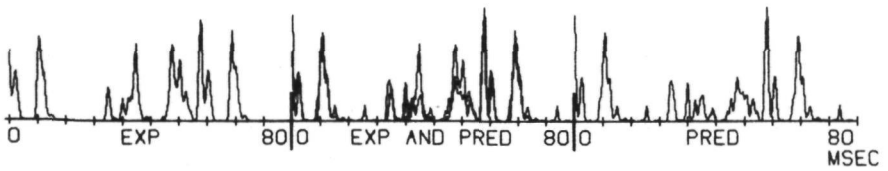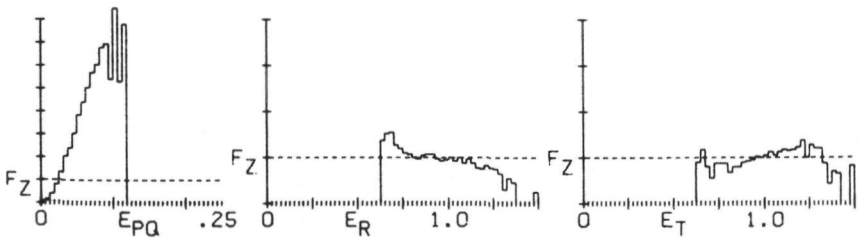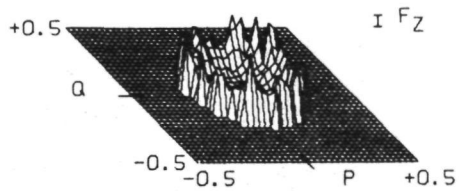
The last two figures (III-25 and III-26) may be seen as an abstract
of the results obtained:
High frequency units, so no R(.).

With the help of the shifting procedure an $R_1(\tau)$ was obtained
which gave clear results for $f(z|P,Q)$ and $f(z|E_{PQ})$.

The predicted PSTH agrees well with the experimentally obtained
one.

From this result we can conclude that indeed the P,Q-analysis,
including the shifting procedure, also is a reasonable functional
description for higher frequency units.

The prediction, however, deviates at two peaks in the PSTH. We
cannot blame this to adaptation, but possibly suppression effects
may cause this.

Another possibility could be that the used $R_1(\tau)$ is in some
respects not the best one. One could try a slight modification
for $R_1(\tau)$ and see if the prediction fits better, but an iteration
of that kind would be very time consuming, and convergence
cannot a priori be expected.

64-5

VCN

0

-70

15000

-30

11242

64

0.000
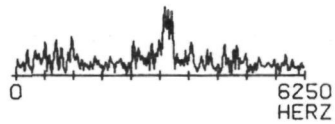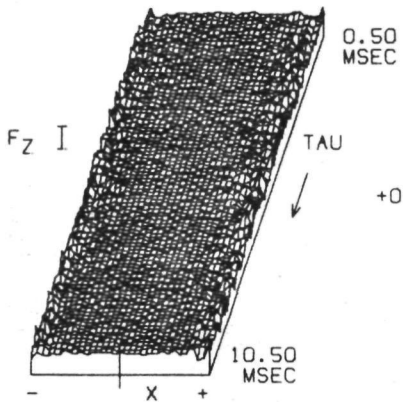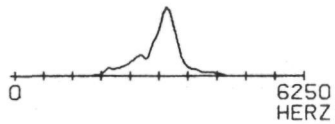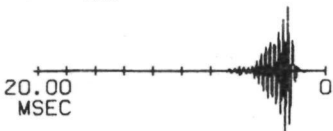
3.34

0.18

4 47

0.54

0.60

2.416

0.987

1.016

5.06

6.27
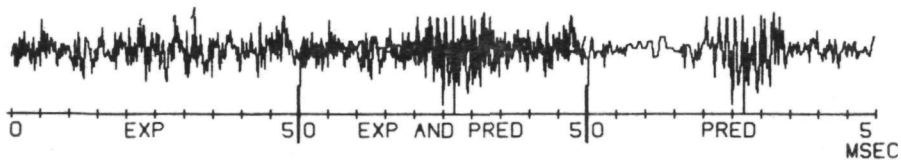
0.81

0

Fig. III-25   for explanation of figures see pages 68 and 69

99
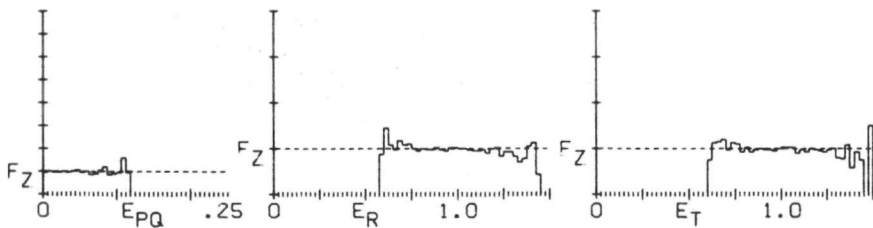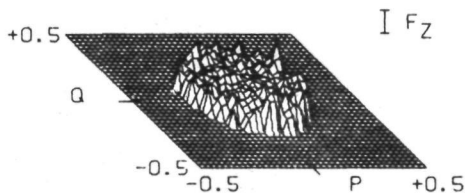
6.67
MSEC

0   18740
                      HERZ

← TAU

6.67
MSEC

0   18740
                      HERZ

UNIT   65– 1

+0.5   I F_Z

Q

–0.5
    –0.5   P   +0.5

F_Z
0   E_{PQ} .25   0 E_R 1.0   0 E_T 1.0

F_Z F_Z

0   EXP   80|0   EXP AND PRED   80|0   PRED   80
                                                              MSEC
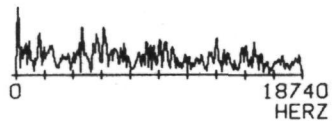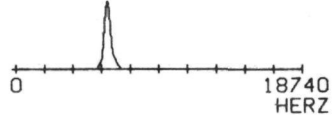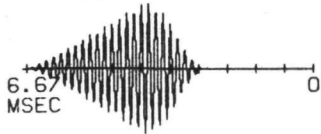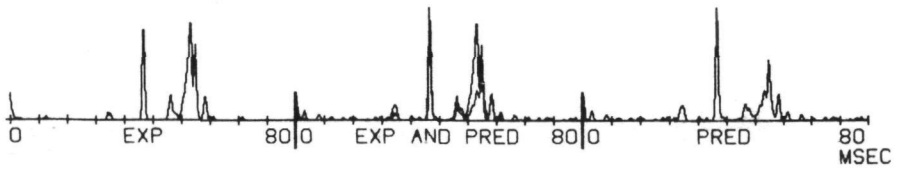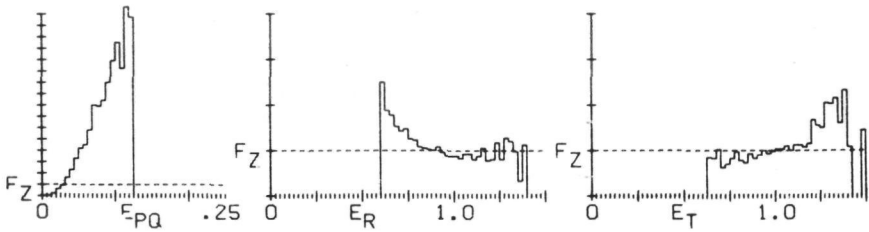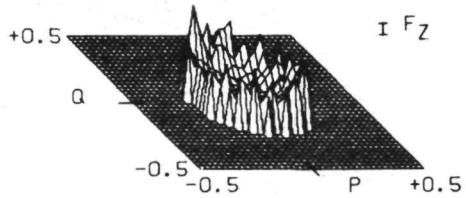
The comments to the previous figure should also be applied here.

One comparison, however, will be made to show that the spectrum of the $R_1(\tau)$ obtained by the shifting procedure fits rather well the IFS for this unit.
This $R_1(\tau)$ was obtained by starting with estimate wave forms (see appendix I) of resp. 5 and 7 kHz and these frequencies have disappeared completely.

65-1

VCN

0

-75

15000

-40

9244

34

0.000

5.89

0.15

4.17

0.65

0.61

2.815

0.984

1.021

2.17

1.80

1.21
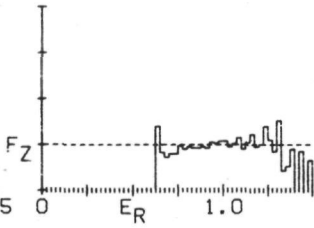
0
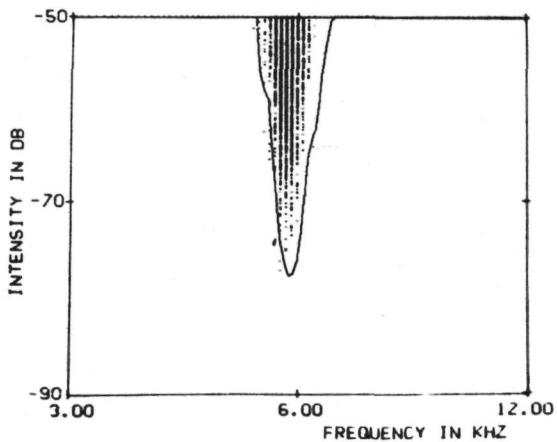
Fig. III-26 for explanation of figures see pages 68 and 69

This is to assist the reading of the right column on the preceding pages. Please cut this page along the line and stick it onto the following page where indicated.

unit number

location

spont act sp/sec

CF threshold dB

upper limit noise

intens. noise dB

number of spikes

$F_Z = f(z)$ sp/sec

$|\vec{R}| = \sqrt{E}$

μ_f kHz

σ_f kHz

μ_τ msec

σ_τ msec

$\Delta = \sigma_\omega \sigma_\tau$

$\overline{E_{PQ}|z} / \overline{E_{PQ}}$

$\overline{E_R|z} / \overline{E_R}$

$\overline{E_T|z} / \overline{E_T}$

N spikes pred.

N spikes rec.

$\dfrac{N \text{ pred.}}{N \text{ rec.}}$

time shift pred. msec
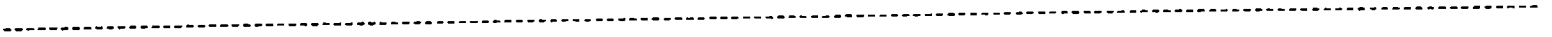
Please stick here

Reviewing the figures on the previous pages it appears that the most important variations in the cochlear nuclei are variations in the form of the different predictors and these variations are rather continuous. But so far we did not succeed in quantifying these forms. This we only did for $R(\tau)$, which will be treated extensively in Chapter IV.

However, the average firing rate under stimulation must still be commented on.
In an attempt to stimulate all neurons at the same relative level the stimulus intensity was chosen 20 dB above the audible threshold for noise stimulation.
In figure III-27 the relation between the average firing rate $f(z)$ and the spontaneous activity is shown. As expected there is a general trend. This trend, however, seems to be more an equal absolute increase in the firing rate than a relative one. The scatter in figure III-27 may indicate deviations of this general trend as well as the difficulty in determining the audible threshold mentioned above.

An interesting relation is found between the relative mean $E_{PQ}|z$ and $f(z)$ as given in figure III-28. For the interpretation of $\overline{E_{PQ}|z}/\overline{E_{PQ}}$ the following can be said:
The $f(E_{PQ})$ is the same for all units (intensity of stimulus = 1), so $\overline{E_{PQ}}$ is constant (=0.020), and thus the form of $f(z|E_{PQ})$ is related to the form of $f(E_{PQ}|z)$. Now it appears that the $f(E_{PQ}|z)$ all belong to the same class of distributions for which $\overline{E_{PQ}|z}$ is an indication of the form of $f(E_{PQ}|z)$. So $\overline{E_{PQ}|z}/\overline{E_{PQ}}$ can be interpreted as some kind of form factor for the $f(z|E_{PQ})$. The normalization with respect to $\overline{E_{PQ}}$ is only made to obtain figures that are easier to interprete.

On the other hand $\dfrac{f(z)}{(\overline{E_{PQ}|z}/\overline{E_{PQ}})-1}$ can be interpreted as a measure for the relative sensitivity of the unit during stimulation (relative sensitivity because we assume that all units are stimulated at the same relative level and the absolute intensity is disregarded).
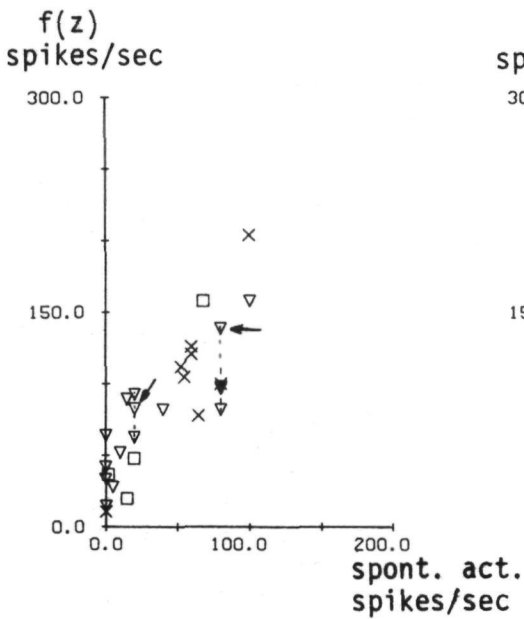
Fig. III-27 Average firing rate
during stimulus versus
spontaneous activity.
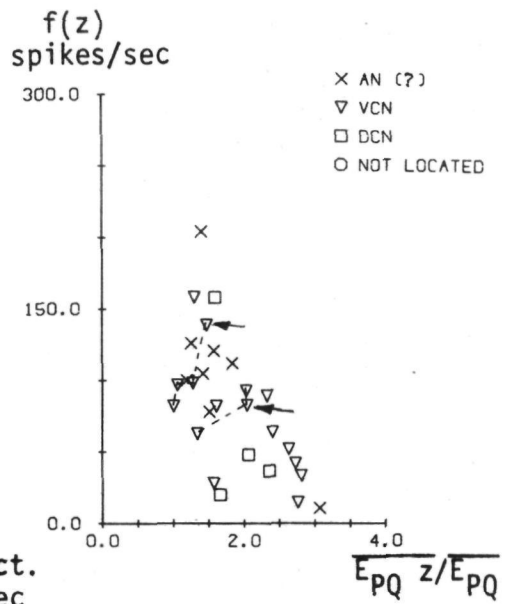
Fig. III-28 Average firing rate
during stimulus versus
relative mean relevant
energy $\overline{E_{PQ}|z/E_{PQ}}$.

Data connected by an interrupted line belong to the same unit stimulated
at different intensities. Arrows indicate the intensity that have to
be compared with the other units.

So units that have the same line connecting its symbol with (f(z)=0 ,
$\overline{E_{PQ}|z/E_{PQ}}$=1) have the same relative sensitivity. Note, however, that the
$\overline{E_{PQ}|z/E_{PQ}}$ cannot be chosen by the experimentalist, but are the result of
the analysis. It thus appears that the units stimulated at different
intensities have about the same relative sensitivity at these different
intensity levels.
Figure III-28 shows a definite relation between f(z) and $\overline{E_{PQ}|z/E_{PQ}}$
(apart from some symbols the deviations of which will be explained).
From figures III-28 and III-27 the conclusion can be drawn that units
with high spontaneous activity are relatively more sensitive than units
with lower spontaneous activity.

In figure III-28 several points deviate from the general trend. These are the points for units 54-3 and 65-2 for the lowest intensities, but also the points in the lower left corner (units 42-3 and 64-1). About these units we concluded earlier that the P,Q-analysis gave an incomplete description and thus $\overline{E_{PQ}|z}$ can be assumed to be too low.

III.4   CONCLUSIONS

From the results obtained with the P,Q-analysis we may accept this analysis to be a relevant functional description of the processes underlying the probabilities of the generation of spikes in the auditory system. With the results of this analysis we now have the opportunity to describe several properties of the neuron.

1. Uncorrelated activity
    Under stimulation it is not possible to discern directly spontaneous activity, but only uncorrelated activity, i.e. activity evoked for P-Q=0 or $E_{PQ}=0$. When we now assume that under stimulation no uncorrelated spikes should occur, apart from spontaneous spikes, the spikes in $f(P,Q|z)$ at P=Q=0 are all spontaneous spikes. And while the $f(P,Q|z)$ for spontaneous spikes, i.e. spikes at random moments, is equal to $f(P,Q)$ for the SE distribution, we can separate $f(P,Q|z)$ into an evoked and a spontaneous part. Whether this separation is correct can be verified by a prediction with the calculated evoked $f(z|P,Q)$, to which the proper amount of random spikes is added.

2. The amount of phaselock (timelock)
    Having obtained the $f(z|P,Q)$ predictor we can predict responses to all kinds of stimuli, therefore also the responses to sinusoidal stimuli. (The correctness of these predictions has not been verfied). It is thus possible for any definition of phaselock to derive a measure of phaselock for the unit from $f(z|P,Q)$.

3. Dynamic range
    Although stationary stimuli have been used, some insight is obtained about the (local) dynamic range from the $f(z|E_{PQ})$, while a stationary stimulus has a constant mean power over longer time durations, but

106

averaged over short time durations (10 msec) variations around this mean power are found. When different intensities are given to the same neuron (unit 54-3, figures III-15 to 17 and unit 65-2, figures III-18 to 21) the tentative conclusion may be drawn that at different intensities, so different adaptation states, a comparable behaviour is observed. (cf. Werblin 1973)

4   Threshold

From our results for $f(z|E_{PQ})$ it can be concluded that no threshold can be found for any one unit.

5. Optimal stimulus

All $f(z|P,Q)$ increase up to ultimate P,Q values. From the equivalent results for $f(z|P)$ and $f(z|\cos\phi)$ (when we disregard phase effects) we now can infer that the stimulus with greatest similarity to $R(\tau)$ for a certain energy, i.e. the greatest $\cos\phi$ will elicite more spikes than any other stimulus. Therefore $x(t-\tau)=R(\tau)$ can be considered as an optimal stimulus.

The concept of the Pre-Event Stimulus Ensemble, which we introduced here, adequately describes the functional properties of the neurons, as can be judged by the resulting predictors.
With the introduction of the shifting procedure the above applies also to high frequency units yielding an $R(\tau)$ being identical zero.
However, very few DCN units have been incorporated and the results shown for unit 42-3 (figure III-22) already indicate that for complex units difficulties may arise. So far, now special attention has been given to inhibitory effects and it is not yet possible to estimate to what extend and in which situation inhibition is comprised in $R(\tau)$ if at all. The use of stationary stimuli causes that no adaptation effects emerge in the predictions, so the analysis must be extended by using non-stationary stimuli.

It is thus clear that this study is only the beginning of a long story. However, the results obtained so far are promissing enough to continue this story, which, it is hoped, will have a happy end in the not too distant future.

IV   THE CHARACTERIZATION OF THE AVERAGE PRE-EVENT STIMULUS OF NEURONS IN
        THE CAT'S COCHLEAR NUCLEI. *

J.L. Grashuis, P.I.M. Johannesma, G.H.F. Olde Heuvelt, J.A.M. v. Gisbergen,
A.J.H. Vendrik.
Laboratory of Medical Physics and Biophysics, University of Nijmegen.

Table of contents

INTRODUCTION

The well known click-PSTH's of Kiang et al (1965) are the first
electro-physiological measurements of some kind of a (rectified)
single unit impulse response of the auditory system up to the auditory
nerve. In system theory it is well known that the impulse response
of a linear system can be obtained by crosscorrelating a Gaussian white
noise (GWN) input and the output of that system.

De Boer and Kuyper and de Jongh (1968-1974) have shown that for their
model of the peripheral auditory system (a linear band-pass filter
followed by a threshold-trigger element) the crosscorrelation between
the GWN input and the output pulses is a mixture of the impulse
response of the linear filter and its time derivative

$$\phi_{xz}(\tau) = b \, h(-\tau) + \sqrt{\frac{2}{\pi}} \, \dot{h}(-\tau) \qquad\qquad (IV-1)$$

where $h(\tau)$ is the impuls response of the linear filter and b is the
threshold.
In the derivation of (IV-1) it was furthermore assumed that the input
and output of the linear filter have a power of unity.

In the model of Johannesma (1969, 1971) (a linear band-pass filter
followed by a one sided linear rectifier, an integrator and a threshold-
trigger element, where the integrator is reset when the trigger
produces a pulse) the crosscorrelation is in fact the impulse response
itself

$$\phi_{xz}(\tau) = \frac{1}{0-x_0} \, h(\tau) \qquad\qquad (IV-2)$$

where 0 is the threshold and x_0 is the resetlevel (Johannesma 1969).
The spike generating element of neurons, however, contains neither
a simple threshold nor an integrator followed by a threshold, and
for secundary or higher neurons, models will be more complicated.
Therefore, Johannesma et al (1972) developed a general theory, which
treats the crosscorrelation function (or reverse correlation function,
de Boer) as precisely what it is : the average pre-event stimulus
(APES).

When an auditory stimulus $x(t)$, which we will assume to be Gaussian white noise, with a power of unity and a total duration of T_0 is presented to the ear, a sequence of action potentials $z(t) = \sum_{n=1}^{N} \delta(t-t_n)$ will be elicited in the neuron.

Therefore the crosscorrelation, representing the linear relationship between $x(t)$ ans $z(t)$, is as follows

$$\phi_{xz}(\tau) = \frac{1}{T_0} \int_0^{T_0} x(t-\tau) \, z(t) \, dt \qquad \text{(IV-3)}$$

$$= \frac{1}{T_0} \int_0^{T_0} x(t-\tau) \sum_{n=1}^{N} \delta(t-t_n) \, dt$$

$$= \frac{1}{T_0} \frac{N}{N} \sum_{n=1}^{N} \int_0^{T_0} x(t-\tau) \, \delta(t-t_n) \, dt$$

$$= \frac{N}{T_0} \frac{1}{N} \sum_{n=1}^{N} x(t_n - \tau)$$

When $x(t_n-\tau)$ is the stimulus preceding the nth spike, which we will call the nth pre-event stimulus $x_n(\tau)$, we divide $\phi_{xz}(\tau)$ into two parts: the average firing frequency $\frac{N}{T_0}$ and the average pre-event stimulus

$$R(\tau) = \frac{1}{N} \sum_{n=1}^{N} x_n(\tau) \qquad \text{(IV-4)}$$

(Note that $R(\tau)$ is thus defined for a stimulus of power of unity)

So $\qquad \phi_{xz}(\tau) = \frac{N}{T_0} R(\tau) \qquad \text{(IV-5)}$

A more complete description and an analysis of the ensemble of $x_n(\tau)$, the Pre-Event Stimulus Ensemble (PESE) will be presented in a future paper (Chapter III of this thesis).

Now because of the generalisation, $R(\tau)$ is the best linear approximation of the impulse response of the whole auditory system up to the neuron and describes adequately the response of a neuron to a certain class of stimuli, as indicated in IV.3.2.1 (see also Chapter III).

In Chapter IV-4 an attempt is made to extract a number of characteristics out of $R(\cdot)$.

To enable more extensive numerical computations as well as a comparison of different levels in the auditory system, we propose in Chapter IV-5 a mathematical function describing $R(\tau)$.

In this paper we will not deal with the average firing frequency $\frac{N}{T_0}$.

Furthermore the effects on $\frac{N}{T_0}$ and $R(\tau)$ due to different stimulus intensities are not yet studied.

Obviously $R(\tau)$ deviates from residual noise, only when there is a time lock between stimulus and response (often called phaselock). When this timelock deteriorates, due to low pass filtering or jitter effects, $R(\tau)$ will diminish. When the uncertainty in time of the spikes is of the order of one half to one period of the characteristic frequency (CF) of the unit, $R(\tau)$ can no longer be distinguised from the residual noise.

So any analysis of $R(\tau)$ can be done only of neurons the cross-correlation of which yields a nonzero result, unless a procedure can be found to eradicate the jitter effects and to recover $R(\tau)$ when the crosscorrelation is residual noise only. Such a procedure has in fact been developed (see appendix I) so the present analysis can be extended to neurons with CF up to 10 kHz.

IV.2   EXPERIMENTAL METHODS

Only a brief description will be given about the preparation, as a more detailed description of the experimental setup is given elsewhere (van Gisbergen, 1974).

Single units were recorded from the cochlear nuclei of anaesthetised cats, that were fixed by means of a metal ball, screwed onto the skull. Through a hole in the skull the cochlear nuclei were reached stereotactically with glass micropipettes (tip diameter ~ 1 μm) filled with 0.5 M sodium acetate and 2% Pontamine sky blue 6Bx.

112

The sound was presented through an acoustic coupler (volume about 2 cm^3) to the intact external ear to simulate a free field condition. The coupler was filled with a damping material to prevent resonances. In the coupler also a monitor microphone was present. The sound source and the microphone both were $\frac{1}{2}$" condenser microphones (Bruel and Kjaer 4134). In this configuration the frequency characteristic is flat within 10 dB in the main frequency range and a maximum sound pressure level of 80 to 90 dB SPL can be reached. By using a condenser earphone driver like Molnar et al (1968) distorsion was limited to 2%.

The noise used as stimulus was generated by a noise generator (HP 3722-H01). In most experiments a pseudonoise was used, namely the lowpass filtered version of a maximum length series of 20 stages. To obtain a better approximation of GWN than was present in the HP 3722-H01 we modified its maximum length series with extra feedback from the stages 11 and 15. At an upper frequency limit of 5 kHz, the duration of one sequence was 10.48 sec., which we repeated as often as necessary until about 10,000 spikes were recorded. The intensity of the stimulus used was set at 20 to 30 dB above the threshold of the neuron for the noise stimulus and we started with the recording of the spikes when a steady state in the firing rate was reached. The spike moments, related to the beginning of the pseudonoise sequence, with a resolution of 10 µsec, were sent to the computer (PDP-9, Digital Equipment Corporation).

The pseudonoise is checked to give the same results as real Gaussian white noise, yet for computer calculations the pseudonoise offers the advantage of having to be recorded only once on computer tape, and during the experiments only the spikemoments need to be sent to the computer.

The details of the main computer program that computes characteristics and parameters are given in appendix II.

The noise stimulus was presented to 41 neurons in the cochlear nuclei 32 of which gave a crosscorrelation function unequal to residual

UNIT 42 6
11902 SPIKES
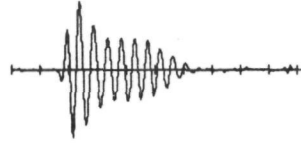
UNIT 45 3
39849 SPIKES

UNIT 52 7
16691 SPIKES
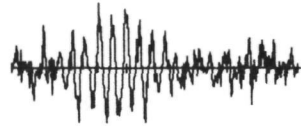
UNIT 54 2
 6418 SPIKES

UNIT 54 3
32881 SPIKES

0   20.00
                     MSEC

⟶ TAU

fig. IV-1 Crosscorrelation functions for several units (upper two
           possibly auditory nerve fibers, lower three ventral cochlear
           nucleus). All functions are amplified to equal magnitude.

114

noise. We succeeded in extracting a function for 6 of the remaining
9 neurons. 33 neurons were anatomically located, of which 9 are
thought to be auditory nerve fibres, 14 ventral cochlear nucleus units
and 10 dorsal cochlear nucleus units.

IV.3 OBSERVATIONS

IV.3.1 Direct observations

Figure IV-1 shows some examples of $R(\tau)$, amplified to equal magnitude.
By observation only, differences can be noted in 'signal to noise'
ratio, starting point, duration and frequency content. The latter two
will be dealt with in Chapter IV.3.2.
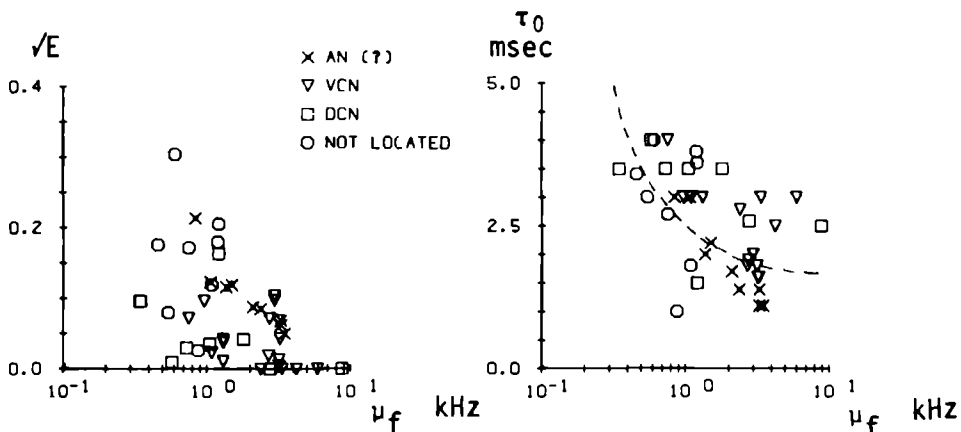
fig. IV-2 Strengths of crosscorrelation
           functions versus mean
           frequency.

fig. IV-3 Delay between spike and
           beginning of $R(\tau)$, determined
           by visual inspection. The
           interrupted line indicates the
           mean of Kiang latency data
           (Kiang, 1965) corrected for an
           extra acoustic delay of 0.2 msec.
           of the acoustic system.
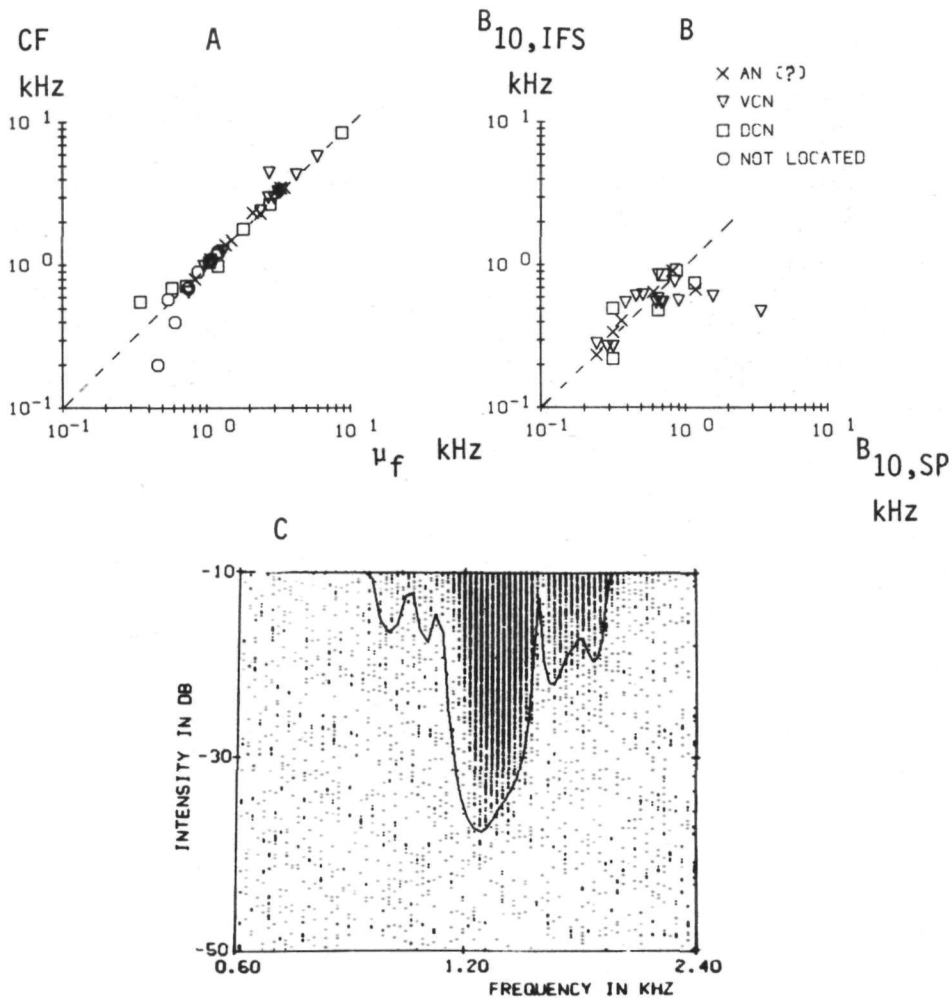
fig. IV-4 Comparison of spectral data for noise- and tone stimulation.
A. characteristic frequency determined from tonal
   stimulation versus mean frequency of the spectrum of R(τ).
B. 10 dB bandwidth of intensity frequency scan (tonal) versus
   10 dB bandwidth of spectrum of R(τ).
C. comparison of intensity frequency scan (IFS) with spectrum
   of R(τ) for unit 54-3. The intensity of the spectrum is
   shifted to match the IFS.

116

The 'signal to noise' ratio is dependent on the number N of pre-event
stimuli (or spikes) used. However, when an equal number of spikes had
been used a difference in the magnitude of $R(\tau)$ remains, due to
different strengths of $R(\tau)$. This strength will be defined as the
square root of the energy E contained in $R(\tau)$ (as will be defined in
equation (IV-17)) The strength is dependent on the CF (for high CF
no $R(\tau)$ can be obtained) but also on the location of the neuron in the
cochlear nuclei (figure IV-2). The abcissa is the mean frequency as
defined in equation (IV-20).
The units that were supposed to be auditory nerve fibers (AN(?))
(although recorded in the cochlear nuclei) all showed relatively large
strengths at least up to 3.5 kHz.
The units in the ventral cochlear nucleus (VCN) vary in strength from
large to zero, whereas the dorsal cochlear nucleus (DCN) units nearly
all have low to zero strength (cf. also Levine, 1971).
The starting points τ_0, determined by visual inspection are given in
figure IV-3. Although τ_0 is not the same as the latency as defined
for click PSTH's by Kiang, in figure 3 the mean of Kiang's latency data
(1965) are given for comparison.

IV.3.2   Indirect observation

IV.3.2.1 The spectrum

The first indirect observation to be made is the frequency content or
the spectrum of $R(\tau)$.

$$\hat{R}(\omega) = \int_{-\infty}^{+\infty} R(\tau) \; e^{-i\omega\tau} \; d\tau \qquad\qquad (IV-6)$$

and in particular $|\hat{R}(\omega)|$, the amplitude spectrum or spectral envelope.
The characteristics to be extracted from this spectral envelope are the
first two moments, the mean and the variance (see Chapter IV.4).
Furthermore, while pure tone experiments were also carried out (van
Gisbergen, 1974) the opportunity exists to compare responses to
broadband and pure tone stimulation.

Figure IV-4A represents the relation between CF, measured with pure tones and the mean frequency of $|\hat{R}(\omega)|$ (as defined in equation IV-20), figure IV-4B shows the relation between the 10 dB bandwidths of spectral envelope and response area for those units where both measurements are carried out, and figure IV-4C gives an example of a comparison of the spectral envelope and the response area for unit 54-3. (The response area here, is in fact an intensity frequency scan as described by van Gisbergen (1974)).

The absolute intensity of the spectrum in figure IV-4C is chosen in order to match the response area.

It can be concluded that in general narrow- and broadband stimulation give comparable responses, and no systematic differences are found, with the exception of some units, for which the differences can be explained. The units that have a lower CF than μ_f (in figure IV-4A) are units that have an apparent convergence (spectrum is multimodal and asymmetric), and the units with a higher CF than μ_f lost their high frequency part of the spectrum, due to the influence of time lock. The latter argument also explains the deviations in figure IV-4B at the greater bandwidth (cf Johannesma, 1971).

IV.3.2.2 The time course

Looking in more detail at the time course of $R(\tau)$, we can distinguish between the oscillation of the signal and the form of the envelope that covers the oscillation. In general $R(\tau)$ has one dominant frequency (which also follows from the spectrum) suggesting $R(\tau)$ to be an amplitude modulated sinusoid.

To obtain the time envelope we define the analytic signal,

$$\rho(\tau) = R(\tau) + i\tilde{R}(\tau) \tag{IV-7}$$

where $\tilde{R}(\tau)$ is the quadrature signal or Hilberttransform of $R(\tau)$ (Deutsch, 1969, Gabor, 1946).

$$\tilde{R}(\tau) = \frac{1}{\pi} \int_{-\infty}^{+\infty} \frac{R(t)}{\tau-t} \, dt \tag{IV-8}$$

(the symbol $\int$ stands for the Cauchy principal value).

118

It can be shown that the spectra of $R(\tau)$ and $\tilde{R}(\tau)$ are related as

$$\overset{\sim}{\hat{R}}(\omega) = -i \; \text{sign}(\omega) \; \hat{R}(\omega)$$
$$= i\hat{R}(\omega) \qquad\qquad \omega < 0$$
$$= 0 \qquad\qquad\qquad \omega = 0 \qquad\qquad (\text{IV-9})$$
$$= -i\hat{R}(\omega) \qquad\qquad \omega > 0$$

with the consequence that

$$\hat{\rho}(\omega) = \hat{R}(\omega) + i\{-i \; \text{sign}(\omega) \; \hat{R}(\omega)\}$$
$$= 0 \qquad\qquad\qquad \omega < 0$$
$$= \hat{R}(\omega) \qquad\qquad \omega = 0 \qquad\qquad (\text{IV-10})$$
$$= 2\hat{R}(\omega) \qquad\qquad \omega > 0$$

Thus the spectrum of $\rho(\tau)$ vanishes for $\omega < 0$ (cf. the well known situation of a causal time function $f(t)$, $f(t) = 0$ for $t < 0$, where the real and imaginary parts of the spectrum are Hilberttransforms (Papoulis, 1962)). From equation (IV-9) it is clear that the spectral envelopes of $R(\tau)$ and $\tilde{R}(\tau)$ are equal, but the phase is shifted over $\frac{\pi}{2}$ for all frequencies, so their time envelopes are equal and they are orthogonal functions.

The most common Hilbert pair is $\cos \omega t$ and $\sin \omega t$, which indeed have the same frequency content, $\frac{\pi}{2}$ phase shift and equal time envelope, and which are orthogonal.

Equation IV-10 also gives an easy way to compute $\tilde{R}(\tau)$ (see appendix II). Now the time envelope of $R(\tau)$ can be defined as

$$A(\tau) = |\rho(\tau)| = \sqrt{R^2(\tau) + \tilde{R}^2(\tau)} \qquad\qquad (\text{IV-11})$$

and from the phase of $\rho(\tau)$

$$\phi(\tau) = \text{arctg} \; \frac{\tilde{R}(\tau)}{R(\tau)} \qquad\qquad (\text{IV-12})$$

an instantaneous frequency

$$\Omega(\tau) = \frac{d\phi(\tau)}{d\tau} \qquad\qquad (\text{IV-13})$$

can be defined.

TIME SIGNAL   UNIT 65 2 3
                                     ORIGINAL CURVE

                                     20.00 MSEC

HILBERT TRANSFORM OF TIME SIGNAL

                                     20.00 MSEC

TIME ENVELOPE   UNIT 65 2 3
                                     ORIGINAL CURVE

                                     20.00 MSEC

'PHASE' IN TIME DOMAIN
50 PI

                                     20.00 MSEC
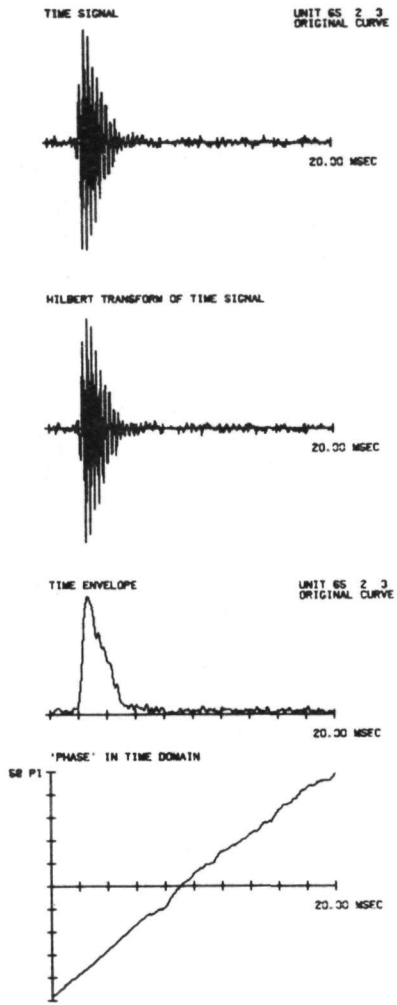
fig. IV-5   Crosscorrelation function R(τ) for unit 65-2, with its
            Hilberttransform R̂(τ), its envelope A(τ) and 'phase' φ(τ).
            Note that the phase is a straight line in the region where
            A(τ) is large, indicating a constant frequency.

120

So now

$$\rho(\tau) = A(\tau) \, e^{i\phi(\tau)} \tag{IV-14}$$

Figure IV-5 gives an illustration of $R(\tau)$, $\tilde{R}(\tau)$, $A(\tau)$ and $\phi(\tau)$ for unit 65-2.

At this point we can verify the amplitude modulation idea, mentioned before. Amplitude modulation means that the oscillation has a constant instantaneous frequency or in terms of (IV-12) and (IV-13), $\phi(\tau)$ must increase linear with time. In general this is the case, at least in the significant part of $R(\tau)$ (figure IV-5).
Therefore (IV-14) can be written as

$$\rho(\tau) = A(\tau) \, e^{i\omega_0\tau} \tag{IV-15}$$

having the consequence that in the frequency domain

$$\hat{\rho}(\omega) = \hat{A}(\omega-\omega_0) \tag{IV-16}$$

signifying that at least $\hat{\rho}(\omega) = 2\hat{R}(\omega)$, $\omega > 0$, must be symmetrical around ω_0 and vanish at $\omega = 0$.
This gives a second clue to verify the amplitude modulation hypothesis. (See also figure IV-4A, a symmetrical spectrum has a mean frequency equal to the CF).

IV.4   COMPUTATION OF CHARACTERISTICS

IV.4.1   Preprocessing

When looking at the $R(\tau)$ as shown in figure IV-1 it will be clear that characteristics extracted from them are strongly influenced by the residual noise. Therefore some preprocessing is necessary. We have chosen for a weighting procedure, both in time- and frequency domain. (See also appendix II).
In the time domain the original $R(\tau)$ is weighted with a function as shown in figure IV-6. The edges were drawn by hand by means of a joy stick on the computerdisplay for every individual $R(\tau)$. The weighted function was fouriertransformed and a similar weighting was performed

R(τ)

weighting function
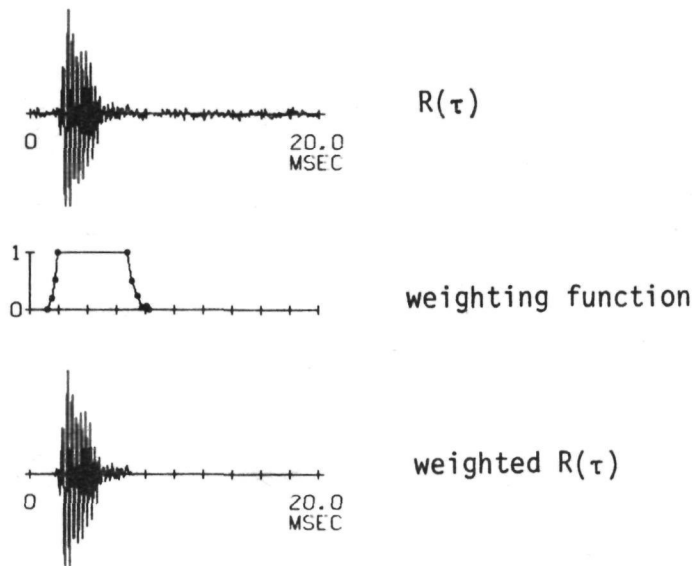
weighted R(τ)

fig. IV-6   Weighting function in the time domain :   R(τ) is weighted
            with the weighting function, which is drawn with a joystick
            on a computerdisplay.   With the joystick the circles in the
            weighting function are indicated and a linear interpolation
            is carried out between them.   The weighting function is
            determined for the envelope but used for the time function
            itself.   A similar procedure is carried out in the frequency
            domain.

in the frequency domain. The weighted spectrum underwent an inverse

fourier transform and the new time function was compared with the

original one. When by visual inspection the relevant parts of R(τ) were

not affected and the non-relevant parts were removed sufficiently

the weighting procedure was terminated, otherwise the weighting procedure

was restarted either with the weighted function or with the original.

With this procedure continuous control is possible in both, time- and

frequency domain, because a too rigorous weighting in one domain,

immediately introduces a broadening in the other.

122

In general the decisions that have to be taken regarding the drawing
of the weighting function are difficult, owing to the uncertainties in
the transitions between the relevant part and the nonrelevant noise
(in both domains)
In most cases, however, different experimentalists have chosen similar
weighting functions with similar results.
The weighting procedure still gives rise to the main errors and
uncertainties in the computations.

IV.4.2   Definition of the characteristics

For the description of $R(\tau)$ a limited set of characteristics will be
introduced, which will be extracted, as already mentioned, from the
weighted function.
The set of characteristics to be chosen are the low-order moments in
both domains, 1 e. the energy contained in $R(\tau)$ and the first two
moments in time- and frequency domain.
As usual in physics and signal theory we will define these moments with
respect to the energy density distributions in both domains, i.e. the
square of the envelopes, rather than with respect to the envelopes
themselves (Gabor, 1946).
We then arrive at the following set
1. The energy contained in $R(\tau)$

$$E = \int_{-\infty}^{+\infty} d\tau \; \rho^*(\tau) \; \rho(\tau) = \int_{-\infty}^{+\infty} d\tau \; A^2(\tau) \qquad\qquad (IV-17)$$

$$= \frac{1}{2\pi} \int_{-\infty}^{+\infty} d\omega \; \hat{\rho}^*(\omega) \; \hat{\rho}(\omega)$$

(the asterisk denotes the complex conjugate)
The strength as used in IV.3.1 now is equal to $\sqrt{E}$.
2. The mean of the time envelope

$$\mu_\tau = \frac{1}{E} \int_{-\infty}^{+\infty} d\tau \; \rho^*(\tau) \; \tau \; \rho(\tau) \qquad\qquad (IV-18)$$

$$= \frac{1}{E} \int_{-\infty}^{+\infty} d\tau \; A^2(\tau) \; \tau$$

123

It may be useful to divide μ_τ into two components.

a. the sum of a number of pure time delays τ_0.

This is the time at which the oscillation starts, and which is already given in figure IV-3.

τ_0 is supposed not to be related to any property of the supposed filter, but is a composition of the acoustic delay, the travelling time along the cochlea, the synaptic delay and the conduction time along the auditory nerve.

b. a component due to the filter properties $\mu_\tau - \tau_0$

3. The standard deviation of the time envelope, which is a measure for the time duration or time width

$$\sigma = \left\{ \frac{1}{E} \int_{-\infty}^{+\infty} d\tau \, \rho^*(\tau) \, \tau^2 \, \rho(\tau) - \mu_\tau^2 \right\}^{\frac{1}{2}} \qquad \text{(IV-19)}$$

$$= \left\{ \frac{1}{E} \int_{-\infty}^{+\infty} d\tau \, A^2(\tau) \, \tau^2 - \mu_\tau^2 \right\}^{\frac{1}{2}}$$

4. The mean of the spectral envelope

$$\mu_f = \frac{1}{E} \int_{-\infty}^{+\infty} df \, \hat{\nu}^*(f) \, f \, \hat{\rho}(f) \qquad \text{(IV-20)}$$

$$= \frac{2}{E} \int_{0}^{+\infty} df \, |\hat{R}(f)|^2 \, f$$

We have chosen the mean frequency, rather than the frequency of the maximum, as is usual in neurophysiology (characteristic frequency), because the mean is a better characteristic as it is influenced by the whole spectrum (for most units, however, the CF and μ_f do not differ very much, figure IV-4A).

5. The standard deviation of the spectral envelope or the spectral width

$$\sigma_f = \left\{ \frac{1}{E} \int_{-\infty}^{+\infty} df \, \hat{\rho}^*(f) \, f^2 \, \hat{\rho}(f) - \mu_f^2 \right\}^{\frac{1}{2}} \qquad \text{(IV-21)}$$

$$= \left\{ \frac{2}{E} \int_{0}^{+\infty} df \, |R(f)|^2 \, f^2 - \mu_f^2 \right\}^{\frac{1}{2}}$$

6. The combined time- frequency property

$$\Delta = \sigma_\omega \sigma_\tau = 2\pi\sigma_f \sigma_\tau \qquad\qquad\qquad\text{(IV-22)}$$

where σ_f and σ_τ are defined as in equation (IV-21) and equation (IV-19). According to the uncertainty relation (Gabor, 1946) there is a lower limit to this product of time width and spectral width

$$\Delta = \sigma_\omega \sigma_\tau \geq 0.5$$

The lower limit can only be reached by signals with a Gaussian time envelope $e^{-\alpha t^2}$, that also have a Gaussian spectral envelope (elementary signals according to Gabor).

Since Gaussian envelopes are not causal, the lower limit of Δ cannot be reached by causal time functions. However it can be sufficiently approached by the causal time function introduced in Chapter IV.5 (Papoulis, 1962).

This characteristic Δ can be seen as a combined time- frequency resolution or as a measure for the optimality of a filter. The smaller Δ, the better is the time resolution for a given frequency resolution or vice versa.

IV.4.3   Results of characterization

Table I gives the characteristics extracted from the weighted curves for all the units, together with their location.

Some attention must be given to units 53-4 and 64-1. They gave an $R(\tau)$ but their spectra did not fit the response area, and showed only an overlap in the low frequency part. This means that the time lock is good enough for these low frequencies, but not for the high frequencies (Johannesma, 1971). Also the shifting procedure did not work, because of the dominant role of the low frequency part.

Figure IV-7 gives the characteristics as a function of μ_f. Although no differences can be observed with respect to the location, different symbols are used for the locations, because location is an independent variable.

Figure IV-7A and B both indicate that the time width of $R(\tau)$ is decreasing with increasing μ_f, but they represent different aspects.
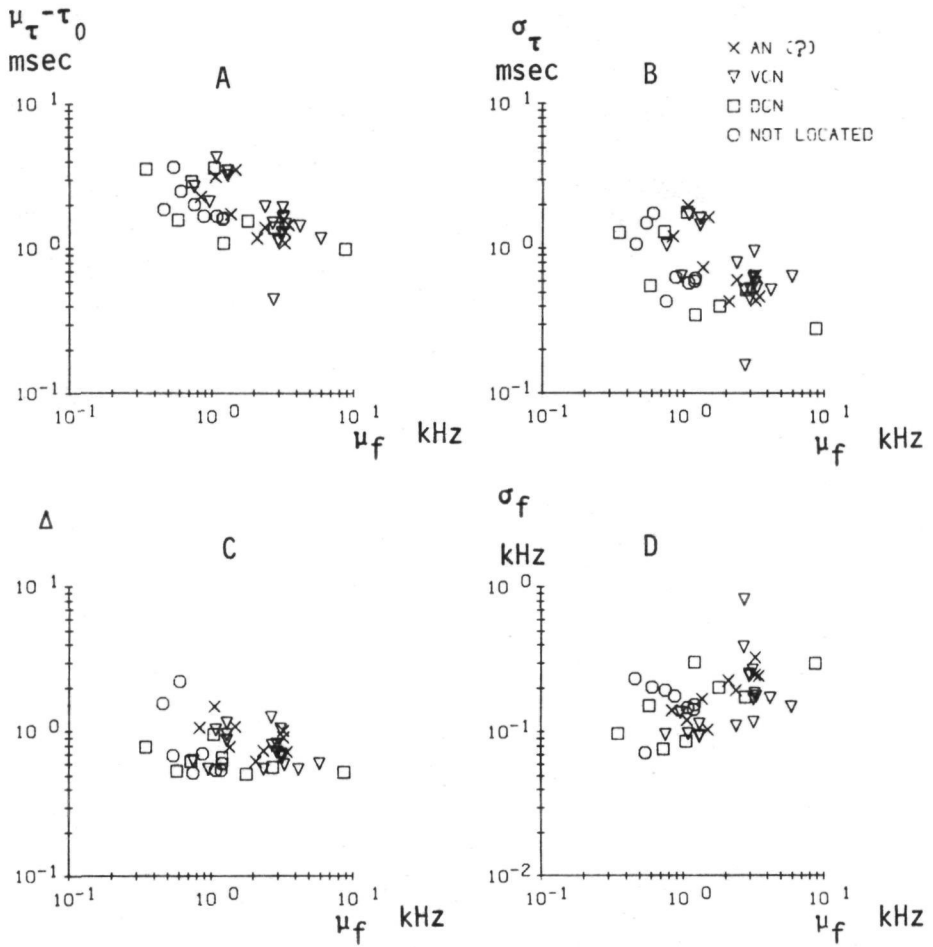
Fig. IV-7 Results of the characterization
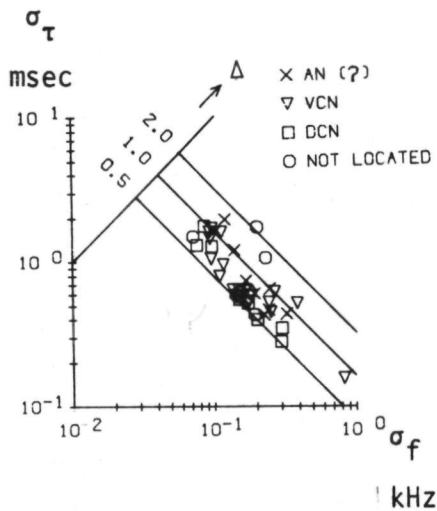
Fig. IV-8   Relation between σ_τ, σ_f and Δ.
　　　　　With figure 7C it is clear that Δ is independent from μ_f as
　　　　　well as from σ_f or σ_τ.
　　　　　Note : $\Delta = \sigma_\omega \sigma_\tau = 2\pi\sigma_f\sigma_\tau$.

Figure IV-7D shows that σ_f is increasing with increasing μ_f, but not
proportional, causing an increasing bandwidth of the same order as found
in literature (Møller, 1972). This is another indication (like
figure IV-4B) that there are no systematic differences in the responses
to broadband and narrowband stimulation.

However, σ_f is increasing in the mean as fast as σ_τ is decreasing, which
gives rise to a constant Δ (apart from the scatter), (figure IV-7C),
which indicates that along the basilar membrane a constant time-frequency
resolution is maintained.

Figure IV-8 shows that the constancy of Δ also is maintained over the
whole σ_f- and σ_τ range respectively.

The two units with highest Δ (25-9 and 28-5) are units with
multimodal spectra, suggesting strongly convergence and causing
relative high σ_f.

Furthermore it can be seen that primary units (AN (?)) never have very
small Δ values.

The results for Δ suggest that Δ may be an important characteristic for the neuron. In general being constant, the individual variations might indicate relevant differences in the population of neurons.

IV.5   MATHEMATICAL APPROXIMATION AND PARAMETER EXTRACTION

IV.5.1   The function

In the previous chapter we described $R(\tau)$ in a general way by its moments. When, however, we want to use $R(\tau)$ in some numerical way (models, mathematical manipulation, etc.) the characteristics of Chapter IV.4 are too general and it should be preferable to describe $R(\tau)$ by a mathematical function.

Now looking at the $R(\tau)$'s it becomes apparent that many of them have similar time courses and spectra, so the introduction of a mathematical function indeed may be possible.

The following considerations are made with regard to the choice of the function. The function is only intended to describe the simple $R(\tau)$'s. Those which have an apparent convergence cannot be described by the same function as the simple ones.

For the so-called simple $R(\tau)$'s the amplitude modulation hypothesis, mentioned above (IV.3.2.2), fairly holds true, judged by the conditions stated there. This means that we will approximate $R(\tau)$ by $R'(\tau)$

$$R'(\tau) = A'(\tau) \cos(\omega_0 \tau + \phi_0) \tag{IV-23}$$

where $\omega_0 = 2\pi_{\vdash f}$

Because of causality $A'(\tau)$ must be zero for $\tau < 0$ and moreover it appears that the leading edge is always steeper than the trailing edge. Furthermore we would like $A'(\tau)$ to have only a few parameters and a simple spectrum.

Therefore we suggest for $A'(\tau)$

$$A'(\tau) = c \left[\frac{\tau-\alpha}{\beta}\right]^{\gamma-1} e^{-\frac{\tau-\alpha}{\beta}} \qquad \tau \geq \alpha \tag{IV-24}$$

$$= 0 \qquad\qquad\qquad \tau < \alpha$$

128

with the spectral envelope

$$|\hat{A}'(\omega)| = c \ \Gamma(\gamma) \ \beta \ (1 + \omega^2\beta^2)^{-\gamma/2} \qquad\qquad (IV-25)$$

where $c = \left|\dfrac{E}{\dfrac{\beta \ \Gamma(2\gamma-1)}{2^{2\gamma-1}}}\right|^{\frac{1}{2}}$ is a scaling factor to give $R(\tau)$ and $R'(\tau)$

equal energy (this factor will be ignored in the following), α is a pure time delay, β can be considered as a time scaling factor and γ is a factor indicating the form of $A'(\tau)$. A small γ means a very asymmetric and a great γ means a symmetric envelope. (for $\gamma \to \infty$ $A'(\tau)$ will approach a Gaussian envelope). In the literature equation (IV-24) is known as a generalised gamma distribution or a Pearson type III distribution.

So now $R(\tau)$ is approximated by

$$R'(\tau) = \left(\frac{\tau-\alpha}{\beta}\right)^{\gamma-1} e^{-\frac{\tau-\alpha}{\beta}} \cos(\omega_0\tau + \phi_0) \qquad\qquad (IV-26)$$

and $\qquad \hat{R}'(\omega) = \dfrac{\Gamma(\gamma) \ \beta \ e^{\pm i(\alpha\omega_0 + \phi_0)}}{(1 \mp i\omega_0\beta + i\omega\beta)^\gamma} \qquad\qquad (IV-27)$

The spectrum (IV-27) indicated a filter with γ polepairs at

$$p = i\omega = \frac{-1 \pm i\omega_0\beta}{\beta} = -\frac{1}{\beta} \pm i\omega_0 \qquad\qquad (IV-28)$$

each having a quality factor

$$q = \frac{\beta\omega_0}{2} \qquad\qquad (IV-29)$$

and having the minimum phase property.

Already here it should be noted that if $\beta \propto \dfrac{1}{\omega_0}$ then $A'(\tau)$ is of the form

$$w(t,\omega_0) = v(\omega_0 t) \ t^b \qquad t > 0 \qquad\qquad (IV-30)$$

which according to Gambardella (1968, 1969) means that the form invariance property in short time spectral analysis holds. Furthermore, it must be remembered that Flanagan (1965) for his model

$$A'(\tau) = \left(\frac{\tau-\alpha}{\beta}\right)^{\gamma-1} \exp\left[-\left(\frac{\tau-\alpha}{\beta}\right)\right]$$

α = 3.0 msec
β = 1.0 msec
γ = 2.5

$$E'(\tau) = \left\{\left(\frac{\tau-\alpha}{\beta}\right)^{\gamma-1} \exp\left[-\left(\frac{\tau-\alpha}{\beta}\right)\right]\right\}^2$$

$$\mu'_\tau = \alpha + \beta(\gamma - \tfrac{1}{2})$$
$$\sigma^2_\tau = \tfrac{1}{2}\beta(2\gamma-1)$$
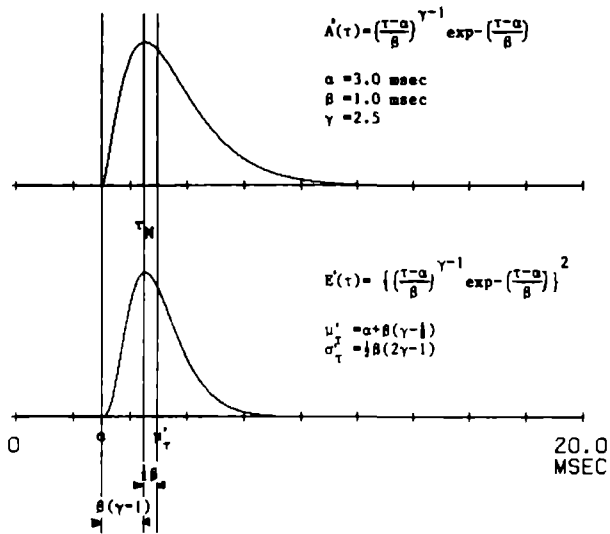
Fig. IV-9   Example of the proposed mathematical approximation $A'(\tau)$ and the energy density distribution $E'(\tau) = A'^2(\tau)$

of the basilar membrane of the human ear, introduced the function

$$(t\omega_0)^2\, e^{-\,t\omega_0/2} \qquad\qquad (IV-31)$$

which also apparently satisfies equation (IV-30).

Figure IV-9 shows an example of the proposed $A'(\tau)$ and its square, the energy density distribution $E'(\tau) = A'^2(\tau)$ with an indication of the influences of the parameters α, β and γ

Note that the moments we defined in IV.4 2 are the moments of the energy density distribution in time and frequency domain, whereas the parameters α, β and γ are introduced for the time envelope itself.

130

Also note that $E'(\tau)$ $(= A'^2(\tau))$ belongs to the same class of functions

$$E'(\tau) = \left[\left(\frac{\tau-\alpha}{\beta}\right)^{\gamma-1} e^{-\frac{\tau-\alpha}{\beta}} \right]^2 \qquad (IV\text{-}32)$$

$$= \left(\frac{\tau-\alpha}{\beta}\right)^{2\gamma-2} e^{-\frac{\tau-\alpha}{\beta/2}}$$

$$= \frac{1}{2^{2\gamma-2}} \left(\frac{\tau-\alpha}{\beta/2}\right)^{2\gamma-2} e^{-\frac{\tau-\alpha}{\beta/2}}$$

which can be written with $\alpha_1 = \alpha$, $\beta_1 = \beta/2$, $\gamma_1 = 2\gamma-1$, as

$$E'(\tau) = \frac{1}{2^{\gamma_1-1}} \left(\frac{\tau-\alpha_1}{\beta_1}\right)^{\gamma_1-1} e^{-\frac{\tau-\alpha_1}{\beta_1}} \qquad (IV\text{-}33)$$

so equation (IV-33) and equation (IV-24) have the same form.

IV.5.2 The estimation

Now the question arises how to estimate $R(\tau)$ by an $R'(\tau)$ i e. how to find the parameterset α, β, γ, ω_0, ϕ_0.
One possibility can be some kind of iteration procedure that leads to a minimum mean square deviation. But because of the emphasis we laid on the moments, we have chosen the method of moments i.e. the equation of the first two moments in both time and frequency domain of $R(\tau)$ and $R'(\tau)$.
So the parameters α, β, γ and ω_0 will be computed from μ_τ', σ_τ', μ_f' and σ_f', which get their values from μ_τ, σ_τ, μ_f and σ_f respectively. The remaining parameter ϕ_0 finally is formed by extrapolating the μ_f-oscillation of $R(\tau)$ to $\tau = 0$. The relations between α, β, γ and ω_0 and the moments μ_τ', σ_τ', μ_f' and σ_f' can be derived to be
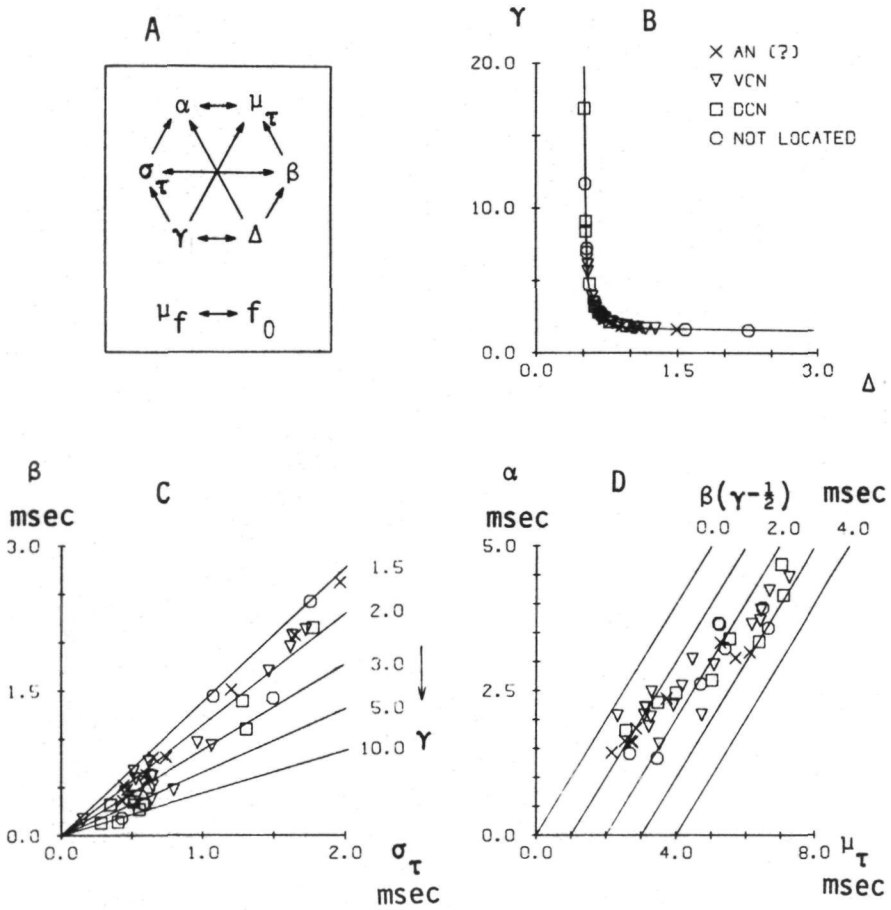
Fig. IV-10A   Influences of the characteristics on the parameters and
               vice versa.
       10B,C,D Relations between α, β, γ and Δ, σ_τ, μ_τ. The solid
               lines represent the relations of equation IV-36 and the
               points the experimental data.

132

$$\mu_f^! = \omega_0/2\pi \quad \text{or} \quad \mu_\omega = \omega_0$$

$$\sigma_f^! = \frac{1}{2\pi} \{\beta^2(2\gamma-3)\}^{-\frac{1}{2}} \quad \text{or} \quad \sigma_\omega^! = \{\beta^2(2\gamma-3)\}^{-\frac{1}{2}}$$

$$\mu_\tau^! = \alpha + \beta(\gamma-\tfrac{1}{2}) \tag{IV-34}$$

$$\sigma_\tau^! = \frac{1}{\sqrt{2}} \beta(\gamma-\tfrac{1}{2})^{\frac{1}{2}}$$

and
$$\Delta^! = \sigma_\tau^! \sigma_\omega^! = \tfrac{1}{2}\left(\frac{2\gamma-1}{2\gamma-3}\right)^{\frac{1}{2}}$$

By inverting these relations and substituting

$$\mu_f^! = \mu_f$$
$$\sigma_f^! = \sigma_f$$
$$\mu_\tau^! = \mu_\tau \tag{IV-35}$$
$$\sigma_\tau^! = \sigma_\tau$$
$$\Delta^! = \Delta$$

we arrive at

$$\alpha = \mu_\tau - \beta(\gamma-\tfrac{1}{2})$$

$$= \mu_\tau - \sigma_\tau \left(\frac{2\Delta^2}{\Delta^2-\tfrac{1}{4}}\right)^{\frac{1}{2}}$$

$$\beta = \frac{\sigma_\tau \sqrt{2}}{(\gamma-\tfrac{1}{2})^{\frac{1}{2}}} \tag{IV-36}$$

$$= \left(2\sigma_\tau^2 - \frac{1}{2\sigma_\omega^2}\right)^{\frac{1}{2}}$$

$$\gamma = \frac{\Delta^2}{\Delta^2 - \tfrac{1}{4}} + \tfrac{1}{2}$$

$$\omega_0 = 2\pi\mu_f$$

From equation (IV-36) it follows that the set μ_τ, σ_τ, μ_f and Δ is more suitable than the set μ_τ, σ_τ, μ_f and σ_f, so we will use Δ instead of σ_f. The influences of the sets α, β, γ, ω_0 and μ_τ, σ_τ, μ_f, Δ upon each
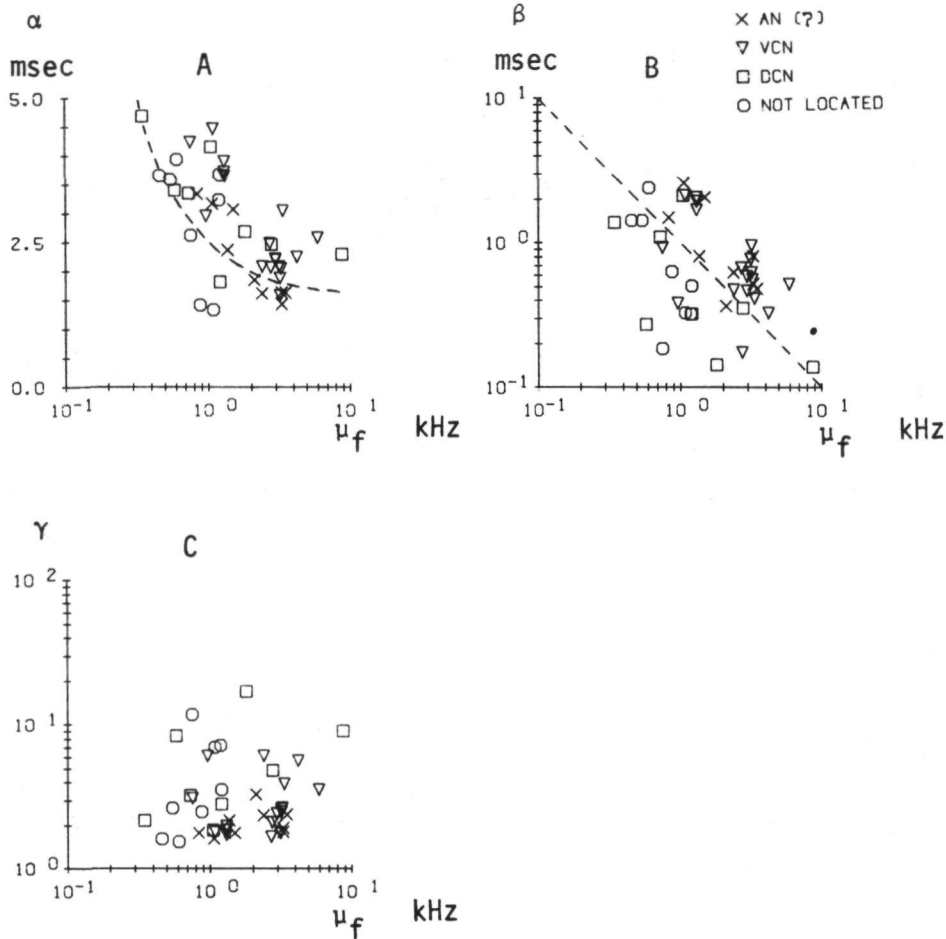
Fig. IV-11 The extracted parameters as a function of the mean frequency.
The interrupted line in A is the mean of Kiang latency data
(Kiang, 1965) corrected for an acoustic delay of 0.2 msec.
(as in figure IV-3).
The interrupted line in B indicates $\beta = \frac{1}{\mu_f}$.

other can be visualized as in figure IV-10A.

Furthermore the relations (IV-36) are given as the solid lines in figure IV-10B,C,D.

Note that for Gaussian envelopes ($\Delta=0.5$) γ will go to infinity and β to zero, while for very skew envelopes (Δ is large) γ has a minimum of 1.5.

IV.5.3   Results of the parameter extraction

To the $R(\tau)$ of the neurons reported in Chapter IV.4.3 an $R'(\tau)$ is connected resulting in the parameter values of α, β, γ, ω_0 and ϕ_j as given in table II.

Figures IV-10B,C,D display the results in relation to the dependences between the parameters α, β, γ, and the characteristics μ_τ, σ_τ and Δ. From figure IV-10B it is clear that for small Δ, γ increases very fast, so computation errors in σ_f and σ_τ in this region have tremendous effects on γ.

Figure IV-10C also indicates that the greater γ-values occur in the small β,σ_τ region and shows that for small β $\beta<\sigma_\tau$ whereas for large β $\beta>\sigma_\tau$. (This can be seen in more detail in figure IV-12)

Figure IV-10D shows a positive correlation between α and $\beta(\gamma-\frac{1}{2})$, $-\alpha$. Both are increasing for increasing μ_τ.

Figures IV-11 A to C show α, β and γ as a function of μ_f.

In all figures there is a lot of scatter and no clear distinction can be made between VCN and DCN units. The AN(?) units seem to have less scattering, so it is possible that for the primary units stronger relations can be inferred (cf. de Boer and de Jongh, 1974), which are disturbed in the cochlear nuclei.

Figure IV-11A shows α, and about the same relation can be seen as for τ_0 (figure IV-3), as could be expected. However, α and τ_0 are determined in very different ways : τ_0 by visual inspection of the starting point, and α is computed from the moments, and thus α is influenced by the whole $R(\tau)$. As in figure IV-3, in figure IV-11A the mean of Kiang latency data (1965) is given, although as τ_0, α is not the latency α for instance is not intensity dependent, and the latency certainly is.
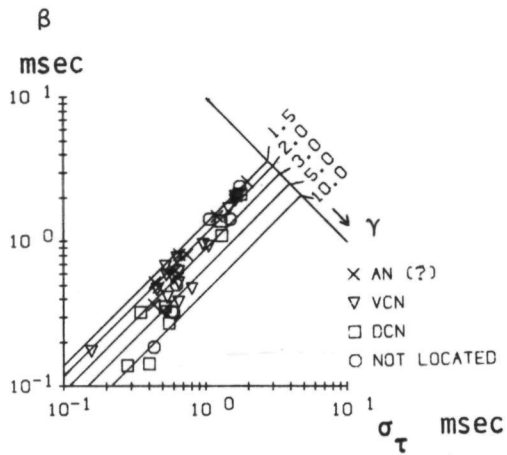
Fig. IV-12   The (β, σ_τ, γ) relation on logarithmic coordinates.
Note that the point with lowest σ_τ is unit 64-1
(cf. Chapter IV.3.2.1) of which the σ_τ is evidently too
small.
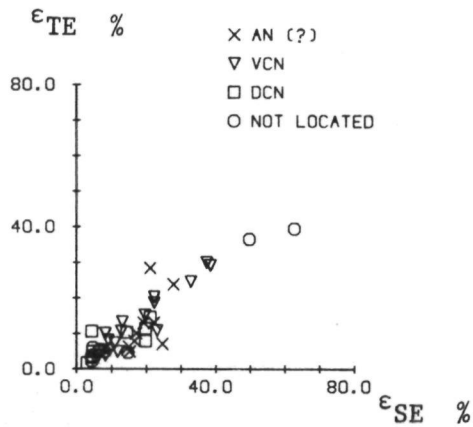
Fig. IV-13 ϵ_{SE} versus ϵ_{TE}
The units with greatest ϵ_{SE} are unit 25-9 (63%) and unit 28-5
(50%) which show an apparent convergence, unit 54-3-3 (39%)
fits badly because of the bad resolution of R(τ), and units
53-4 (37%) and 64-1 (33%) where the spectrum does not fit the
response area.

Figure IV-11B gives $\beta = f(\mu_f)$. Through the large amount of scatter only a weak relation to μ_f can be observed. However, looking at the AN(?) results and data of de Boer and de Jongh (1974), possibly a $\beta \propto 1/\mu_f$ relation can be observed in the auditory nerve. In the cochlear nuclei this relation is far more disturbed. The $\beta \propto 1/\mu_f$ result indicates that the form invariance property as mentioned in Chapter IV.5.1 may hold to some extend, although there is no evidence that the auditory system indeed exploits this property. Figure IV-11C shows γ to be independent of μ_f, as already the result for Δ (figure IV-7C) indicated The very great γ-values may be due, as mentioned above, to computational errors as γ is very sensitive in the higher values.

In figure IV-12 once more the β, σ_τ, γ relation is given, but now on logarithmic coordinates. As can be seen more clearly than in figure IV-10C there is a correlation between β and γ. The implication of this correlation is not understood yet.

The parameter ϕ_0 is not displayed, as it seems to have a random distribution between $+\pi$ and $-\pi$ (ϕ_0 can only be determined mod(2π)). Also the distribution of $\Psi_0 = \phi_0 + a\omega_0$ does not give any relation to μ_f. These results, however, may be due to the mod(2π) computation. If it were possible to compute ϕ_0 or Ψ_0 not mod(2π) we certainly would expect some kind of relation.

In table II also are given the root mean square deviations of both time and spectral envelopes, ϵ_{TE} and ϵ_{SE} defined as

$$\epsilon_{TE} = \left(\frac{\int \{A(\tau) - A'(\tau)\}^2 \, d\tau}{\int A^2(\tau) \, d\tau} \right)^{\frac{1}{2}} \cdot 100\% \qquad (IV-37)$$

$$\epsilon_{SE} = \left(\frac{\int \{|\hat{R}(\omega)| - |\hat{R}'(\omega)|\}^2 \, d\omega}{\int |\hat{R}(\omega)|^2 \, d\omega} \right)^{\frac{1}{2}} \cdot 100\% \qquad (IV-38)$$

The ϵ_{SE} and ϵ_{TE} are shown together in figure IV-13.

137

To illustrate the figures for τ, figure IV-14 shows two time envelopes with ε_{TE} being 14% and 2% respectively (units 60-8 and 44-3).

UNIT 44 3
CUTCURVE AND FITCURVE

$\varepsilon_{TE} = 2\%$

0.   20.00 MSEC

UNIT 60 8
CUTCURVE AND FITCURVE

$\varepsilon_{TE} = 14\%$

0.   20.00 MSEC
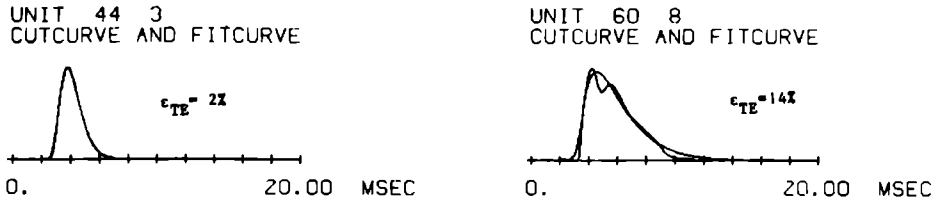
Fig. IV-14 Envelopes of weighted curve and approximation curve (cutcurve and fitcurve) to illustrate the fit.

IV.5.4 Characteristic times and time constant

Having introduced the mathematical approximation curve, we are in the position to give proper definitions of several characteristic times.

1. A pure time delay T_0, which obviously is

$$T_0 = \alpha \qquad\qquad (IV-39)$$

2. A rise time T_+

The time in which $A(\tau)$ reaches its maximum value is $\tau_M = \alpha + \beta(\gamma-1)$. We thus define the rise time

$$T_+ = \tau_M - \alpha \qquad\qquad (IV-40)$$

$$= \beta(\gamma-1)$$

3. A decay time T_-

Because of the influence of β and γ on the trailing edge, it is impossible to define a time constant for the decay. Also the time at which $A'(\tau)$ or $E'(\tau)$ decayed to 1% of their maximal value or at which 99% of their area is passed cannot be given in an analytical expression.

The best measure, therefore, is a measure in terms of the moments of $A'(\tau)$. The first two moments of $A'(\tau)$ expressed in β and γ, are

138

$$m_\tau = \int_0^\infty A'(\tau)\ \tau\ d\tau \qquad\qquad (IV\text{-}41)$$

$$= \alpha + \beta\gamma$$

$$s_\tau = \{ \int_0^\infty A'(\tau)\ \tau^2\ d\tau\ -\ m_\tau^2\ \}^{\frac{1}{2}} \qquad\qquad (IV\text{-}42)$$

$$= \beta\sqrt{\gamma}$$

The moments m_τ and s_τ must not be confused with μ'_τ and σ'_τ, which are the moments of $E'(\tau) = A'^2(\tau)$ as defined in Chapter IV.4.2.

We now propose as a decay time T_-

$$T_- = m_\tau + \lambda s_\tau - (T_+ + T_0) \qquad\qquad (IV\text{-}43)$$

$$= \alpha + \beta\gamma + \lambda\beta\sqrt{\gamma} - (\beta(\gamma-1) + \alpha)$$

$$= \beta(1 + \lambda\sqrt{\gamma})$$

The choice of the constant λ still depends on the appropriate requirements (for $\lambda=2$, the area outside $T_0 + T_+ + T_-$ is about 4%, for $\lambda=3$, about 1%).

4. An asymptotic time constant τ_∞. For very large τ the slope of $A'(\tau)$ is fully determined by $e^{-\frac{\tau-\alpha}{\beta}}$, so the asymptotic time constant is

$$\tau_\infty = \beta \qquad\qquad (IV\text{-}44)$$

The quantities defined above are once more depicted in figure IV-15.
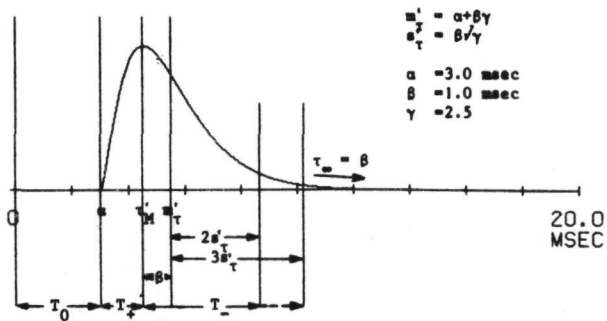
Fig. IV-15   Characteristic times and time constant

139

The present paper reports a first attempt to characterize and parameterize crosscorrelation functions obtained from the cochlear nuclei. Very much remains to be done and the number of neurons investigated is too low (certainly for the not time locked units) to draw definite conclusions. However, there are several more or less tentative conclusions that come forward.

1. The only property from the neurons that is related to the location in the cochlear nuclei is the strength and so the energy of $R(\tau)$. For the other properties no definite interrelations can be found. It appears that relations in the auditory nerve between several characteristics or parameters are somewhat stronger than in the cochlear nuclei, where much more scatter is found in the data.

2. The amplitudespectra or spectral envelopes of the $R(\tau)$'s do not differ systematically from the response areas, i.e. no significant differences can be found in the spectral sensitivity for broadband and narrow band stimulation. For time properties no such conclusions can be drawn.

3. The combined time-frequency resolution, expressed in the value of Δ does not systematically depend on the frequency of the neuron, whereas σ_τ and σ_ω both do. Roughly these can be expressed as (figure IV-7)

$$\sigma_\tau \propto \mu_f^{-\frac{1}{2}} \qquad\qquad\qquad (IV\text{-}45)$$

$$\sigma_\omega \propto \mu_f^{\frac{1}{2}}$$

$$\Delta = \text{constant}$$

4 For simple $R(\tau)$ a mathematical function can be found which adequately describes $R(\tau)$

$$R'(\tau) = c\left(\frac{\tau-\alpha}{\beta}\right)^{\gamma-1} e^{-\frac{\tau-\alpha}{\beta}} \cos(\omega_0\tau + \phi_0) \qquad (IV\text{-}46)$$

140

the parameters being approximately

$$\alpha = \alpha_0 + \frac{\alpha_1}{\mu_f}$$ (figure IV-11A) (IV-47)

$$\alpha_0 = 1.5 \text{ msec}$$

$$\alpha_1 = 2$$

$$\beta \propto \frac{1}{\mu_f}$$ (figure IV-11B) (IV-48)

$$\gamma = 2.5 \text{ (independent of } \mu_f) \quad \text{(figure IV-11C)}$$ (IV-49)

$$\omega_0 = 2\pi\mu_f$$ (IV-50)

ϕ_0 random ?

The relations (IV-47) to (IV-50) are disturbed by very large individual deviations, but with the individual parameters a rather good estimate for $R(\tau)$ is found.

5. It is possible to define a proper delay time and several characteristic times which opens the possibility to separate latencies in delay times and integration times.

141

unit	loc *)	$\sqrt{E}$ **)	μ_f kHz	σ_f kHz	μ_τ msec	σ_τ msec	Δ	τ_0 msec
21- 2	NL	0.120	1.08	0.15	3.47	0.58	0.54	1.8
24- 3	NL	0.027	0.87	0.18	2.68	0.64	0.71	1.0
24-12	NL	0.172	0.75	0.19	4.72	0.43	0.52	2.7
25- 7-1	NL	0.180	1.20	0.14	5.41	0.60	0.54	3.8
25- 7-2	NL	0.206	1.22	0.16	5.22	0.62	0.61	3.6
25- 9	NL	0.305	0.61	0.20	6.49	1.76	2.25	4.0
28- 5	NL	0.177	0.46	0.23	5.26	1.08	1.58	3.4
28- 6	NL	0.081	0.54	0.07	6.66	1.50	0.68	3.0
30- 7	DCN	0.096	0.35	0.10	7.05	1.28	0.78	3.5
30-10	VCN	0.097	0.96	0.14	5.10	0.64	0.55	3.0
30-11	VCN	0.072	0.75	0.10	6.69	1.06	0.64	4.0
32-11	DCN	0.010	0.60	0.15	5.57	0.56	0.54	4.0
32-12	VCN	0.000	--	--	--	--	--	-
33- 7	DCN	0.043	1.80	0.20	5.04	0.40	0.52	3.5
34- 5	DCN	0.164	1.21	0.30	2.58	0.35	0.66	1.5
36-11	DCN	0.036	1.06	0.09	7.10	1.78	0.96	3.5
38- 8	AN(?)	0.088	2.09	0.23	2.88	0.44	0.62	1.7
38-10	DCN	0.000	8.79	0.30	3.49	0.28	0.53	2.5
38-11	DCN	0.000	--	--	--	--	--	-
42- 1	DCN	0.000	--	--	--	--	--	-
42- 3	DCN	0.030	0.73	0.08	6.39	1.31	0.63	3.5
42- 6	AN(?)	0.086	2.38	0.19	2.78	0.61	0.74	1.4
44- 3	DCN	0.000	2.78	0.18	4.00	0.52	0.57	2.6
44- 8	VCN	0.000	4.21	0.17	3.93	0.52	0.56	2.5
44- 9	AN(?)	0.063	3.29	0.25	2.71	0.66	1.03	1.4
44-13	AN(?)	0.069	3.29	0.33	2.19	0.44	0.92	1.1
44-14	AN(?)	0.050	3.47	0.25	2.55	0.47	0.73	1.1
45- 3	AN(?)	0.123	1.08	0.12	6.12	1.97	1.49	3.0
52- 6	VCN	0.105	2.96	0.25	3.14	0.53	0.82	2.0
52- 7	VCN	0.098	2.97	0.25	3.12	0.46	0.72	2.0
53- 4	VCN	0.019	2.71	0.39	3.30	0.52	1.26	1.8
54- 2	VCN	0.023	1.10	0.10	7.25	1.72	1.04	3.0
54- 3-1	VCN	0.042	1.30	0.10	6.17	1.47	0.88	3.0
54- 3-2		0.039	1.30	0.09	6.42	1.62	0.96	3.0
54- 3-3		0.012	1.31	0.11	6.45	1.63	1.16	3.0
54- 4	AN(?)	0.120	1.51	0.10	5.71	1.65	1.08	2.2
56- 7	VCN	0.000	2.39	0.11	4.75	0.80	0.55	2.8
59- 5	AN(?)	0.117	1.38	0.17	3.73	0.74	0.79	2.0
60- 8	AN(?)	0.214	0.84	0.14	5.27	1.21	1.08	3.0
64- 1	VCN	0.072	2.73	0.83	2.35	0.16	0.82	1.9
64- 5	VCN	0.000	3.34	0.18	4.47	0.54	0.60	3.0
65- 1	VCN	0.000	5.89	0.15	4.17	0.65	0.61	3.0
65- 2-1	VCN	0.069	3.14	0.27	3.08	0.62	1.06	1.8
65- 2-2		0.044	3.21	0.18	3.28	0.59	0.68	1.6
65- 2-3		0.014	3.19	0.17	3.22	0.65	0.69	1.6
65- 2-4		0.005	3.21	0.12	3.52	0.96	0.71	1.6

Table I   Results of characterization

*)   NL : not located, AN(?) : possibly auditory nerve fibre, VCN :
     ventral cochlear nucleus, DCN : dorsal cochlear nucleus.

**)   power of stimulus = 1.000

unit	loc *)	f_0 kHz	α msec	β msec	γ	ϕ_0	ε_{SE} %	ε_{TE} %
21- 2	NL	1.08	1.34	0.33	6.94	1.05	4.4	3.7
24- 3	NL	0.87	1.42	0.63	2.49	1.41	8.0	5.1
24-12	NL	0.75	2.63	0.19	11.67	0.96	4.8	6.2
25- 7-1	NL	1.20	3.24	0.32	7.21	1.92	4.4	2.2
25- 7-2	NL	1.22	3.68	0.51	3.55	0.30	7.0	5.4
25- 9	NL	0.61	3.95	2.42	1.55	0.88	62.9	39.6
28- 5	NL	0.46	3.66	1.44	1.61	1.44	50.0	36.5
28- 6	NL	0.54	3.59	1.43	2.66	1.67	14.6	4.7
30- 7	DCN	0.35	4.69	1.40	2.19	1.94	19.8	7.8
30-10	VCN	0.96	2.96	0.38	6.07	0.86	8.2	3.8
30-11	VCN	0.75	4.24	0.94	3.10	1.33	9.0	8.2
32-11	DCN	0.60	3.40	0.27	8.40	0.53	4.8	5.0
32-12	VCN	--	--	--	--	--	--	--
33- 7	DCN	1.80	2.70	0.14	16.88	0.93	4.5	10.7
34- 5	DCN	1.21	1.83	0.32	2.83	0.61	19.9	11.5
36-11	DCN	1.06	4.16	2.15	1.87	1.62	21.3	14.8
38- 8	AN(?)	2.09	1.86	0.37	3.28	0.48	15.3	5.0
38-10	DCN	8.79	2.30	0.14	9.07	0.44	4.7	3.4
38-11	DCN	--	--	--	--	--	--	--
42- 1	DCN	--	--	--	--	--	--	--
42- 3	DCN	0.73	3.36	1.11	3.23	1.64	14.5	10.3
42- 6	AN(?)	2.38	1.62	0.63	2.35	0.22	19.3	13.2
44- 3	DCN	2.78	2.48	0.35	4.79	0.26	3.1	1.9
44- 8	VCN	4.21	2.25	0.33	5.65	0.02	6.5	4.0
44- 9	AN(?)	3.29	1.64	0.81	1.81	0.56	16.7	7.9
44-13	AN(?)	3.29	1.44	0.52	1.92	1.71	24.8	7.2
44-14	AN(?)	3.47	1.64	0.48	2.40	1.38	15.0	6.3
45- 3	AN(?)	1.08	3.17	2.62	1.63	1.20	28.0	24.0
52- 6	VCN	2.96	2.20	0.59	2.09	1.15	11.8	4.9
52- 7	VCN	2.97	2.23	0.47	2.41	1.82	12.8	10.8
53- 4	VCN	2.71	2.50	0.67	1.68	0.45	37.3	30.2
54- 2	VCN	1.10	4.47	2.14	1.80	0.16	13.1	13.4
54- 3-1	VCN	1.30	3.65	1.70	1.98	1.86	22.2	20.5
54- 3-2		1.30	3.73	1.95	1.88	0.29	22.3	18.9
54- 3-3		1.31	3.90	2.08	1.73	1.62	38.5	29.3
54- 4	AN(?)	1.51	3.08	2.07	1.77	1.78	21.2	28.6
56- 7	VCN	2.39	2.10	0.48	6.07	1.13	5.7	3.8
59- 5	AN(?)	1.38	2.37	0.82	2.16	1.20	17.3	10.1
60- 8	AN(?)	0.84	3.34	1.51	1.78	1.72	22.3	13.2
64- 1	VCN	2.73	2.07	0.18	2.09	1.08	32.8	24.7
64- 5	VCN	3.34	3.06	0.41	3.90	0.52	8.3	10.1
65- 1	VCN	5.89	2.58	0.52	3.53	0.31	6.4	5.0
65- 2-1	VCN	3.14	2.08	0.78	1.78	1.49	23.2	10.9
65- 2-2		3.21	2.05	0.56	2.67	0.79	9.2	5.2
65- 2-3		3.19	1.90	0.63	2.61	0.78	10.9	7.4
65- 2-4		3.21	1.59	0.97	2.49	0.63	19.5	15.4

Table II   Results of parametrization

← *)
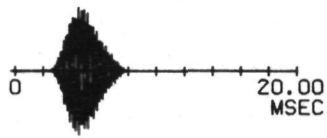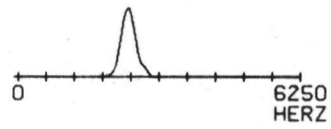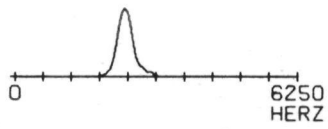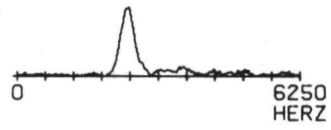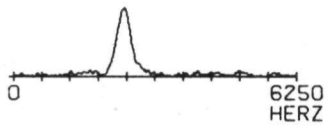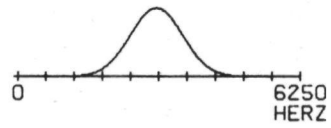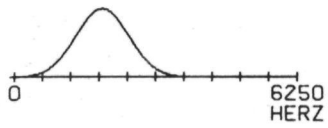
The shifting procedure

When the crosscorrelation does not yield an $R(\tau)$ which deviates clearly from the residual noise, we will assume that this is caused by some kind of jitter in the time of occurrence of the spikes. The origin of this jitter is not important here, the point is that the spikes are not originated at the moments that they should, in relation to the input signal. Consequently the problem to be solved is to find the original times of occurrence. We have solved it as follows :
We know from the obtained $R(\tau)$'s that the spikes are related to some wave form of the CF, and the CF we can obtain by other experiments. We now assume some waveform $R_0(\tau)$ of the CF with an arbitrary envelope like the proposed mathematical one, or a Gaussian one, and compute the crosscorrelation function of this $R_0(\tau)$ and the stimulus preceding the spike at $t = t_n$, $x(t_n - \tau) = x_n(\tau)$

$$\phi_{R,x_n}(v) = \frac{1}{T} \int_0^T R_0(\tau) \, x_n(\tau+v) \, d\tau \tag{AI-1}$$

Now $\phi_{R,x_n}(v)$ obviously will have some maximum in the neighbourhood of the spike, say at $v_{n,M}$. The assumption then is that in the case where no jitter was present, the spike should have been originated at this maximum, so at $t_n - v_{n,M}$ instead of t_n, and the spike is shifted

← Fig. AI-1   Adaptive shifting procedure for unit 56-7.

From top to bottom :
starting functions $R_{o,o}(\tau)$ of 1.9 kHz and 3.0 kHz resp.
spectra $\hat{R}_{o,o}(\omega)$
results of shifting procedure $R_{o,n}(\tau)$
spectra $\hat{R}_{o,n}(\omega)$
weighted $R_{o,n}(\tau)$
weighted $R_{o,n}(\omega)$
the two weighted functions in the same picture.

from t_n to $t_n - \nu_{n,M}$. This shifting is performed for all N spikes,
and a new crosscorrelation $R_1(\tau)$ can be made with the shifted spikes

$$R_1(\tau) = \frac{1}{N} \sum_{n=1}^{N} x_n(\tau + \nu_{n,M}) \qquad (AI-2)$$

Now, while $R_0(\tau)$ was arbitrary, $R_1(\tau)$ is not, and we can start another
shifting, by crosscorrelating the $x_n(\tau)$ with $R_1(\cdot)$, to see if there is
convergence to some waveform.

In the procedure above, we are crosscorrelating all $x_n(\tau)$ with the same
waveform, $R_0(\tau)$ or $R_1(\tau)$, which may lead to a stable, but wrong result.
Therefore we developed a second procedure, which is an adaptive one,
and in which the waveform, with which $x_n(\tau)$ is crosscorrelated, is
updated after every performed shifting.
We then start with an arbitrary waveform $R_{0,0}(\tau)$ that after n-1 spikes
will assumed to be $R_{0,n-1}(\tau)$. The crosscorrelation for $x_n(\tau)$ then will
be

$$\phi_n(\nu) = \frac{1}{T} \int_0^T R_{0,n-1}(\tau) \, x_n \, (\tau+\nu) \, d\tau \qquad (AI-3)$$

with a maximum at $\nu_{n,M}$.
We now update $R_{0,n+1}(\tau)$ by adding $x_n(\tau+\nu_{n,M})$ to it and obtain

$$R_{0,n}(\tau) = (1-a) \, R_{0,n-1}(\tau) + ax_n(\tau+\nu_{n,M}) \qquad (AI-4)$$

where a is a weighting constant.
When all N spikes are treated in this way again a second run can be
made, but now starting with $R_{1,0}(\tau) = R_{0,N}(\tau)$, to verify convergence.
We found that in general there are two possible results.
1. The result of the first method resembles $R_0(\tau)$ and diverges in the
   updating procedure, so the shifting failed. This may be the case,
   when the unit is not responding chiefly to one dominant frequency
   or when the simple 'only jitter' hypothesis is not true. This
   failure was found for 3 out of 9 neurons that were treated.
   It is not surprising that with the first method, there will always
   be a resulting waveform. In white noise all frequencies are present
   and at all times can we force the spike to the place required, i.e.

where the resemblance to the constant $R_0(\tau)$ is maximal. Even with a random pulse sequence, the $R_0(\tau)$ waveform will appear.

2. $R_1(\tau)$ or $R_{0,N}(\tau)$ is the result we searched for, may be apart from some minor details. At this moment we cannot substantiate this result , but this will be done in a future paper (Chapter III). However, we can make it plausible
When we use the shifting procedure twice on one unit, starting with $R_{0,0}(\ )$ having the wrong frequency (20% too high or too low
respectively) both results will have the right frequency. When we then remove residual noise and keep the common parts of the spectra (cf. Chapter IV 4.1), the two waveforms are practically identical, and we may assume that they are the right ones (see figure AI-1)

The shifting procedure was successful with 6 out of 9 units, up to 9 kHz.

The shifting procedure is, as mentioned, not always successful. The conditions to succeed are not totally clear yet as is the choice between the two mentioned methods. A lot of human interaction to the computer program is still necessary. However, the results seem to open the possibility to extend the analysis, related to the cross-correlation procedure, to higher frequency ranges.

The computerprogram BIREV

BIREV is a Fortran program written for a PDP-9 (Digital Equipment
Corporation) in which all the calculations and drawings for the complete
parametrisation of $R(\tau)$ are performed. In the main part the (fast)
fourier- and hilberttransforms are done together with the calculations
of the respective parameters and other data and the drawings.
A simplified scheme of this main part is given in figure AII-1
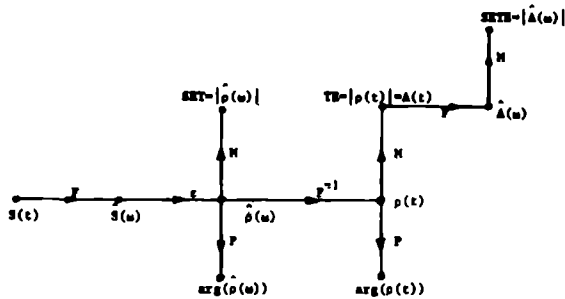
Fig. AII-1   Scheme of the main part of BIREV

$S(\tau)$	the appropriate inputsignal
F	fast fourier transform
	deletion of negative frequency components
	(see equation (IV-10)
F^{-1}	inverse fast fourier transform, yielding
	$\rho(t) = S(t) + i\, \tilde{S}(t)$
M.P	calculate modulus and argument (= phase) for the
	complex signal
SET	spectral envelope of time signal
TE	time envelope
SETE	spectral envelope of time envelope
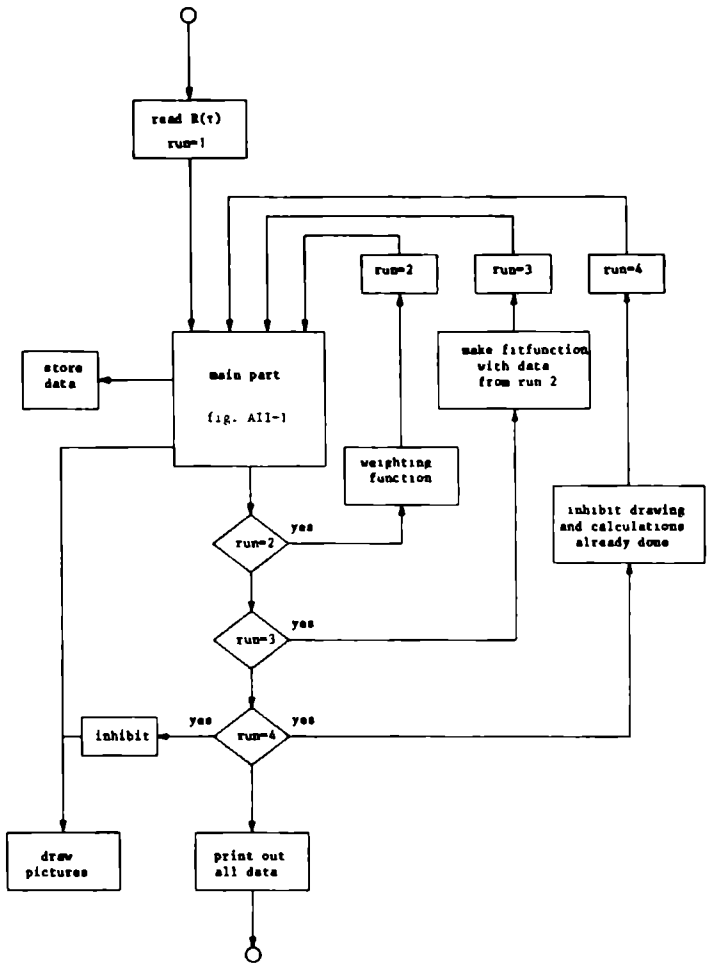
Fig. AII-2 Flow scheme of BIREV

| TIME SIGNAL UNIT 65 2 ORIGINAL CURVE | TIME SIGNAL UNIT 65 2 CUTCURVE | TIME SIGNAL UNIT 65 2 FITCURVE |

20.00 MSEC   20.00 MSEC   20.00 MSEC

| SPECTRAL ENVELOPE OF TIME SIGNAL UNIT 65 2 ORIGINAL CURVE | SPECTRAL ENVELOPE OF TIME SIGNAL UNIT 65 2 CUTCURVE | SPECTRAL ENVELOPE OF TIME SIGNAL UNIT 65 2 FITCURVE |

6250. HERZ   6250. HERZ   6250. HERZ

| TIME ENVELOPE UNIT 65 2 ORIGINAL CURVE | TIME ENVELOPE UNIT 65 2 CUTCURVE | TIME ENVELOPE UNIT 65 2 FITCURVE |

20.00 MSEC   20.00 MSEC   20.00 MSEC

| SPECTRAL ENVELOPE OF TIME ENVELOPE UNIT 65 2 ORIGINAL CURVE | SPECTRAL ENVELOPE OF TIME ENVELOPE UNIT 65 2 CUTCURVE | SPECTRAL ENVELOPE OF TIME ENVELOPE UNIT 65 2 FITCURVE |

0.   3125. HERZ   0.   3125. HERZ   0.   3125. HERZ

Fig. AII-3 Example of the several curves for unit 65-2.

This main part is passed through four times for every R(τ). The first
run computes data and draws pictures for the original curve, the second
run for the weighted curve (cutcurve), the third run for the approximation
(fitcurve) and the fourth run computes the root mean square deviations
of the envelopes of the second and third runs. (This fourth run is
necessary because of the limited memory size of the computer ($<$4K,
recently 32K). In this fourth run no drawings or other calculations
are made).

After the first run, separately, the weighting procedure, as described
in Chapter IV.4.1, is done and run two started with the weighted function.
During run two the parameters necessary to make the approximation curve
are computed and between run two and three this function is made so the
third run can start with the fitfunction. We have chosen this equal
treatment of the three functions (original, cut- and fitcurve) for
better comparison at every point in the main part of the program. An
overall flow scheme is given in figure AII-2 and the results for one
unit are given in figure AII-3 (apart from the vast numerical datalist).

REFERENCES

Boer E. de (1967)
        Correlation studies applied to the frequency resolution of
        the cochlea
        J. Audit. Res. 7, 209-217
Boer E. de (1968)
        Reverse correlation I
        Proc. Kon. Acad. v. Wetenschappen, C 71, 472-486
Boer E. de and Kuyper P. (1968a)
        Triggered correlation
        IEEE Tr. on Biomed. Eng. BME-15, 169-179
Boer E. de (1969)
        Reverse correlation II
        Proc. Kon. Acad. v. Wetenschappen, C 72, 129-151
Boer E. de (1969a)
        Encoding of the frequency information in the discharge
        pattern of auditory nerve fibers
        Intern. Audiology, 8, 547-556
Boer E. de and Jongh H.R. de (1971)
        Computer simulation of cochlear filtering
        Proc. 7th Intern. Congr. on Acoustics, paper 20H 12, 393-396
Boer E. de (1973)
        On the principle of specific coding
        J. of Dynamic Systems, Measurements and Control
        95-G, 3, 259-273
Boer E. de and Jongh H.R. de (1974)
        On cochlear excitation
        to be published
Deutsch R. (1969)
        System Analysis Techniques
        Prentice Hall Inc.
Flanagan J.L. (1965)
        Speech analysis,synthesis and perception
        Springer Verlag

Gabor D. (1946)
>Theory of communication
>J. IEE, 93(3), 26, 429-457

Gabor D. (1947)
>Acoustical quanta and the theory of hearing
>Nature 159, May 3, 591-594

Gambardella G. (1968)
>Time scaling and short-time spectral analysis
>J. Acoust. Soc. Am. 44(6), 1745-1747

Gambardella G. (1969)
>Properties of the short-time spectral analysis performed by
>the peripheral auditory system
>Proc. Ist International Congr. on Cybernetics, London
>Chapter II-17

Gestri G. and Petracchi E. (1970)
>The transformation induced by light stimulus on the retinal
>discharge : Study of the interval distribution at high-
>frequencies of sinusoidal stimulation
>Kybernetik, 6, 171-176

Gisbergen J.A.M. van, Grashuis, J.L., Johannesma P.I.M. and Vendrik, A.J.H.
>(1971)
>Single cells in the auditory system investigated with
>stochastic stimuli
>Proc. XXV Congress on Physiol. Sciences, München.

Gisbergen J.A.M. van (1974)
>Characterization of responses to tone and noise stimuli of
>neurons in the cat's cochlear nuclei.
>Thesis, Lab. Med. Physics and Biophysics
>University of Nijmegen, Nijmegen, The Netherlands

Goblick Th.J. and Pfeiffer R.R. (1969)
>Time domain measurements of cochlear non-linearities using
>combination click stimuli.
>J. of Acoust. Soc. Am., 46, 924-938

Johannesma P.I.M. (1968)
        Diffusion models for the stochastic activity of neurons
        in : Caianello, E.R. (ed.), Neural networks, 116-144
        Springer Verlag, Berlin

Johannesma P.I.M. (1969)
        Stochastic neural activity
        Thesis, Lab. Med. Physics and Biophysics
        University of Nijmegen, Nijmegen, The Netherlands

Johannesma P.I.M. (1971)
        Dynamical aspects of the transmission of stochastic neural
        signals
        Proc. First European Biophysics Congress, Wiener Med. Akademie,
        V, 329-333

Johannesma P.I.M., Gisbergen J.A.M. van and Grashuis J.L. (1971a)
        Forward and backward analysis of temporal relations between
        sensory stimulus and neural response
        Internal report, Lab. Med. Physics and Biophysics
        University of Nijmegen, Nijmegen, The Netherlands

Johannesma P.I.M. (1972)
        The pre-response stimulus ensemble of neurons in the cochlear
        nucleus
        Proc. of the IPO Symp. on hearing Theory (ed. Cardozo, B.L.)
        Eindhoven, 58-69

Jongh H.R. de (1972)
        About coding in the VIIIth nerve
        Proc. of the IPO Symp. on Hearing Theory (ed. Cardozo, B.L.)
        Eindhoven, 70-77

Jongh H.R. de (1973)
        Analysis of a spike generator
        Third IFAC Symp. on identification and parameter estimation
        Den Haag, The Netherlands

Kiang N., Watanabe T., Thomas E.C. and Clark L.F. (1965)
        Discharge patterns of single fibers in the cat's auditory
        nerve
        Cambridge, MASS., M.I.T. Press

Koldewijn G.J.R. (1973)

     Modelstudie aan het perifere auditief systeem

     Afstudeerverslag Lab. Med. Fysica en Biofysica, Nijmegen /

     afd. Electrotechniek T.H. Eindhoven

Lavine R.A. (1971)

     Phase-locking in response of single neurons in cochlear

     nucleus complex of the cat to low-frequency tonal stimuli

     J. of Neurophysiol. 34, 467-483

Møller A.G. (1970)

     Studies of the damped oscillatory response of the auditory

     frequency analyzer

     Acta physiol. Scand., 78, 299-314

Møller A.G. (1972)

     Coding of sounds in lower levels of the auditory system

     Quart. Rev. Biophys., 5, 59-155

Molnar Ch.E., Loeffel R.G. and Pfeiffer R.R. (1968)

     Distortion compensating, condensor-earphone driver for

     physiological studies

     J. of Acoust. Soc. Am., 43, 1177-1178

Nevenzel G. (1974)

     Coding and cytoarchitecture in the cochlear nucleus of the cat

     Afstudeerverslag Lab. Med. Fysica en Biofysica, Nijmegen

Olde Heuvelt G.H.F. (1971)

     Computer analyse van average pre-response stimuli

     Afstudeerverslag Lab. Med. Fysica en Biofysica, Nijmegen

Ruggero M.A. (1973)

     Response to noise of auditory nerve fibers in the squirrel

     monkey

     J. of Neurophysiol , 36, 569-587

Siebert W.M. (1965)

     Some implications of the stochastic behavior of primary

     auditory neurons

     Kybernetik, 2, 206-215

Werblin F.S. (1973)

     The control of sensitivity of the retina

     Scientific American, 228,1, 70-79

SUMMARY

In neurophysiology it is common practise to analyse the properties
of the stimulus-evoked series of actionpotentials by means of
post stimulus time histograms (for repetitive stimuli) and interval-
distributions and autocorrelation functions. The stimulus here is a
properly defined one and the investigations concerne about the neural
responses.

The analyses described in this thesis approach the investigations of
neurons from another side. The stimulus applied is an unstructured and
complex one, and need not to be controllable, but only observable. The
elicited actionpotentials are recorded and the analyses focus upon those
parts of the stimulus that immediately preceded an actionpotential
(neural event). The entire ensemble of stimuli preceding an event forms
the pre-event stimulus ensemble (PESE) The hypothesis now is, that
the functional properties of a neuron can be found by the analysis
of this pre-event stimulus ensemble.

In Chapter II a number of necessary concepts are introduced, like the
(already mentioned) pre-event stimulus ensemble (PESE), the (original)
stimulus ensemble and the post-stimulus response ensemble. Furthermore,
it will be shown that these concepts are related through the Bayes
relation.
This Bayes relation is a very important factor in this study.

In Chapter III the analyses of the PESE are described and from the Bayes
relation predictors are derived. These predictors open the possibility
to predict the responses to stimuli that are not applied. (The Bayes
relation appears to act as a generalized transfer function.)
Verifications of the predicted responses with experimentally recorded
responses affirm that with these analyses indeed a proper functional
description for a number of neurons is obtained.
So far the analyses have been made for stationary complex stimuli and
as yet only can be applied to this kind of stimulus.

156

Chapter IV is a detailed study about the average of the PESE. It appears that a fair approximation of the average of the PESE can be given by a mathematical function being an amplitude modulated sinusoid of which the envelope is described by four parameters.

157

In de neurophysiologie is het gebruikelijk om de eigenschappen van door stimulatie opgewekte neurale pulsreeksen te analyseren door middel van post stimulus tijd histogrammen (voor repeterende stimuli) en intervalverdelingen en autocorrelatiefuncties. De stimulus is hierbij en de studie betreft de neuronale responsies.

De in dit proefschrift beschreven analyses benaderen het onderzoek aan neuronen van een andere kant. De stimulus die wordt aangeboden is ongestructureerd en complex en hoeft zelfs niet controleerbaar te zijn, doch slechts observeerbaar. De door deze stimulus veroorzaakte aktiepotentialen worden geregistreerd en het onderzoek richt zich op die delen van de stimulus die direct voorafgingen aan een aktiepotentiaal ('neural event'). De totale verzameling van stimuli voorafgaande aan een aktiepotentiaal vormt het pre-event stimulus ensemble. De hypothese is nu dat de functionele eigenschappen van een neuron gevonden kunnen worden door bestudering van dit pre-event stimulus ensemble.

In hoofdstuk II worden een aantal noodzakelijke begrippen ingevoerd, zoals het (reeds genoemde) pre-event stimulus ensemble (PESE), het (originele) stimulus ensemble en het post-stimulus response ensemble. Daarnaast wordt aangetoond dat deze gegrippen aan elkaar gerelateerd zijn via de Bayes relatie. Deze Bayes relatie neemt een zeer belangrijke plaats in in het gehele onderzoek.

In hoofdstuk III worden de analyses van het PESE beschreven en via de Bayes relatie worden voorspellers afgeleid. Deze voorspellers geven de mogelijkheid om responsies op niet gegeven stimuli te voorspellen (de Bayes relatie blijkt hier een gegeneraliseerde overdrachtsfunctie op te leveren).
Toetsingen van voorspelde responsies aan gemeten responsies tonen aan dat met deze analyses inderdaad een goede functionele beschrijving van een aantal neuronen gegeven wordt.

Een en ander is onderzocht voor stationaire complexe stimuli en is vooralsnog ook slechts op deze stimuli van toepassing.

Hoofdstuk IV geeft een nadere bestudering van het gemiddelde van het PESE. het blijkt mogelijk om met redelijke benadering het gemiddelde van het PESE voor diverse neuronen te beschrijven met een analytische uitdrukking, te weten een amplitude gemoduleerde sinus waarvan de omhullende een viertal parameters bevat.

'Wovon man nicht sprechen kann, darüber muss man schweigen'

Ludwig Wittgenstein
Tractatus logico-philosophicus, 7

14 - 8 - '42 geboren te Delft

'54 - '59 H.B.S.-B te Tilburg

'59 - '68 studie voor natuurkundig ingenieur aan T.H. Delft
           afgestudeerd in de werkgroep Reactorfysica op theorie
           van en metingen aan epithermische neutronen spectra.

'68 - '69 militaire dienst

'69 - '73 werkzaam op laboratorium voor medische fysica en biofysica,
           universiteit van Nijmegen
           onderzoek aan signaalverwerking in het auditieve systeem
           van de kat.

behorende bij het proefschrift "The Pre-Event Stimulus Ensemble"

- 1 -

Responsies van neuronen op stationaire complexe stimuli zijn minder
complex dan responsies op in de neurofysiologie gebruikelijke
niet-stationaire stimuli.

- 2 -

Het verdient aanbeveling om bij auditief neurofysiologisch onderzoek
meer aandacht te besteden aan stimuli die gesuperponeerd zijn op een
achtergrond.

- 3 -

Voor het verklaren van het afnemen van phaselock in net auditief
systeem bij toenemende karakteristieke frequentie of hogerop in het
auditief systeem is het niet noodzakelijk om een jitter te introduceren.

- 4 -

Het is onjuist om aan te nemen dat de zonder stimulatie aanwezige
spontane activiteit onder stimulatie onveranderd aanwezig blijft.
Over de vraag of er onder gestimuleerde condities een onderscheid te
maken is tussen spontane en opgewekte activiteit kan door een hierop
gerichte analyse van het pre-event stimulus ensemble een uitspraak
gedaan worden.

- 5 -

Bij het presenteren van resultaten in duidelijke plaatjes wordt
vaak te veel geld en tijd gespendeerd om deze plaatjes extra mooi te maken.

- 6 -

Het verdient aanbeveling om op scholen het vak "godsdienst" te vervangen,
vooraf te laten gaan dan wel te begeleiden door een vak als algemene
filosofie.

De salarisongelijkheid die met name bij de overheid bestaat tussen
mensen met gelijke capaciteiten en arbeidsprestaties doch verschillende
diploma's is uitermate onrechtvaardig.

Medisch fysici moeten ervoor waken dat zij, zodra zij nader in contact
komen met, dan wel werken in de kliniek, niet de daar bestaande
inkomensfilosofie, onder meer betreffende de goed betaalde bijverdiensten
en de betaling per verrichting, als vanzelfsprekend overnemen.

Een opvallend verschil tussen de voor- en tegenstanders in de discussie
rond de abortus provocatus is dat in het algemeen de voorstanders
voor een vrije discussie en vrije beslissing zijn en de tegenstanders
tegen abortus.

Het is verwonderlijk dat een niet functionerend (al dan niet electronisch)
apparaat de meeste mensen meer verwondert dan een wel functionerend.

Het verdient aanbeveling om op daartoe geschikte plaatsen (brede
gangen) van gebouwen waarin veel geestelijke inspanning wordt verricht,
zodanige faciliteiten te scheppen (zweeds rek, rekstok, gewichten)
dat op onregelmatige tijden ook lichamelijke inspanning kan worden
verricht.

18 januari 1974   Jan L Grashuis